PERFORMANCE OF SINGLE AND DOUBLE SILLS

FOR STEEP CIRCULAR CULVERTS

by

Manam V. P. Rao, Robert J. Brandes

and Frank D. Masch

Research Report Number 92-5F

Performance of Circular Culverts on Steep Grades

Project 3-5-66-92

Conducted for

The Texas Highway Department

In Cooperation with the

U.S. Department of Transportation, Federal Highway Administration

by

CENTER FOR HIGHWAY RESEARCH

THE UNIVERSITY OF TEXAS
AUSTIN, TEXAS

January 1971

PREFACE

The research reported herein is a study of the performance of single and double sills as a means of producing uniform distribution of flow to the channel downstream of steep circular culverts. All experimental work has been carried out on 18-inch diameter corrugated metal and concrete pipe culverts. Experiments were conducted to determine single and double sill height/s and location/s within the standard Texas Highway Department wing walls to uniformly distribute culvert flow to the downstream channel.

The study was initiated under an agreement between the Texas Highway Department, the Federal Highway Administration and the Center for Highway Research of The University of Texas at Austin. Special acknowledgement is made to Messrs. Sam Fox and Dwight Reagan of the Texas Highway Department and Messrs. Frank Johnson and Edward Kristaponis of the Federal Highway Administration for their valuable suggestions and comments during the investigation.

Special thanks are also due to Armco Metal Pipe Corp. and Gifford-Hill Pipe Co. for providing the corrugated metal and concrete pipe respectively used in this study. The authors also wish to thank Messrs. A. C. Radhakrishnan, A. Sundar and Kenneth Shuler for their assistance in construction of the models and the collection of the data. Finally, the authors wish to thank Mrs. Joyce N. Crum for typing the manuscript and The University of Texas Bureau of Engineering Research for assistance with drafting.

ABSTRACT

The hydraulic performance of steep sloped circular culverts was investigated experimentally using 18-inch diameter corrugated metal and concrete pipe culvert models of different geometrical configurations. One of the effect means found to dissipate the energy of supercritical flows in steep culverts was to force a hydraulic jump to form inside of the culvert pipe by placing a sill within the flared wing walls of the culvert. Although some amount of energy was dissipated by the jump, there still remained the problem of high velocity concentrations in the central region of the downstream channel following the nappe from the jump producing sill. The use of two sills in such cases accomplished more energy dissipation due to the fact that the energy of the nappe was dissipated in the pool created by the second sill. Furthermore, the flow was distributed in the downstream channel more evenly in a shorter distance.

The primary objectives of this investigation was to determine the height and location of the jump producing sill for different culvert geometries over a broad range of discharge factors and to determine the best double sill configuration that would produce uniformly distributed flow in the downstream channel.

Data were collected on water surface profiles, jump locations within the culvert pipe, transverse depths and velocity profiles in the downstream

channel, and head water depths for various discharge factors ranging up to a maximum of 6.5 for different culvert geometries. The measured water surface profiles and jump locations were matched with the computed values. Energy levels in the downstream channel produced by sills were compared to the corresponding energy levels for the case of "no sills". The reductions of velocity concentrations in the downstream channel due to the sills were presented as graphical relationships between different dimensionless parameters pertaining to the geometry of the sills and the flow conditions.

SUMMARY

The main objective of this research report has been to study the performance of single and double sills as means of producing uniform distribution of flow in channels downstream of steep circular culverts. In particular, the study involved the experimental determination of the height and location of single and double sills placed within standard Texas Highway Department wing walls for different culvert geometries and a range of discharge factors. For the double sill arrangement, the best configurations (locations and heights) that would produce a uniform flow distribution in the downstream channel were determined.

Tests were conducted on 18-inch diameter corrugated metal and concrete culverts for discharge factors, $Q/D^{2.5}$, up to 6.5. Water surface profiles, jump locations, transverse depth and velocity profiles in the downstream channel were measured to evaluate the performance of the sill/s.

Although a single sill can be used to force a jump inside a culvert, more efficient performance can be obtained with two sills. The first sill serves to produce a jump while the second creates a pool to dissipate the energy of the falling jet from the first sill and to provide a more uniform distribution of flow in the downstream channel.

With a two sill arrangement, extensive data on downstream depths and velocity distributions for different double sill configurations were collected

in order to select the best combinations of sill heights and locations. Design criteria for these two parameters were recommended for the corrugated metal and concrete pipe culverts.

IMPLEMENTATION STATEMENT

The research indicated that the relationships between the head water depth and the discharge factor for corrugated metal and concrete pipe culverts operating under ventilated conditions and with sharp edged entrances were identical up to a value of $Q/D^{2.5} = 2.5$. Within the range of discharge factors $2.5 \leq Q/D^{2.5} \leq 4.5$, corrugated pipe culverts could be expected to display slug and mixture control. The concrete pipe culverts operated under orifice control up to discharge factors equal to 6.5.

It appeared from the tests on corrugated metal pipe culverts that the hydraulic jump was influenced more by a rough horizontal Unit 3 and the sharp break in grade whereas the jump position in concrete pipe culverts was affected very little by these factors for operation under the same conditions.

A one-dimensional method of analysis to predict water surface profiles and jump locations was found to generally yield satisfactory results provided that the upstream control, downstream control and the friction factor for the pipe were well defined. It has been recommended that the downstream control be taken as the sum of mid-sill height, head over the sill as computed from standard weir formulas, and the velocity head at the pipe outlet.

The study also indicated that two sills were more effective than a single sill in reducing high velocity concentrations in the downstream channel. The more effective double sill configurations were found to be associated with greater sill spacings and smaller end sill heights.

Tests showed that the two sills should be placed at distances of 1.5 and 3.0 pipe diameters from the culvert outlet for steep corrugated metal pipe culverts. For concrete pipe culverts, the recommended distances are 1.5 and 4.6 pipe diameters. The required height of the first sill can be determined from considerations of jump formation but never higher than 0.8D whereas the height of the end sill should be of the order of 0.16D.

TABLE OF CONTENTS

LIST OF FIGURES

Figure	Title	Page

LIST OF TABLES

LIST OF SYMBOLS

B	Width of the downstream channel.
D	Pipe diameter.
E	Specific energy.
E_3	Specific energy at the beginning of Unit 3.
ΔE	Difference in specific energy.
f	Friction factor.
g	Acceleration due to gravity.
H	Total energy.
H_o, H_s	Total energy in the downstream channel at a given section for the cases of 'no sill' and 'with sills' respectively.
ΔH	Difference in total energy.
HW	Head water depth.
L_1, L_2, L_3	Lengths of Units 1, 2 and 3 respectively.
n	Manning's n.
Q	Discharge.
R	Hydraulic mean radius.
s_1, s_2	Sill heights.
S_1, S_2, S_3	Slopes of Units 1, 2 and 3 respectively.
S_f	Friction slope.

V	Velocity.
X	Distance of single sill from culvert outlet.
X_1, X_2	Distances of the two sills from culvert outlet.
X_j	Distance of the toe of the jump from culvert outlet.
ΔX	Relative spacing of the two sills.
Y_1, Y_2	Sequent depths of hydraulic jump.
$\bar{Y}$	Average depth at a specified section of the downstream channel.
Y_3	Depth of flow at the beginning of Unit 3.
y	Depth of flow at a given section of the culvert.
Z	Elevation.
ΔZ	Difference in elevation.
ρ	Mass density of the fluid.
θ	Flare angle of the wing walls.
ϕ	Function.

CHAPTER I

INTRODUCTION

The prediction of the hydraulic performance of culverts on moderate to steep slopes and the subsequent dissipation of energy at the culvert outlets are essential parts of the design of highway cross drainage systems. A satisfactory design must provide an adequate opening to pass flows without excessive build-up of water at the culvert inlet and at the same time insure a safe and even velocity distribution at the end of the downstream wing walls as a safeguard against scour. A design which meets these requirements should lead to minimum maintenance costs and efficient operation over a broad range of flows.

The control of the exit velocity from culverts in which supercritical flows develop is the principal design issue of concern in this investigation. An economical method for modifying the energy levels in the flow leaving the culvert is sought to produce a reasonably uniform distribution of flow to the downstream channel. This would make it possible to eliminate high velocity flow concentrations and minimize potential scour problems.

The design of energy dissipators is not new to highway engineers and there are several standard types used where high velocity flows may be expected. In most cases the creation of a hydraulic jump is an essential feature of the energy dissipator. Because of the excessive length, appertunances within the basin, complex shapes and difficulties in construction many of these basins are not economically practical.

One effective means for dissipating energy at the end of a culvert is to force a hydraulic jump to form with a sill located downstream of the culvert exit. Such a sill not only provides the additional downstream force necessary for jump formation but also aids in distributing the flow uniformly across the width of the downstream channel. Without a sill supercritical flow from a culvert generally maintains the characteristics of a high velocity jet extending for considerable distances into the downstream channel. At high discharges, however, a single sill capable of forcing a hydraulic jump may become excessively high and since it raises the water level above the tail water channel it may again produce a potential scour problem as the flow spills over the sill.

More efficient performance and the production of a hydraulic jump over a broader range of flows can be accomplished by the use of double sills. The first sill serves to produce the force necessary to force the jump while the downstream sill creates a pool for the dissipation of the energy of the falling flow from the first sill and serves to distribute the flow more uniformly to the downstream channel. It is the performance of single and double sills over a broad range of discharges and different culvert configurations that forms the basis for this investigation.

Objectives and Scope

The main objectives of this study are as follows:

1. Determine the sill height and sill location within the standard Texas Highway Department (THD) 30^o flared wing walls necessary to force a hydraulic jump as a function of the discharge and culvert geometry for 18-inch corrugated metal and concrete pipe culverts.

2. Investigate the effectiveness of two sills used simultaneously within standard THD 30^o flared wing walls and determine the most desirable double sill configuration from the stand point of uniformity of the exit velocity.

3. Compare flow patterns in the downstream channel for conditions of no sill, a single sill, and double sills and estimate the energy dissipation in order to compare the effectiveness of the various sill configurations.

Although not primary objectives of this study other necessary data to fully evaluate the sill configurations were collected. These data included:

1. Determination of the head water - discharge relationship for 18-inch corrugated metal and concrete pipe culverts over the range of discharges used in the tests.

2. Prediction of the water surface profiles and jump locations within the culvert for given discharges, culvert geometry and sill configuration.

For each culvert configuration and discharge ratio, minimum sill height/s required to force a hydraulic jump were determined. The efficacy of the double sill arrangement over a single sill is studied by comparing the transverse depth and velocity distributions at sections downstream of the sills over the full range of discharge factors and sill locations. This comparative data for different sill arrangements over a wide range of discharge ratios were useful not only in the determination of the energy levels in the downstream channel but also in the appropriate selection of a double sill arrangement for the corrugated metal and concrete pipe culverts. These data were used to determine the effectiveness of the double sill configuration relative to the single sill. The data were useful also in estimating energy levels in the downstream channel and the distance from the various sills at which uniform flow was re-established in the channel.

Only one type of sill was used for all the experimental tests. Rectangular sill/s uniform in both height and thickness were placed vertically across the entire width of the channel between the flared wing walls and perpendicular to the longitudinal axis of the culvert. Different sill height/s were used in a trial process to determine the sill height/s and location/s that would force a stabilized hydraulic jump upstream of the culvert outlet for a given discharge factor and culvert geometry.

Throughout the entire experimental portion of the study visual observations were made on the flow patterns in the vicinity of the sill/s located at various positions. The water surface profiles of the flow immediately upstream and over the sill/s, the flow concentrations, and the effectiveness of the sill/s in the spreading and distributing the flow across the width of the channel were observed. All these factors entered in the selection of the most effective combination of sill height/s and location/s.

The range of variables used in these tests are near the upper limits for situations encountered in practice except for culverts with improved inlets where the discharge ratios can be significantly higher. The test conditions are believed to produce flow rates and Froude numbers in the realm of those encountered in practice. This together with the fact that scale effects are minimized in the large models should improve confidence in the application of these results to prototype installations.

Literature

A detailed review of the literature as it relates to culvert performance and energy dissipators has been presented previously in Reports 92-2 and 92-4, [Refs. 1, 2] respectively. Since these reports were previously submitted under Project 3-5-66-92 no attempt will be made to repeat this review. Since Report 92-4 [Ref. 2], a paper by McDonald in 1969 [Ref. 3] described an investigation to determine the performance of a hook-type energy dissipator used in large culverts operating with free outlet conditions. In the McDonald work the best configuration of energy dissipator (i.e., best location of staggered hooks downstream from the culvert outlet, their thickness and spacing, end sill height, and sill opening) was determined by experimental testing and comparisons of velocity reductions obtained for each of the few configurations tested.

CHAPTER II

EXPERIMENTAL PROGRAM

All the experimental tests in this study were conducted on 18-inch diameter corrugated metal and concrete pipe culvert models. For each model setup and discharge ratio, data were collected on water surface profiles, head water depths, hydraulic jump locations, sill height/s and location/s and transverse depths and velocity profiles in the downstream channel. These data were collected for the range of discharge factors, $1.5 \quad Q/D^{2.5} \quad 6.5$ and for steep culvert slopes of 8 and 10 percent for each type of culvert. The inlet for all the models was of the sharp edge type and the culvert outlet was followed by standard THD wing walls set at 30^{o} flare to the culvert axis.

In each of the seven geometric configurations tested, the Unit 2 length of the culvert, L_2, was set on a steep grade. In Setups A, B, E and G, Unit 2 was followed by a short length, L_3, of horizontally placed pipe, (Unit 3). In Setup A, a full broken back culvert configuration was tested. A detailed description of each of these setups is given in the following section and pertinent dimensions are summarized in Table 2-1.

Model Setups

A schematic sketch of the head tank, culvert model and tail water channel is shown in Figure 2-1. The hand tank was made of 3/4 inch

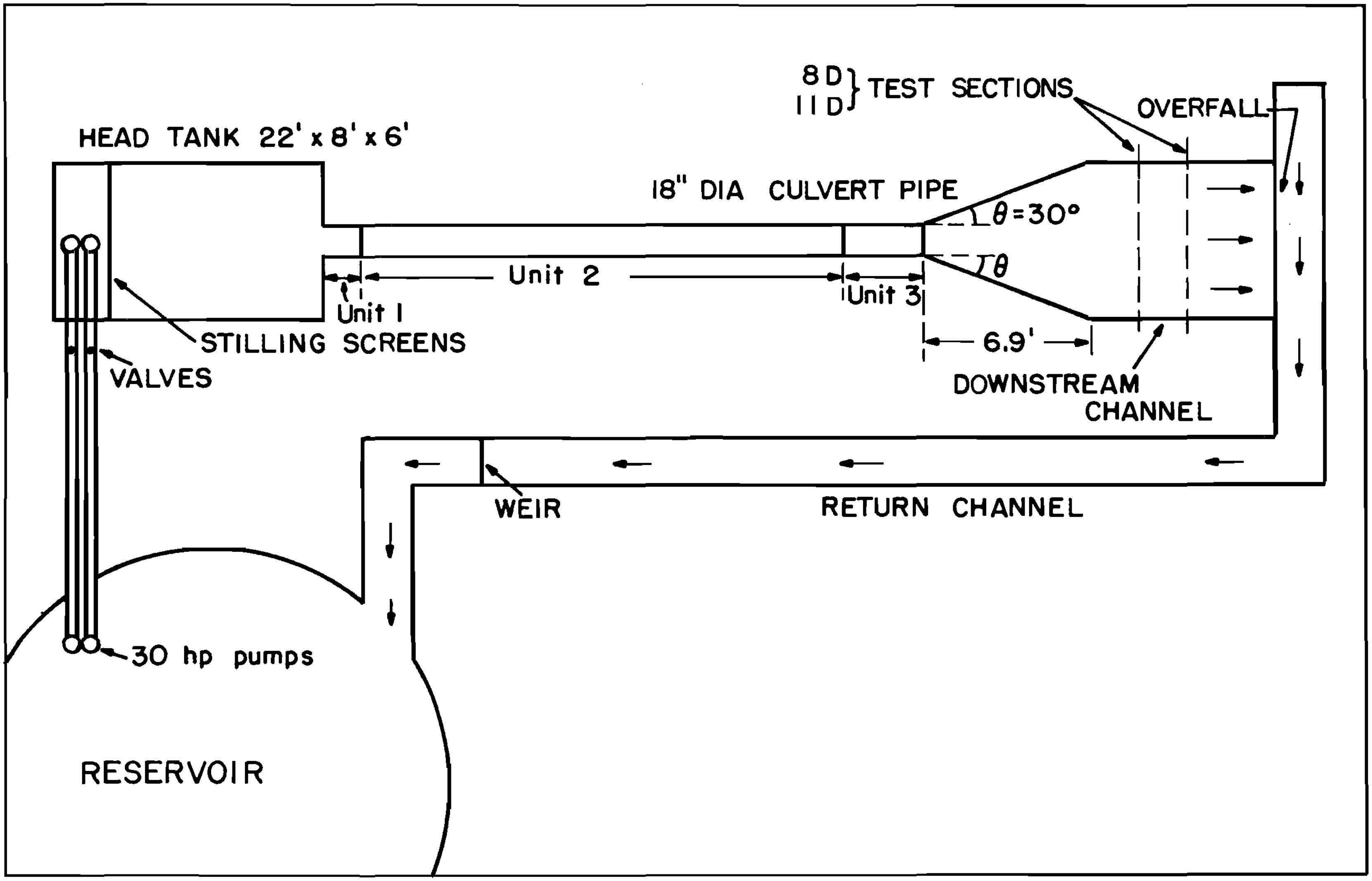

Figure 2-1. Schematic Sketch of the Experimental Setup

plywood and was 22 feet long, 8 feet wide and 6 feet deep. Two pumps each capable of delivering 4,000 gpm supplied water to the head tank through two 14-inch diameter pipe lines with regulating valves. The head tank contained stilling screens to quieten the initial disturbance at the entrance and to smooth the approaching flow upstream of the culvert inlet. The depth of water in the head tank was measured with four piezometers connected to taps located in the bottom of the tank and spaced one foot apart along the central flow line upstream of the culvert inlet.

Dimensions of the various test setups are summarized in Table 2-1. Figures 2-2 and 2-3 show overall views of corrugated metal and concrete pipe corresponding to Setups C and G, respectively. Variations in the slope of the middle section of the culvert were obtained by adjusting the cradle supports to required elevations along the length of the model. Where changes in the total length of the culvert model were made the tail water channel was shortened or lengthened as to provide a closed recirculating system. The water surface profiles in the corrugated metal pipe were measured with pressure taps located along the length of the pipe and connected to a battery of manometers. For the concrete pipe one-inch diameter holes were drilled at one-foot intervals along the top of the pipe and an electrical point gage equipped with neon bulb was used to measure the water surface profiles. In the concrete pipe additional side holes were drilled at regular intervals to supplement observations of the water surface profile and hydraulic jump locations.

TABLE 2-1. SUMMARY OF THE DIFFERENT CULVERT SETUPS

Designation of the Setup	Sloping Lengths of the Individual Units in Feet			Slopes of the Individual Units In Feet per Foot			Size and the Material of the Pipe
	L_1 Unit 1	L_2 Unit 2	L_3 Unit 3	S_1 Unit 1	S_2 Unit 2	S_3 Unit 3	
A	5.3	77.7	11.3	0.0	.079	0.0	Corrugated
B	0.0	63.7	11.3	0.0	.098	0.0	Metal Pipe
C	0.0	63.7	0.0	0.0	.098	0.0	18-inch Diameter
D	0.0	78.0	0.0	0.0	.080	0.0	Concrete Pipe
E	0.0	78.0	12.0	0.0	.080	0.0	18-inch
F	0.0	60.0	0.0	0.0	.104	0.0	Diameter
G	0.0	60.0	12.0	0.0	.104	0.0	

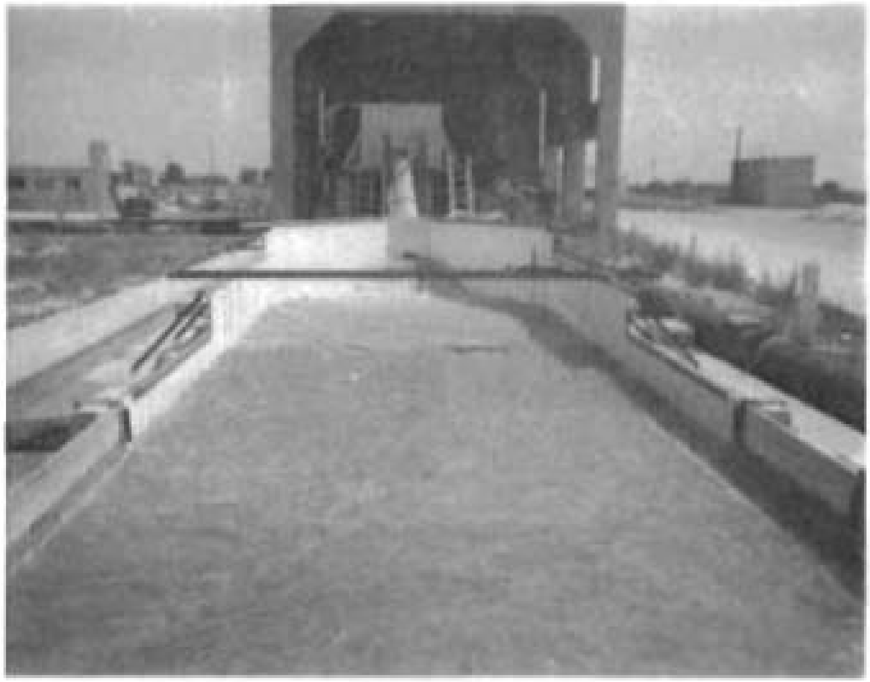

Figure 2-2. Photograph of Setup C

Figure 2-3. Photograph of Setup G

The wing walls at the outlet of the culvert also were made of plywood and flared at an angle of 30° from the central flow line to conform with THD standards. Provisions were made for placing sills within the wing walls at various distances downstream of the culvert outlet. The range of sill locations from the culvert outlet varied up to 4.6D or a maximum distance of 6.9 feet. The wing walls were followed by a tail water channel 9.8 feet wide which led water away from the culvert and into a return channel. A calibrated 15" high sharp crested weir located in the 4-foot return channel was used to determine the flow rates through the culvert models. In all cases the invert of the culvert at the outlet was set to conform with the elevation of the downstream tail water channel.

Rectangular plywood sills that spanned the width of the outlet channel between the wing walls were used to force the hydraulic jump. The sill length was equal to the width of the outlet channel at the particular location between the wing walls. Vertical braces were fixed to the wing walls and also at the central part of the outlet channel to hold the sills in an upright position and perpendicular to the flow. Selection of the proper sill/s to stabilize a jump was a trial and error process using an assortment of varying sill heights. A point gage was used to measure water depths above the sill/s and in the downstream channel. A pitot tube was installed on a sliding frame over the downstream channel so that velocity measurements could be made in the flow over the sill and in the downstream channel.

Experimental Procedure for Single and Double Sill Tests

Since this investigation was primarily experimental in character data collection was a detailed process. All quantities related to the stabilization of the jump by either single or double sills had to be varied in a way that their efficiency could be determined. In this respect the discharge, culvert geometry and sill configurations were all varied systematically. Experiments on single sill performance were conducted on Setups A, B and C which are corrugated metal pipe culvert models.

For each setup a sequence of measurements was followed so that the following determinations could be made:

1. Head water-discharge relationships.
2. Friction factor for both corrugated metal and concrete pipes determined from full pipe flow tests.
3. Water surface profile observations and jump locations for a range of flows with and without sill/s.
4. Transverse depth and velocity profiles in the tail water channel at distances 8D and 11D from the culvert outlet with and without sill/s.
5. Sill height/s and location/s required to produce stabilized hydraulic jumps.

The discharge factor, $Q/D^{2.5}$, was generally varied in increments of 0.5 over the range of 1.5 to 3.5 for the single sill tests and up to 6.5 for double sill tests. This provided a normal range of discharges at which various sill/s could be used to force the hydraulic jump for a given culvert geometry. The discharge factors and corresponding discharges for 18-inch pipe expressed in units of cubic feet per second are listed in Table 2-2.

TABLE 2-2. DISCHARGE RATIOS USED IN MODEL TESTS

$Q/D^{2.5}$	Q, cfs
1.5	4.133
2.0	5.510
2.5	6.888
3.0	8.265
3.5	9.643
4.0	11.020
4.5	12.398
5.0	13.775
5.5	15.153
6.0	16.530
6.5	17.908

For the single sill tests, two locations corresponding to either the mid-point or the end of the wing walls (i.e., X = 2.3D or 4.6D) were investigated in tests on Setups A, B and C. In the case of Setups A and B which had a 11.3-foot long horizontal Unit 3, the hydraulic jump always formed regardless of whether or not a sill was used. However, tests were still carried out to determine if sill height had an effect on jump location and specific energy at the beginning of Unit 3. In all these tests the range of sill height was $6'' \leq s \leq 14.5''$, i.e., $0.333 \leq s/D \leq 0.805$[1]. Results obtained with Setups A and B are illustrative of the influence of a rough length of Unit 3 pipe together with a sharp break in grade between Units 2 and 3.

Upon completion of single sill tests with Setups A, B and C, a new series of tests were undertaken with the objective of determining the best locations for two sills placed within the wing walls. The height of the first sill, s_1, was selected on the basis of its ability to force a jump near the pipe outlet. A second sill of lesser height, s_2, was placed further downstream to dissipate the energy of the falling jet from the first sill and to distribute the flow more evenly to the tail water channel. The locations for the sills were determined by extensive testing on many different sill configurations in which the distances of each sill from the outlet (X_1 and X_2) and the heights of each sill (s_1 and s_2) were varied systematically. Details of nine of the better performing double sill configurations are summarized in Figure 2-4. The criterion used for determining the better double sill configurations

---

[1] It was determined in conference with personnel of the Texas Highway Department and the Federal Highway Administration that the maximum sill height would be limited to 0.8D.

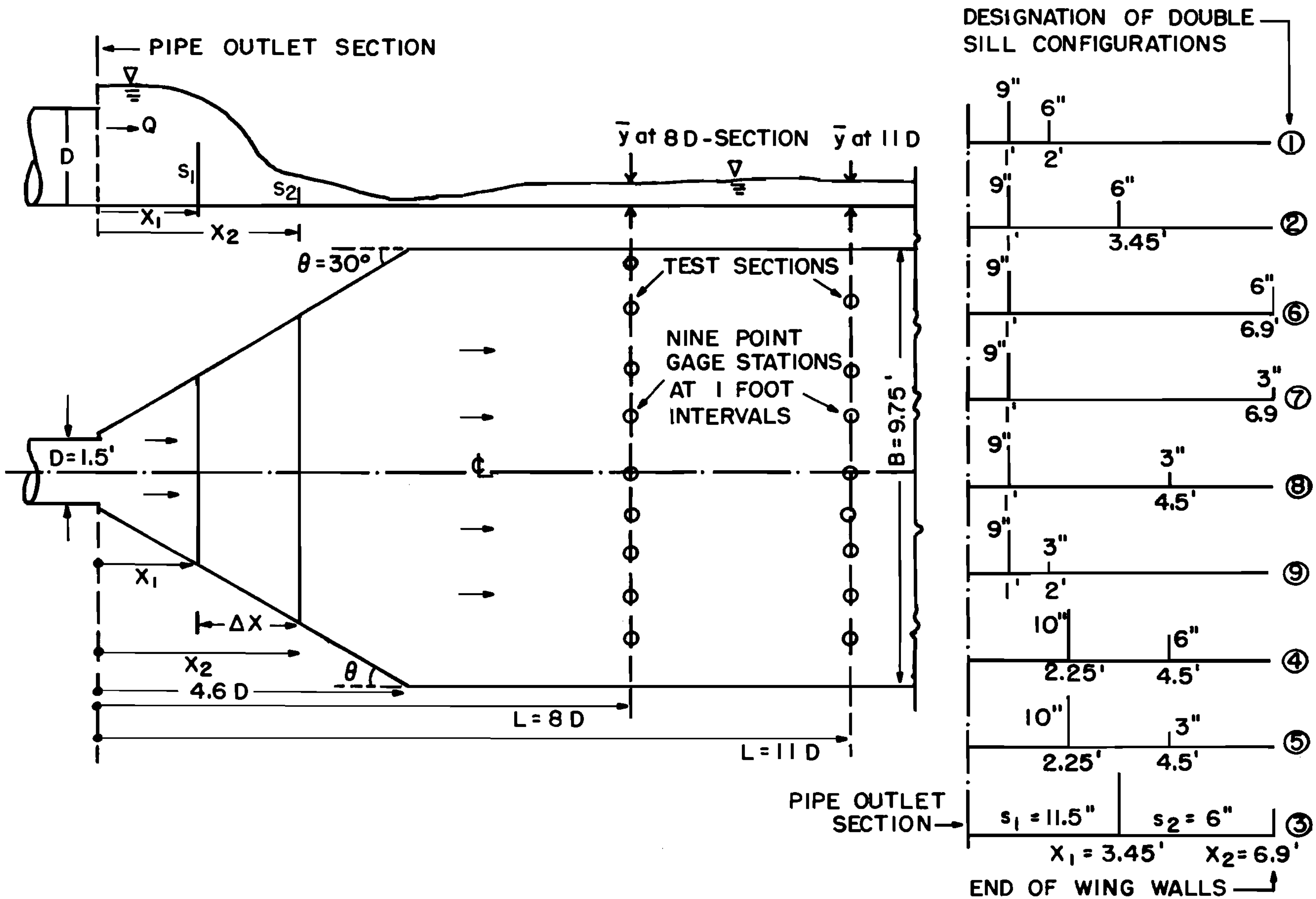

Figure 2-4. Schematic Sketch for the Double Sill Tests

was based upon the transverse depth and velocity profiles measured in the tail water channel at distances 8D and 11D from the pipe outlet.

The basic data collection procedure was similar for all tests. Beginning with 'no sill' condition, a selected discharge was set and allowed to flow through the culvert until steady-state conditions were established. Water surface profiles and transverse depth and velocity profiles were measured. A trial sill or combination of sills was then selected and placed in specific location/s between the wing walls. Depending on the sill height/s and location/s either a jump was formed and forced upstream into the pipe until pressure plus momentum relationship is satisfied and the jump stablized or no jump was formed and supercritical flow remained throughout the entire culvert length and downstream channel. The condition sought was the sill height/s and location/s which would force a stable jump within the pipe, eliminate downstream velocity concentrations, and provide a reasonably uniform distribution of velocity and depths in the tail water channel.

In determining the degree of flow concentrations over the sills and in the downstream channel, vertical velocity profiles were measured across the width of the sills and the transverse velocity distributions were measured across the channel at Sections 8D and 11D downstream of the sills. Of particular interest in these measurements was the downstream section where uniformly distributed flow was established.

CHAPTER III

ANALYTICAL CONSIDERATIONS

A detailed examination of the variables associated with the performance of broken-back culverts aids in understanding the flow behavior within the culvert and provides a basis for presenting data in non-dimensional form. A complete analysis of these variables was presented by Brandes, et al [Ref. 2] and only will be summarized here. With reference to Figure 3-1, the variables necessary to describe the hydraulic behavior in steep culverts are given by the general functional relationship

$$\phi\,[Q, \rho, g, D, L_1, L_2, L_3, S_1, S_2, S_3, s, X, X_j, \theta, f] = 0 \qquad (3\text{-}1)$$

where the variables are as defined in Figure 3-1 and where ρ is the mass density of the fluid, g is the acceleration due to gravity and f is the friction factor for the pipe culvert.

In this investigation the wing wall angle, θ, is maintained constant at 30° throughout the study. The results thus obtained are applicable for this flare angle only which influences the flow divergence at the culvert outlet and determines the tail water depth upstream of the first sill. The friction factor, f, is also considered constant for a given pipe material and pipe size.

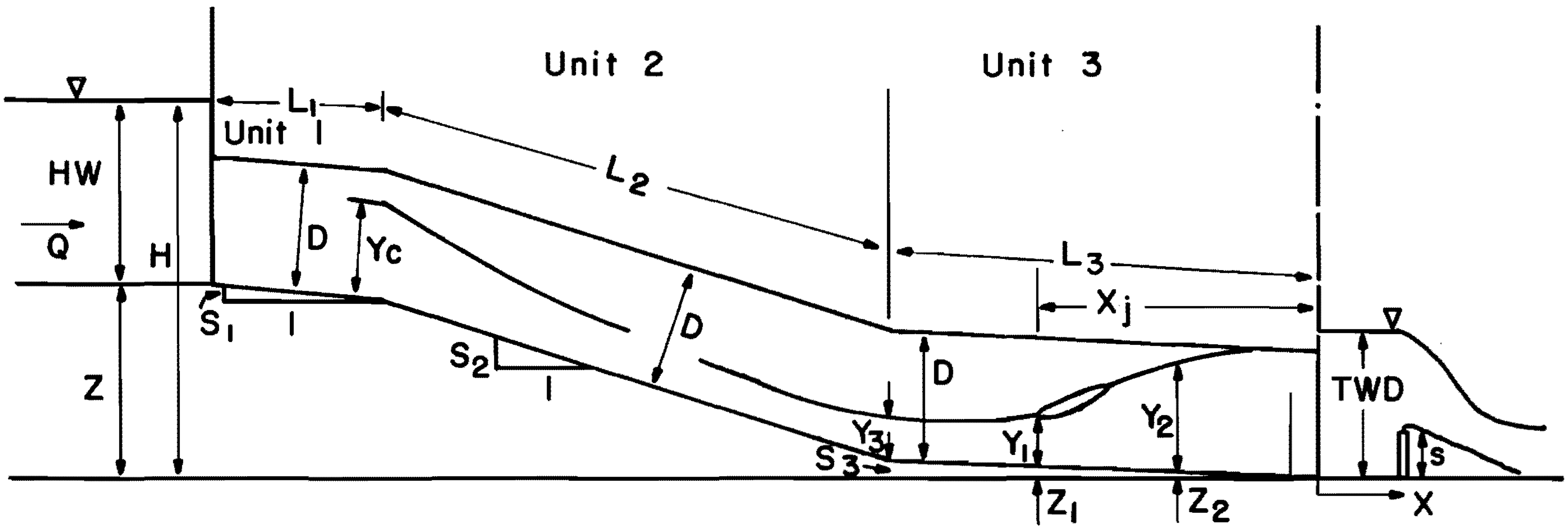

Figure 3-1. Definition Sketch of the Variables

It may be assumed that the specific energy at the beginning of Unit 3 (E_3) is a function of L_1, L_2, S_1, S_2 for a given test setup and discharge factor. Considering E_3 as representative of the above four variables the following relationship between the dimensionless parameters can be written as:

$$\phi[Q/g^{0.5}D^{2.5}, \ L_3/D, \ E_3/D, \ S_3, \ X_j/D, \ s/D, \ X/D, \ f] = 0 \tag{3-2}$$

The above relationship can be plotted from the data obtained from Setup A where several single sill heights at a specified location were tried at the same rate of flow. A plot of E_3/D versus s/D for specified values of $Q/D^{2.5}$, S_3, X_j/D, and X/D would represent the data obtained from Setup A. As an alternative, a plot of L_3/E_3 versus s/L_3 can be made keeping the above parameters constant. The only variable that cannot be held constant is X_j/D, i.e., the hydraulic jump location. However, a range of X_j/D can be stated under such circumstances.

Hydraulic Jump

For the case of the hydraulic jump the following well established functional relationships can be considered:

$$F_1 = \phi[Y_2/Y_1] = \phi[Y_1/E_1] = \phi[Y_2/E_1] \tag{3-3}$$

and

$$F_1 = \phi[\Delta E/E_1] = \phi[\Delta H/H_1] = \phi[H_2/H_1] = \phi[E_2/E_1] \tag{3-4}$$

where the subscripts 1 and 2 refer to sections before and after the jump respectively; F is the Froude Number, E is the specific energy, and H is the total head.

The relationship between sequent depths for hydraulic jumps in rectangular and circular channels are well known. The energy loss due to the jump in a circular channel can be computed from the difference in specific energies across the jump as follows:

$$\Delta E = (Y_1 + V^2{}_1/2g) - (Y_2 + V^2{}_2/2g) \tag{3-5}$$

$$\Delta E/E_1 = [(Y_1 - Y_2) + (V^2{}_1 - V^2{}_2/2g)]/(Y_1 + V^2{}_1/2g) \tag{3-6}$$

Expressing the velocities in terms of the discharge, flow areas, and noting that $F^2{}_2/F^2{}_1 = A^2{}_1 Y_1/A^2{}_2 Y_2$, it can be shown that

$$\Delta E/E_1 = [2(1 - Y_2/Y_1) + F^2{}_1(1 - A^2{}_1/A^2{}_2)]/(2 + F^2{}_1) \tag{3-7}$$

A similar expression can be written with respect to the total energy by considering the bed elevation before and after the jump as follows:

$$\Delta H/H_1 = [2(1 - Y_2/Y_1) + F^2{}_1(1 - A^2{}_1/A^2{}_2)]/(2 + F^2{}_1 + 2\,\Delta Z/Y_1) \tag{3-8}$$

where ΔZ is the difference in bed elevation before and after the jump.

Surface Flow Profiles

In the present study non-uniform flow profiles in the culvert were computed using the computer programs developed by Price and Masch

[Ref. 1] and later refined by Brandes, et al [Ref. 2]. As the programs were described in these earlier reports, they will not be repeated here. A summary of the basic method of calculations will suffice at this point.

For a given flow rate and bed slope (S_o), the distance along the bed (Δx) between any two sections where the depths are y_1 and y_2 respectively can be computed by the direct step method. The accuracy of the computations depends upon the selected values of Δy and the use of the proper friction factor for calculating the friction slope, S_f. The energy equation may be written between two sections spaced Δx apart, as follows:

$$y_1 \cos \theta + \alpha_1 \ V^2{}_1/2g + S_o \ \Delta x = y_2 \cos \theta + \alpha_2 \ V^2{}_2/2g + S_f \ \Delta x \tag{3-9}$$

where θ is the angle of slope; and α_1 and α_2 are the kinetic energy correction factors at each section respectively. From Equation (3-9), Δx can be determined as:

$$\Delta x = E_2 - E_1/S_o - S_f \tag{3-10}$$

where S_f is the average of the friction slopes of the two sections where the depths are y_1 and y_2. The friction slope can be calculated from either of the following equations.

$$S_f = n^2 v^2 / 2.22 R^{4/3} \tag{3-11}$$

$$S_f = f v^2 / 8 g R \tag{3-12}$$

where R is the hydraulic radius.

It is important to note that the backwater computation program [Ref. 1] is divided into two parts.

1. Upstream control in which the step computations are advanced in the downstream direction beginning with the critical depth at the beginning of the steep slope. A profile thus computed is referred to as a supercritical flow profile.

2. Downstream control in which the step computations are advanced in the upstream direction beginning with a known tail water depth at the culvert outlet caused by a sill. If the sill produces a tail water depth less than the critical depth of flow at the pipe outlet then the critical depth is taken as the downstream control. The profile so computed is referred to as a subcritical flow profile.

Hydraulic Jump Location

When the computations for the subcritical and supercritical flow profiles are performed, the pressure plus momentum at each section also is calculated for each flow profile. The section along the length of the culvert at which the pressure plus momentum values computed for each profile are equal is taken as the jump location. If a sill is placed within the wing walls, a meaningful measurement of the resulting tail water upstream of the sill can be obtained only if the sill is located far downstream of the culvert outlet. The measurement becomes much more difficult as the sill approaches the outlet of the culvert because of the turbulent character of the flow. The measurement of tail water depths in the region upstream of the sill also proved to be very difficult for the case of the concrete culvert where the jump formed very close to the outlet. As an alternative, tail water depths were estimated by approximate methods described in the next chapter. In this case, the estimated tail water depth is then taken as the downstream control and step computations are performed to obtain the subcritical flow profile. It is to be noted that the computed tail water depth depends upon the flow rate and the configuration of the first sill only. Hence the procedure to determine the jump location is the same regardless of the number of sills used.

CHAPTER IV

ANALYSIS OF RESULTS AND DISCUSSION

In this chapter results obtained from the experimental tests and computer runs are presented for different culvert geometries and flow conditions. Although various attempts were made to reduce the data to meaningful dimensionless parameters, all the data collected on the seven culvert setups were not directly amenable to plotting over a broad range of measured variables. For example, the location of the hydraulic jump was anticipated to depend on sill height and location. However, extensive data on jump locations over the range of sill heights, $0.0 \leq s/D \leq 0.81$ and for given $Q/D^{2.5}$ indicated that the jump location was insensitive to changes in sill height or position. This was particularly true for the first two setups (A and B) constructed of corrugated metal pipe. The break in slope between the Units 2 and 3 of the culvert and the rough horizontal section of the culvert dominated the jump location so that the jump always formed in Unit 2. Tests on Setup A indicated the jump could be moved further upstream into Unit 2, but required a sill height greater than 0.8D. Extensive data also were collected for Setup A with different single sill heights at 2.3D and 4.6D respectively to verify the computer model for flow profiles in the large model and to examine the variation of specific energy at the beginning of

Unit 3. These preliminary tests provided considerable insight into the effects of the sills and helped to reduce testing in subsequent setups.

Considering the results obtained from Setup A and the stated objectives of this study the following revised aspects of the data program are considered of primary importance:

1. Determination of head water - discharge ratio relationship.
2. Selection of minimum sill height and location to force a hydraulic jump in cases where the jump does not form without the aid of a sill.
3. Selection of the best double sill configuration for a large range of flows to produce a jump and to obtain relatively uniform distribution of the exit velocities.
4. Comparison of measured and computed water surface profiles and predicted jump locations.
5. Computation of the energy dissipation over a broad range of flows under conditions with (a) no sill, (b) a single sill and (c) double sills.
6. Measurements of velocity and depth distributions in the downstream channel for different flows for conditions with (a) no sill, (b) single sill and (c) double sills.

Head Water-Discharge Relationship

The head water-discharge rating curve for the culvert models is given in Figure 4-1. The basic data from which this figure was prepared is summarized in Appendix A, Table A-1. Also included in Figure 4-1

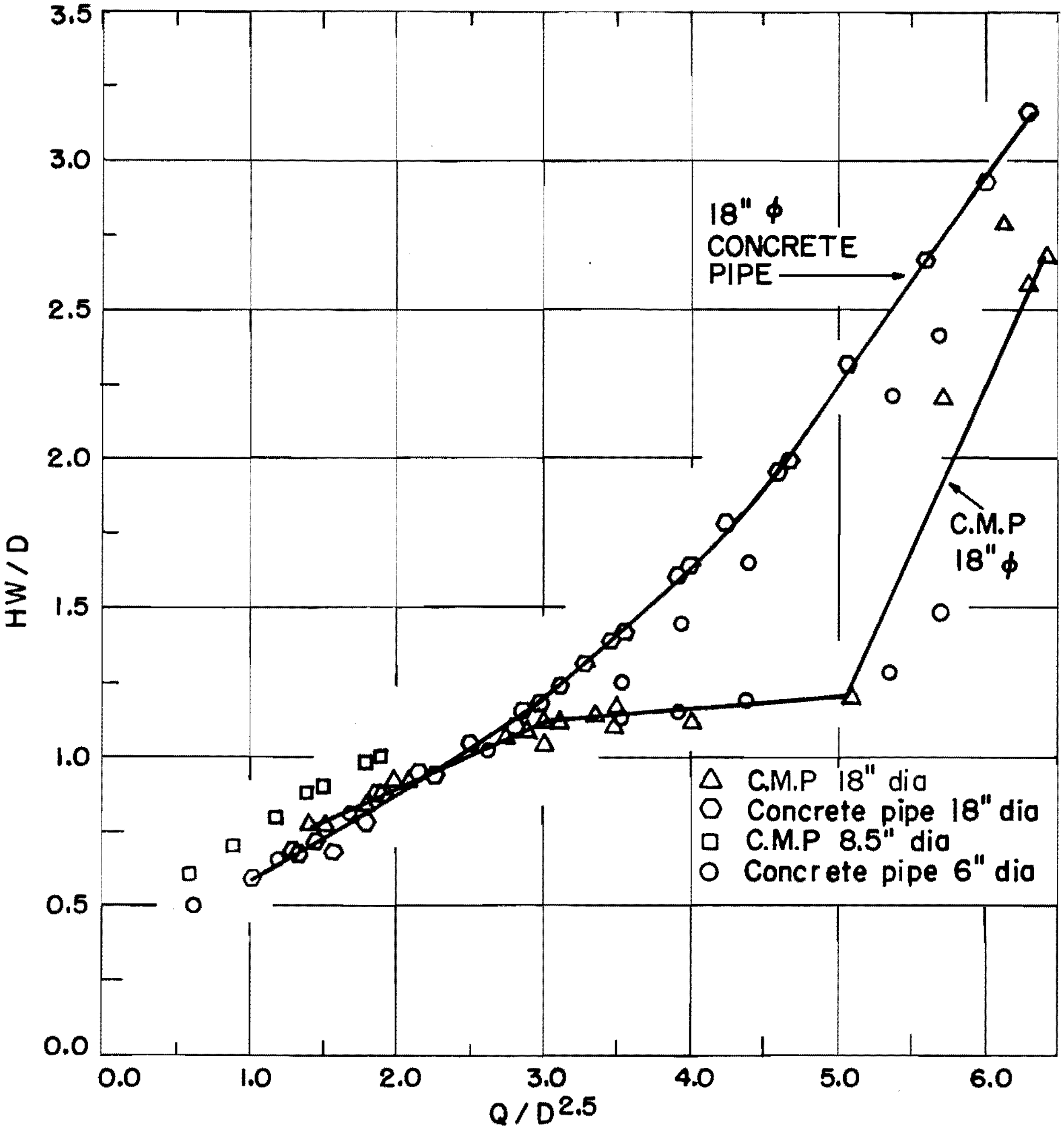

Figure 4-1. Head Water Depth - Discharge Factor Relationship for Corrugated Metal and Concrete Pipe Culverts

are data obtained by Price [Ref. 1] on 6-inch concrete pipe and 8.5-inch diameter corrugated metal pipe. All these data follow the well-known rating curve for highway culverts and the agreement between the data for different sizes of pipes is such to justify the universality of the rating curve for sharp edged entrances.

The principal difference between the performance of the concrete and corrugated metal pipe is to be noted at $Q/D^{2.5} = 2.5$. Beyond this and up to a value of $Q/D^{2.5} = 4.5$ the 18-inch corrugated metal pipe performs in the range of slug and mixture type flow as reported by Blaisdell [Ref. 4]. The performance of concrete pipe is characterized by orifice control for $Q/D^{2.5} \geqslant 2.5$.

Single Sill Investigations

The relationships between the non-dimensional parameters associated with the culvert geometry, flow rate, jump position and single sill configuration were summarized in Chapter III. The effects of sill height on specific energy at the beginning of Unit 3 were discussed by Brandes, et al [Ref. 2], and results presented as a series of curves relating s/L_3 to L_3/E_3. Such graphs are possible to compile provided data are available in which the length, L_3, is varied while all other parameters including discharge factor, culvert geometry, and jump location are maintained constant. Extensive data of this type was not obtained because of the difficulties in modifying the large culvert models and tail water channels for different L_3's and in controlling the hydraulic jump location. Furthermore, it was decided after tests were underway that the major efforts of the study would be shifted to investigation of double sill arrangements. All single sill test data from corrugated metal pipe Setups A, B and C are summarized in Appendix A, Tables A-2 through A-7.

Figures 4-2 through 4-5 do show the relationships obtained with Setup A between s/L_3 and L_3/E_3 and Y_3/L_3 for specified values of $Q/D^{2.5}$, S_3, X/D and a range of X_j/D. These curves display characteristics similar to those given by Brandes, et al [Ref. 2]. As expected, L_3/E_3 decreased as s/L_3 is increased or in other words, the greater the length of L_3, the lower the sill height required for given E_3. A similar variation is noted in the plots relating sill heights to the depth, Y_3, at the beginning of Unit 3. It is also noted that the change in L_3/E_3 or Y_3/L_3 is greater for sills located at X = 2.3D than the sills at X = 4.6D. Generally, an increase in specific energy upstream requires an increase in sill height and when a sill of given height is moved nearer the outlet, the head over the sill is increased due to the reduction in sill length. It is only those sills whose height is sufficient to raise the tail water level at the culvert outlet above critical depth that can be expected to influence energy conditions at the beginning of Unit 3. Accordingly, Figures 4-2 through 4-5 indicate very little changes in specific energy (E_3) or the depth (Y_3) at lower sill heights.

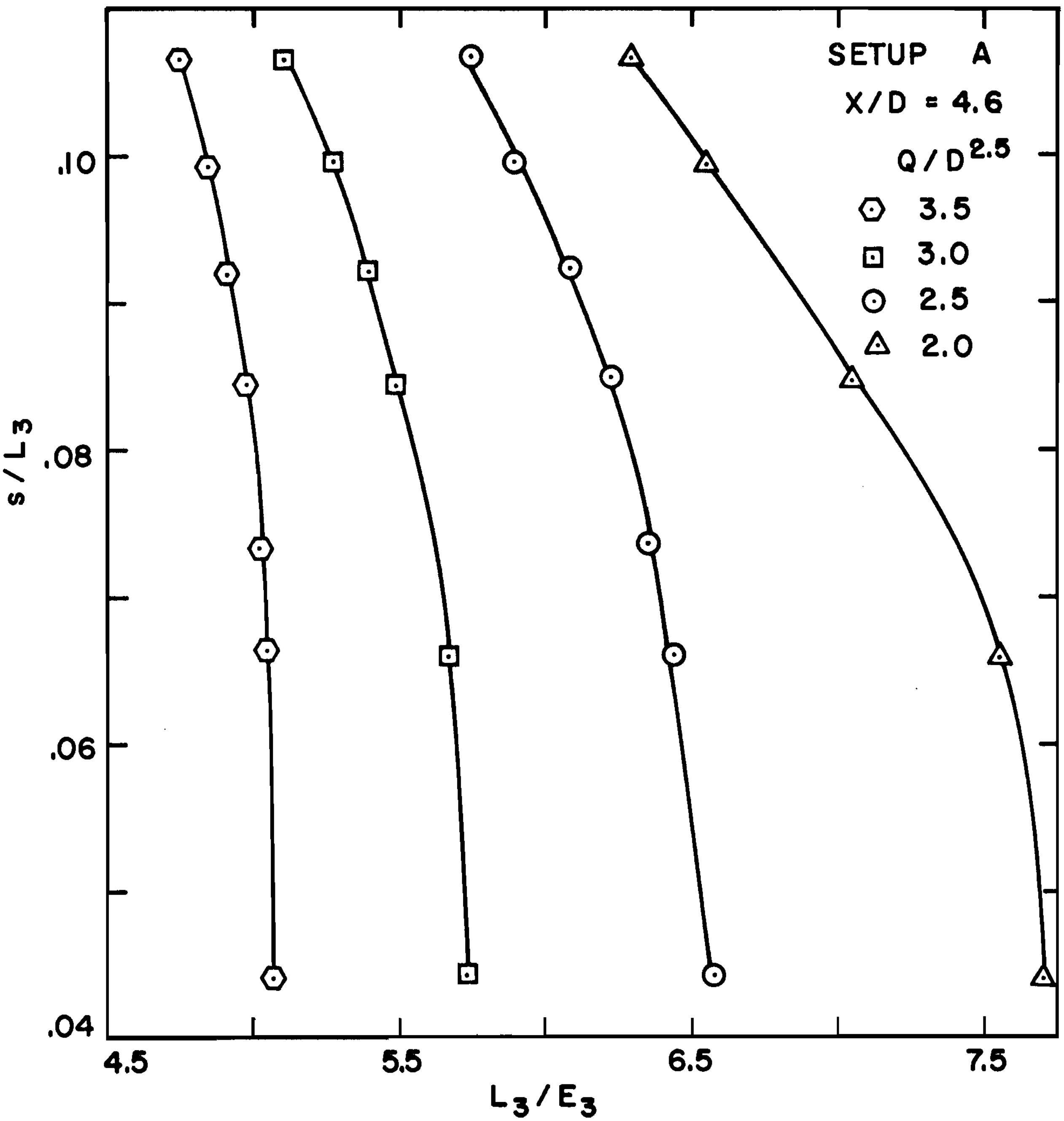

Figure 4-2. Relationship between s/L_3 and L_3/E_3 (End Sills)

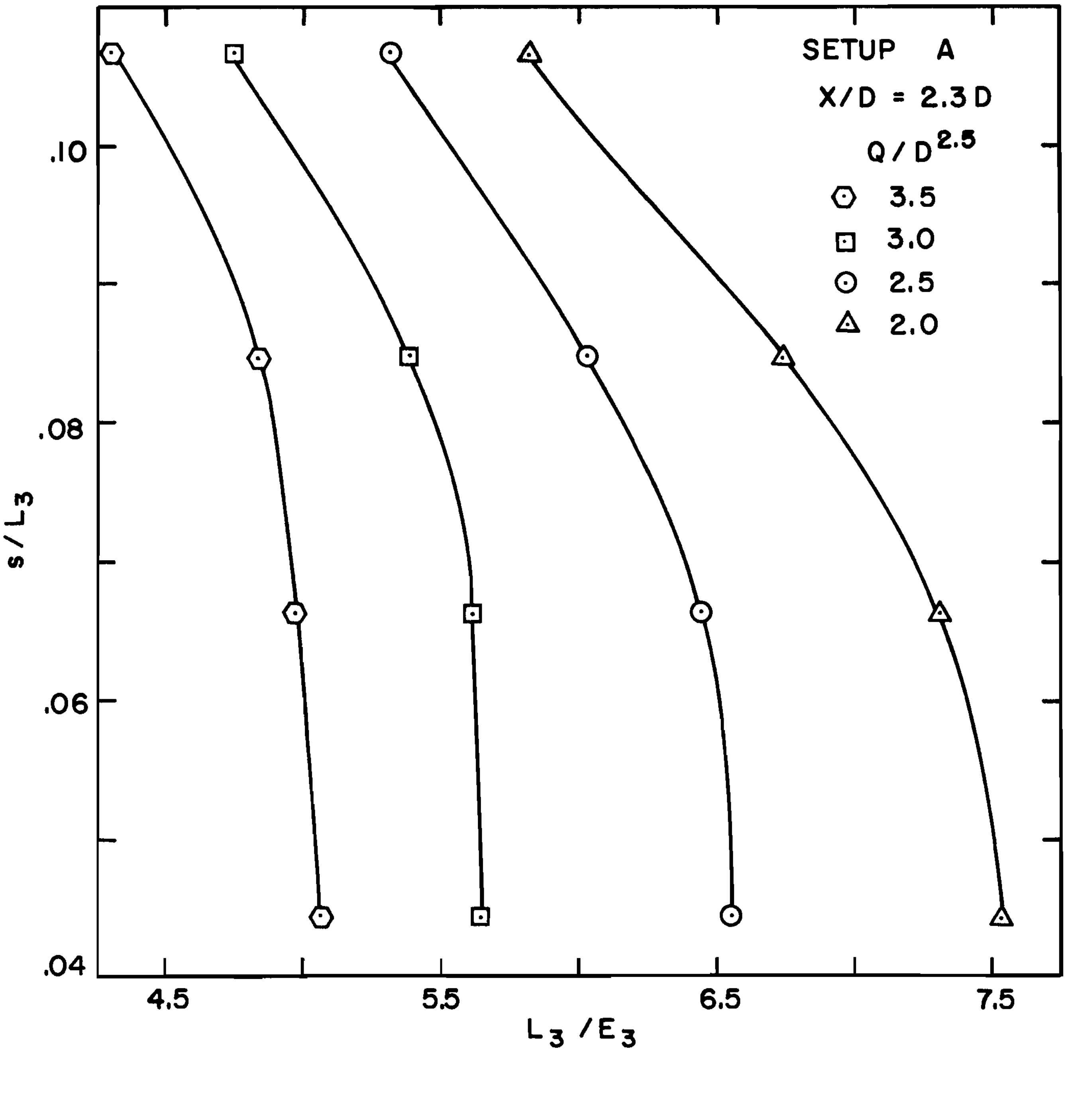

Figure 4-3. Relationship between s/L_3 and L_3/E_3 (Mid Sills)

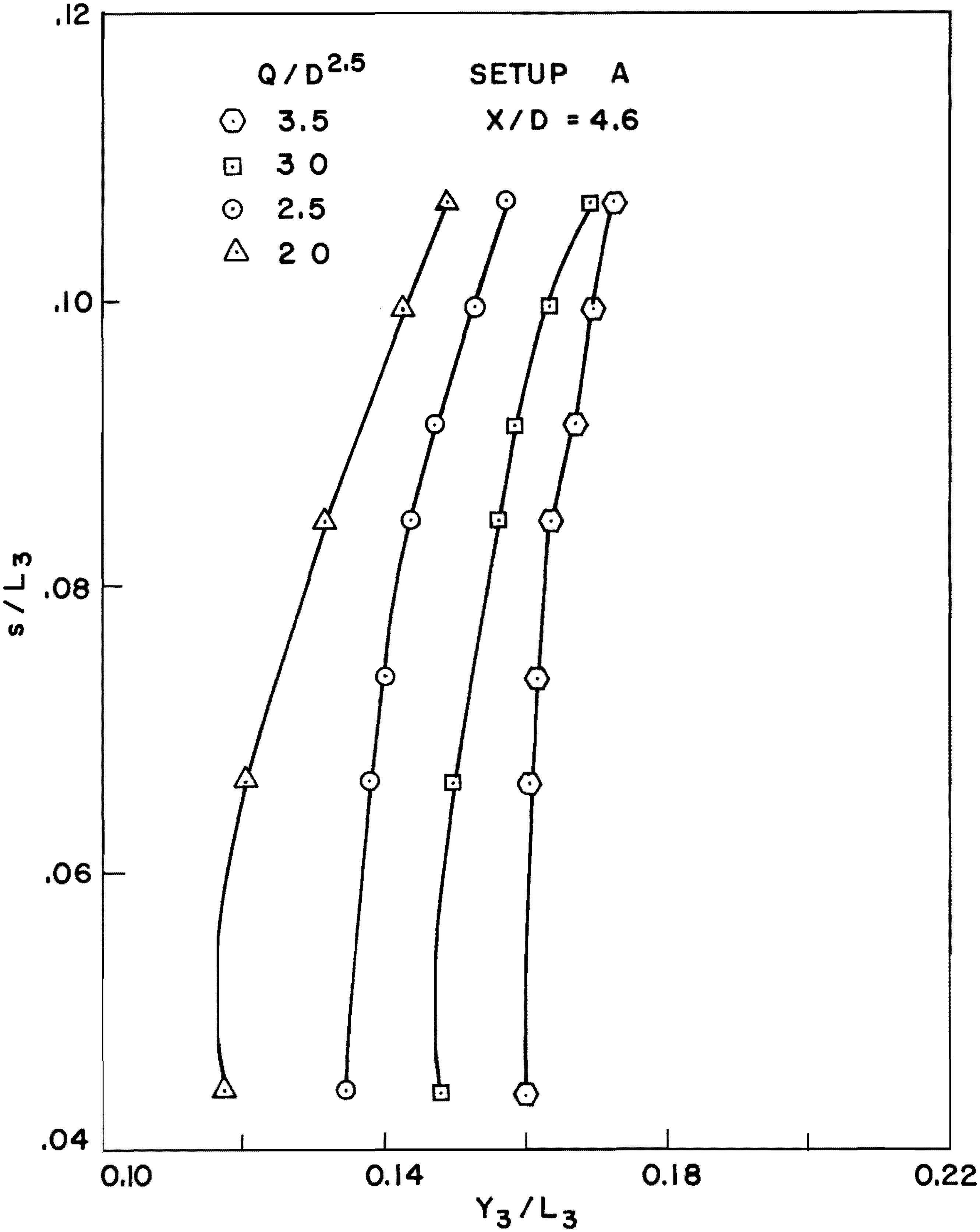

Figure 4-4. Relationship between s/L_3 and Y_3/L_3 (End Sills)

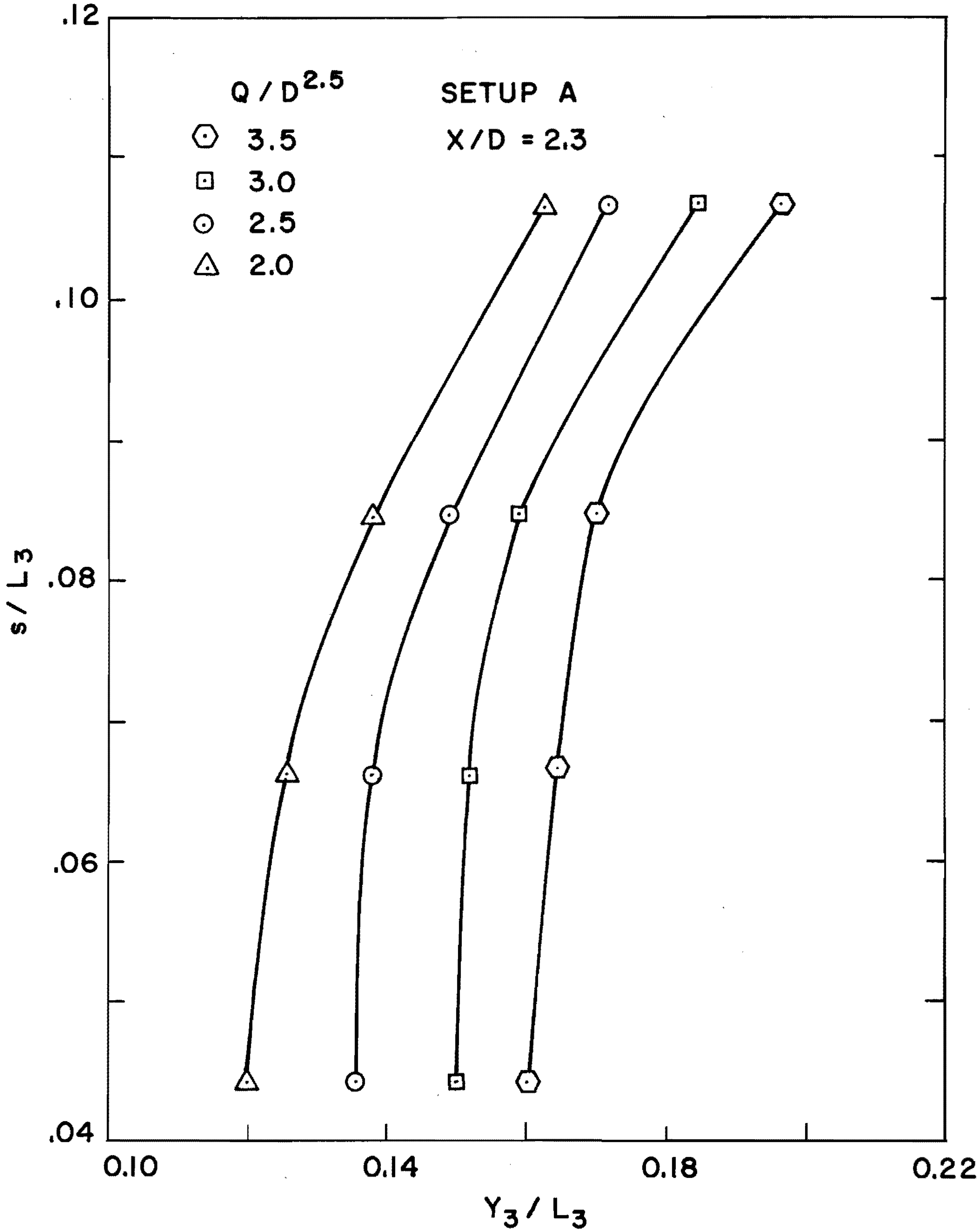

Figure 4-5. Relationship between s/L_3 and Y_3/L_3 (Mid Sills)

Characteristics of the Hydraulic Jump in Circular Culverts

For Setup A the relationships between upstream Froude number, sequent depths, energy loss and jump efficiency also were determined as shown in Figures 4-6 and 4-7. Figure 4-6 defines the relationships between the hydraulic jump depths and the entering Froude number whereas Figure 4-7 illustrates the relationship between the energy losses, jump efficiency and entering Froude number. Both plots conform reasonably well with corresponding plots for jumps in rectangular channels. Most of the scatter occurs at Froude numbers less than 1.5 where the jump is not well-defined and there is little energy dissipation. At higher Froude numbers the percent of energy dissipation is comparable with that obtained for jumps in rectangular channels.

Hydraulic Jump Location

Verification of predicted jump location for various culvert configurations was difficult to obtain in the large scale model. The prediction was based on computing the supercritical and subcritical flow profiles using critical depth as the upstream control and tail water depth as the downstream control. At each section the pressure plus momentum values associated with each of the two profiles were computed and the section at which the computed values were equal was taken as the hydraulic jump location. The jump

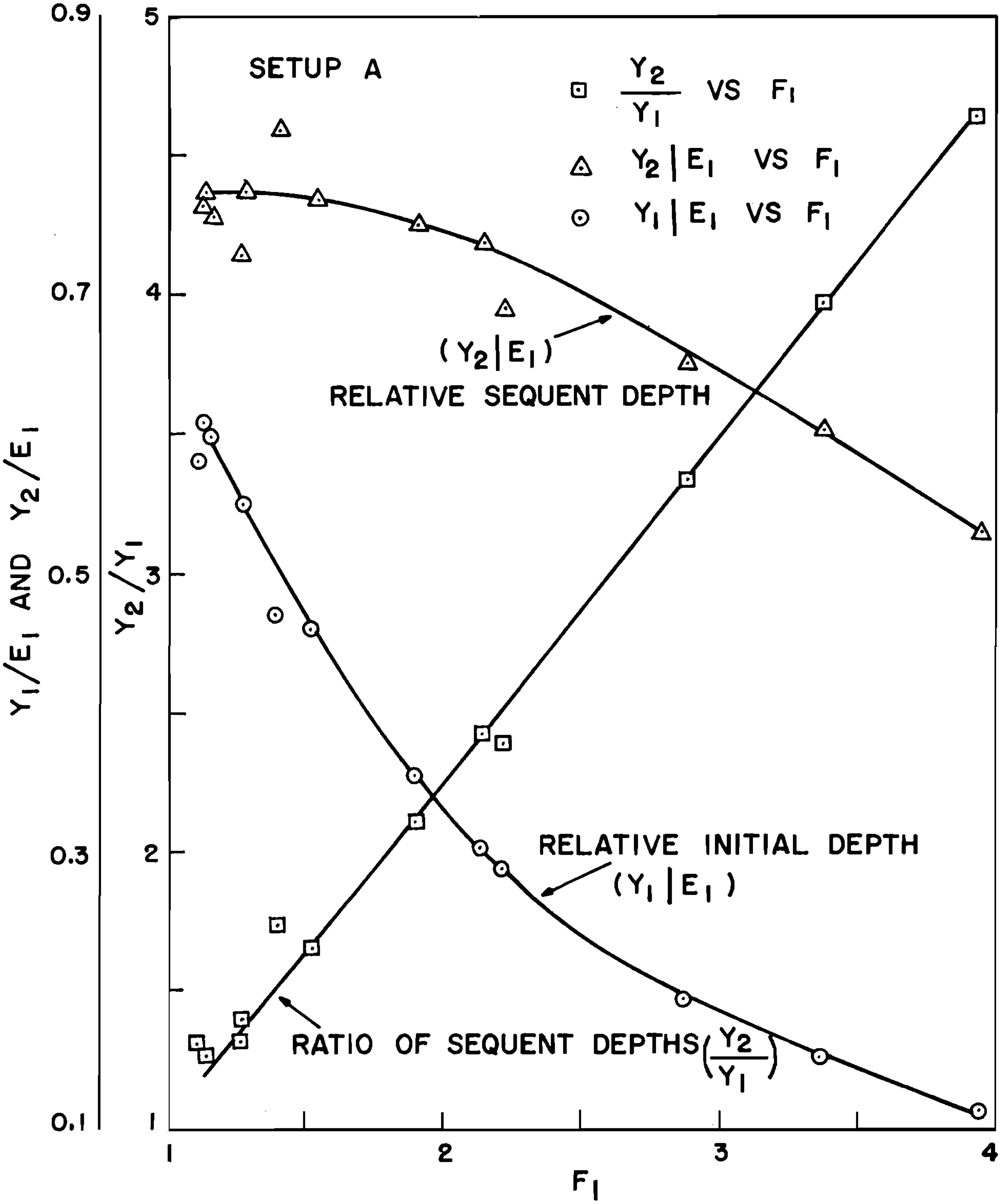

Figure 4-6. Characteristic Curves of the Hydraulic Jump

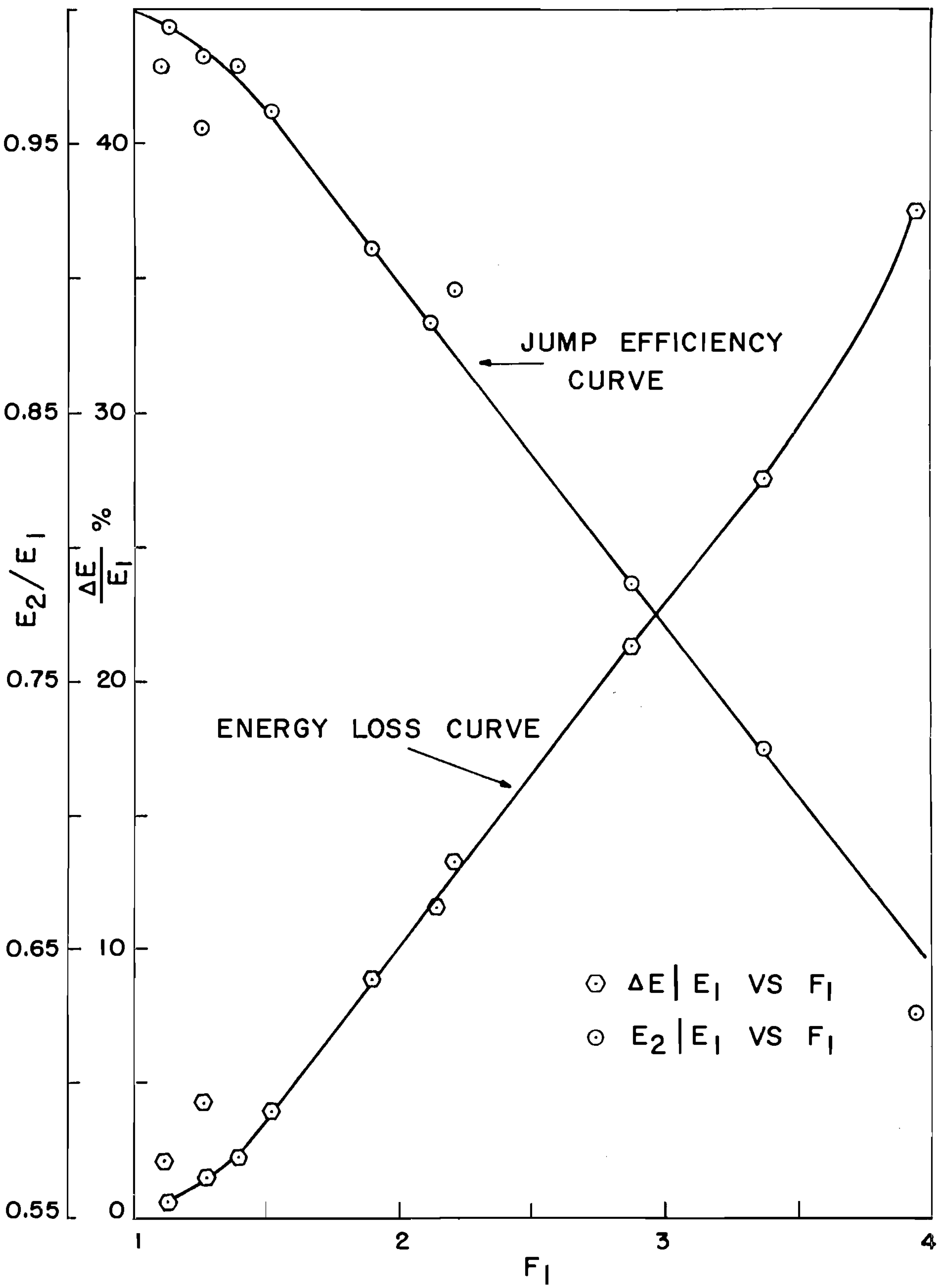

Figure 4-7. Froude's Number as a Function of Energy Loss and Jump Efficiency

location calculated in this manner is governed primarily by the specified tail water used in the computations. Close agreement between the computed and measured jump locations can be expected when the upstream and downstream controls are well-defined.

There are several factors which led to discrepancies between measured and computed jump locations. The first is the fact that the computed jump locations do not take into account the length of the jump. Jump lengths are commonly taken as 5 or 6 times the height of the jump and it is logical to expect an error of this order of magnitude in the predicted location. The second and more important factor which made it difficult to predict jump locations is specification of the tail water at the culvert outlet. Measured tail water depths can reliably be used in situations where flow upstream of the sill is reasonably uniform and steady. However, as the sill is moved closer to the culvert outlet, a great deal of turbulence and irregular flow is produced at the culvert outlet. This makes even average measurements of tail water depths difficult. The third is the use of appropriate value of friction factor or Manning's n in the computation of surface flow profiles. The friction factor for the corrugated metal pipe was determined from full pipe flow tests whereas in the case of concrete pipe models this procedure could not be followed because the models could not be made to run full. Based on the computed friction factor for the corrugated metal pipe, the Manning's n value was found to be 0.0238. In the case of concrete pipe a range of Manning's n values were used in the computer runs. Several computer test runs were made for different sill configurations, flow rates and for different corrugated metal pipe culvert configurations. The number of computer test runs for the concrete pipe were limited because of the jump formation close to the culvert outlet.

Several attempts were made to estimate tail water depths for a given flow in order to achieve better agreement between measured and computed jump locations. The methodology used in these computations may be summarized as follows:

1. Tail water depths were taken as the sill height plus the head over the full length of the sill. Consideration was given to the height of the sill in this computation by use of standard weir formulae. To determine the jump location by this method the pressure applied by the sill was added to the pressure plus momentum values associated with the downstream control profile.

2. Tail water depths were taken as the sill height plus the head over the sill as in the case of the first method. An additional term was added to the computed tail water depth corresponding to the velocity head at the culvert outlet. For cases in which the computed tail water based on Method 1 was greater than or equal to the pipe diameter, the full pipe velocity head was added to the tail water depth. For those cases where the computed tail water elevation was between the crown of the pipe and the critical depth of flow, the corresponding part flow velocity head was added to the tail water depth. Finally, in those cases where the computed tail waters were less than the critical

depth of flow at the pipe outlet, the tail water depth was taken as the pipe critical depth plus the corresponding critical velocity head. This method in effect considers the change in velocity head of the jet at the culvert outlet to pressure head as a consequence of the impact of the jet on the sill.

3. Tail water depths were computed from the sill height and the critical depth over a reduced length of the sill obtained from visual observation of the flow separation and back flow. The flow separation and the resulting back flow near the wing walls had some influence on the irregularity of tail water elevations upstream of the sill. The flow concentrated in the central region of the sill over a length approximately equal to 1.5 feet. The critical depth over the sill was then computed as for a rectangular channel.

4. Tail water depths were computed as the pipe diameter plus the full pipe velocity head assuming that the hydraulic grade line at the culvert outlet pierced the pipe at its crown and that the pipe was running full for all cases. It is further assumed in this method that the velocity head was fully recovered in the form of pressure head.

Tail water depths computed by the first method gave depths in good agreement with measured tail water depths upstream of the sill when the sill location, $X > 1.5D$ and when the hydraulic jump was formed well upstream of the culvert outlet. Use of this method in the computer runs for Setups A and B resulted in good reproduction of the water surface profiles in the downstream region of the culvert. However, predicted jump locations were underestimated for many of the test runs. Hence, an alternate method was sought which would provide a greater pressure plus momentum downstream of the jump. Although this could be accomplished by other three methods for estimating tail water, it was necessary to compromise the agreement between the computed and measured water surface profiles in the downstream region of the culvert to simulate the jump location.

Computer runs for the corrugated metal pipe tests indicate that Method 1 gave good results on jump location and water surface profiles in the downstream region when $s/D > 0.638$ and the additional sill force was added to the pressure plus momentum relationship. Even with sill pressures added, discrepancies between the measured and computed jump locations existed for $s \leq 0.638D$. To obviate these discrepancies, tail waters were recomputed by Methods 2, 3 and 4. It is to be noted that an effective sill length of 1.5 feet is used in Method 3 which naturally results in higher tail water than those obtained by the other methods. Reasonable agreement between measured and predicted jump locations were obtained for all the sill heights by these methods. The principle disadvantage, however, is the poor reproduction of the water surface profiles below the jump. Also to be noted is that Method 4 results in a common tail water for all sill heights and hence may be unreasonable for general application. However, observations of the jump locations indicate the lack of sensitivity of the jump to the sill height except for the highest sill, i.e., $s/D = 0.805$. The results obtained on jump locations computed on the basis of the different methods of tail water estimations are summarized in Tables 4-1 and 4-2 and four representative computer plots of the water surface profiles are shown in

TABLE 4-1. SUMMARY OF COMPUTER MODEL AND EXPERIMENTAL MODEL RESULTS*

(Corrugated Metal Pipe Setup A)

Method of Est. of TWD	X/D	s/D	$Q/D^{2.5} = 3.5$			$Q/D^{2.5} = 3.0$			$Q/D^{2.5} = 2.5$			$Q/D^{2.5} = 2.0$		
			TWD	CJL	MJL	TWD	CJL	MJL	TWD	CJL	MJL	TWD	CJL	MJL
Method 1	2.3	.805	1.828	32.2	34	1.768	31.2	27	1.705	32.9	25	1.638	37.3	27
	4.6	.805	1.647	29.1	27	1.606	28.1	27	1.559	31.0	19	1.512	35.3	17
	2.3	.638	1.568	21.1	27	1.511	19.6	19	1.451	18.6	19	1.383	23.1	15
	4.6	.638	1.392	19.0	27	1.351	14.5	19	1.307	17.3	19	1.259	22.0	14
	2.3	.500	1.350	16.5	26	1.295	12.4	19	1.235	11.7	19	1.170	12.7	14
Method 2	2.3	.805	2.291	30.4	34	2.107	24.7	27	1.941	21.2	25	1.789	19.3	27
	4.6	.805	2.110	26.9	27	1.945	21.9	27	1.795	18.9	19	1.663	17.5	17
	2.3	.638	2.031	25.3	27	1.850	20.2	19	1.691	17.3	19	1.546	15.8	15
	4.6	.638	1.885	22.4	27	1.729	18.1	19	1.584	15.7	19	1.447	14.3	14
	2.3	.500	1.865	22.0	26	1.701	17.6	19	1.542	15.0	19	1.386	13.4	14
	4.6	.500	1.831	21.3	26	1.650	16.8	19	1.480	14.0	19	1.319	12.6	13
	2.3	.333	1.831	21.3	26	1.650	16.8	19	1.470	13.9	19	1.285	12.3	14
	4.6	.333	1.831	21.3	26	1.650	16.8	19	1.470	13.9	19	1.285	12.3	13
Method 3	2.3	.805	2.294	33.5	34	2.189	27.4	27	2.077	23.3	25	1.956	21.7	27
	2.3	.638	2.044	28.5	27	1.939	23.1	19	1.827	19.4	19	1.707	18.1	15
	2.3	.500	1.836	24.3	26	1.731	19.5	19	1.619	16.2	19	1.498	15.1	14
	2.3	.333	1.586	17.7	26	1.481	14.9	19	1.369	12.4	19	1.248	11.9	14

* Computed jump location (CJL) and measured jump location (MJL) are expressed in feet with reference to the culvert outlet.

TABLE 4-2. SUMMARY OF COMPUTER MODEL AND EXPERIMENTAL MODEL RESULTS
(Corrugated Metal Pipe Setups B and C)

Method Est.TWD	Set-up	X/D	s/D	$Q/D^{2.5} = 3.5$			$Q/D^{2.5} = 3.0$			$Q/D^{2.5} = 2.5$			$Q/D^{2.5} = 2.0$		
				TWD	CJL	MJL	TWD	CJL	MJL	TWD	CJL	MJL	TWD	CJL	MJL
1	B	2.3	.638	1.568	17.0	21	1.511	15.7	17	1.451	13.8	13	1.383	17.5	13
		4.6	.638	1.392	7.0	17	1.351	11.8	17	1.307	12.7	13	1.259	16.5	13
2	B	2.3	.638	2.031	19.6	21	1.850	16.7	17	1.691	15.0	13	1.546	14.1	13
		4.6	.638	1.885	17.6	17	1.729	15.1	17	1.584	13.7	13	1.447	13.0	13
3	B	2.3	.638	2.044	23.5	21	1.939	19.9	17	1.827	17.2	13	1.707	15.9	13
2	C	2.3	.805	2.291	7.5	5	2.107	5.7	5	1.941	4.7	4	1.789	4.4	4
		4.6	.805	2.110	5.0	5	1.945	3.6	5	1.795	3.0	4	1.663	2.9	4
		2.3	.638	2.031	3.8	5	1.850	2.4	5	1.691	1.8	4	1.546	1.6	4
		4.6	.638	1.885	1.8	5	1.729	0.8	5	1.584	0.5	4	1.447	0.6	4
3	C	2.3	.638	2.044	4.1	5	1.939	3.9	5	1.827	3.6		1.707	3.9	4

Figures 4-8 to 4-11. The matching of the computed and measured jump locations was found to be poor in the case of concrete pipe models in view of the jump formation close to the culvert outlet.

A factor of lesser importance in the prediction of jump location is the assumption of upstream control at the beginning of the steep sloped unit. Except for very low flows the depth at the culvert inlet is characterized by an unsteadiness especially for those cases when head water is at or near the crown of the pipe. This unsteadiness is caused by vortex formation and intermittent flow of air into the pipe. Both the roughness of the pipe and the inlet geometry are known to have some influence on the head water. Experimental studies [Ref. 5] indicate that critical depth occurs approximately 0.5D downstream of the culvert inlet if it is of square edge type. In this study the distance of the upstream control from the inlet varied with the flow factor. However, no great importance was attached to this since the flow profile based on upstream control is associated with large changes in depth over a short length. This is especially true for the rougher corrugated metal pipe in which supercritical flow profile attains supercritical normal depth in a very short distance from the upstream control section. The pressure plus momentum for the upstream control profile does not change beyond the section of the culvert at which the normal depth is obtained. As the hydraulic jump location is computed from the intersection of the pressure plus momentum curves associated with the upstream and downstream control

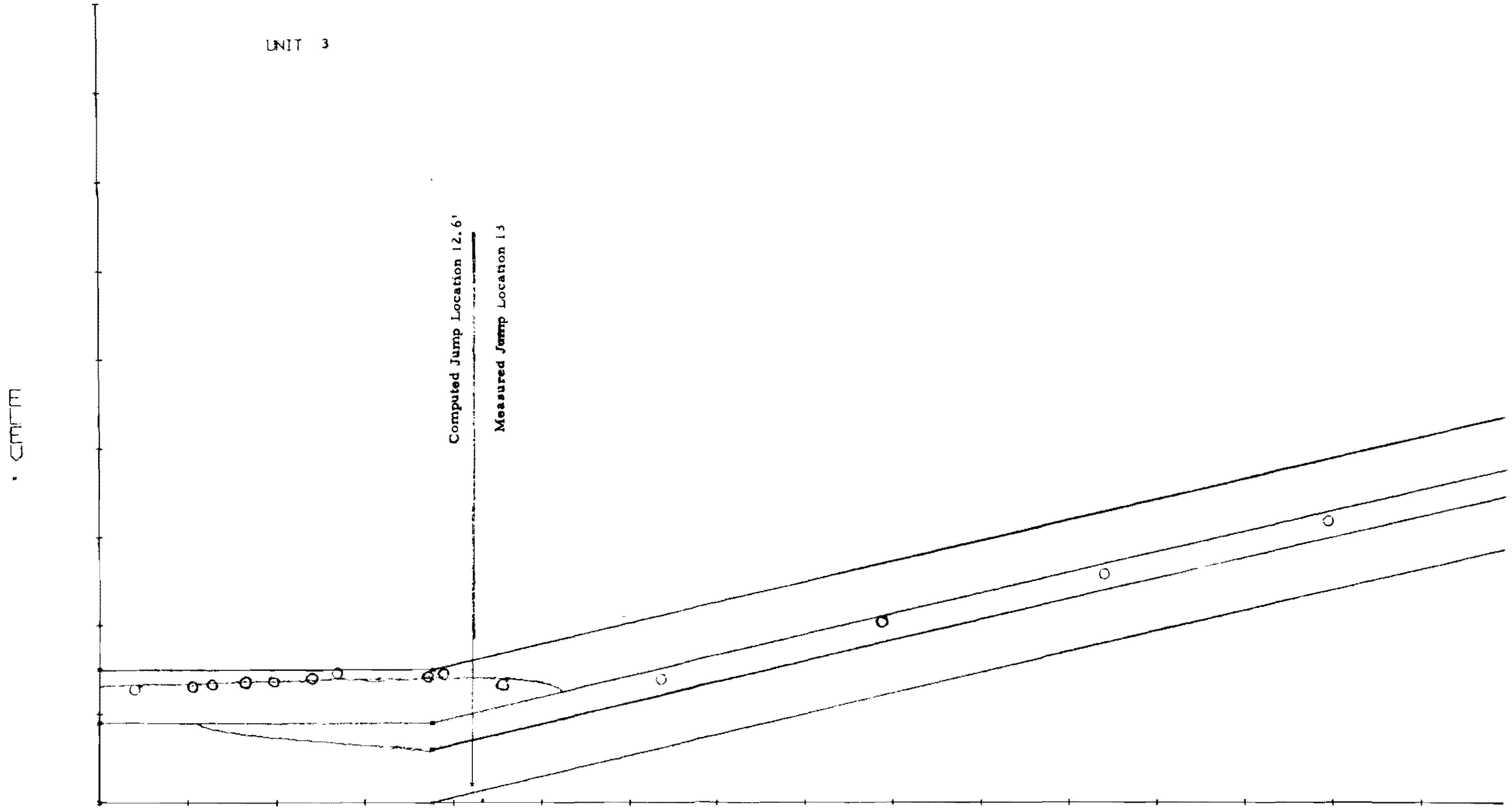

Figure 4-8. Measured and Computed Surface Profiles - Setup A (Continued)

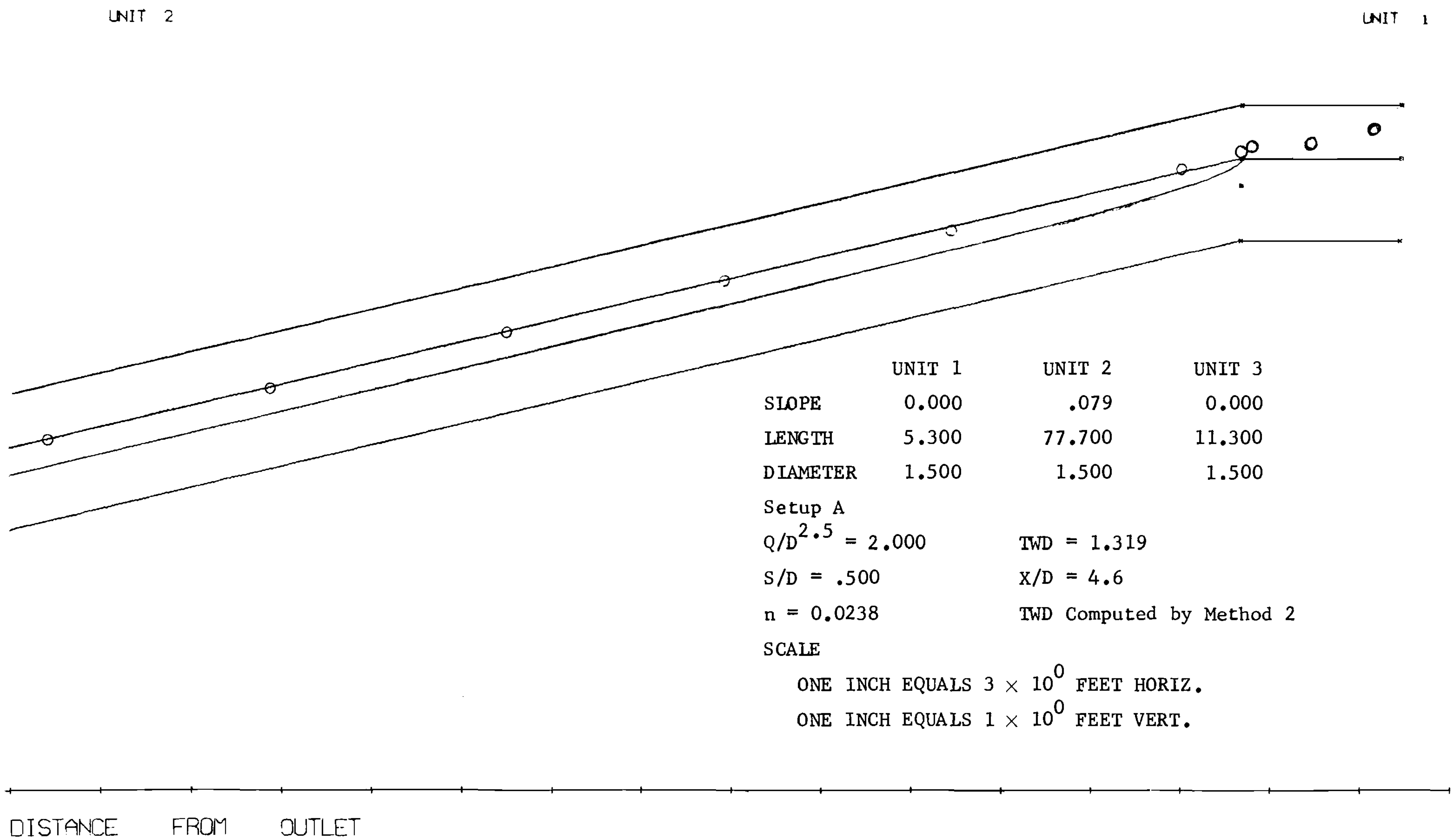

	UNIT 1	UNIT 2	UNIT 3
SLOPE	0.000	.079	0.000
LENGTH	5.300	77.700	11.300
DIAMETER	1.500	1.500	1.500

Setup A

$Q/D^{2.5} = 2.000$ TWD = 1.319

S/D = .500 X/D = 4.6

n = 0.0238 TWD Computed by Method 2

SCALE

ONE INCH EQUALS 3×10^0 FEET HORIZ.

ONE INCH EQUALS 1×10^0 FEET VERT.

Figure 4-8. (Continued)

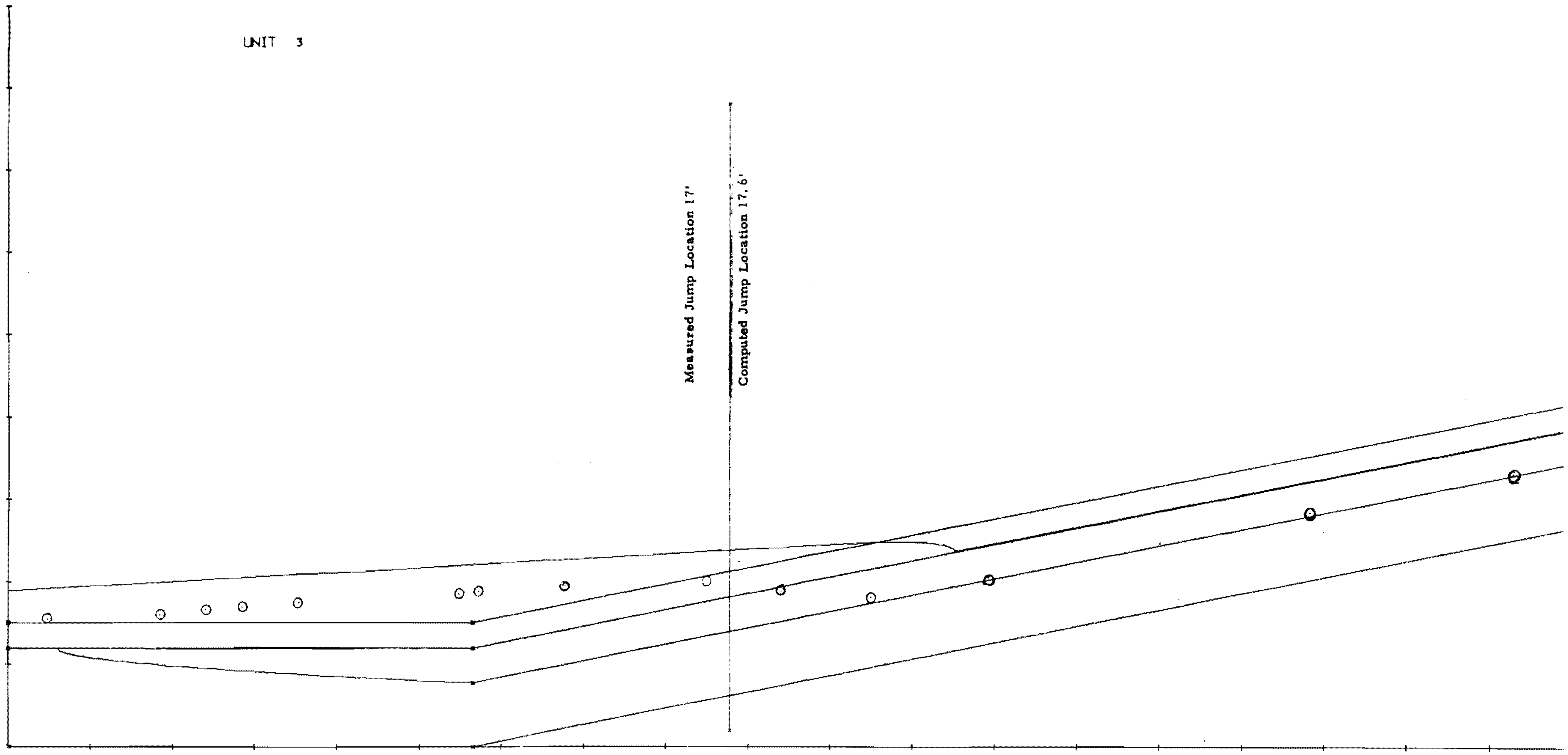

Figure 4-9. Measured and Computed Surface Profiles - Setup B (Continued)

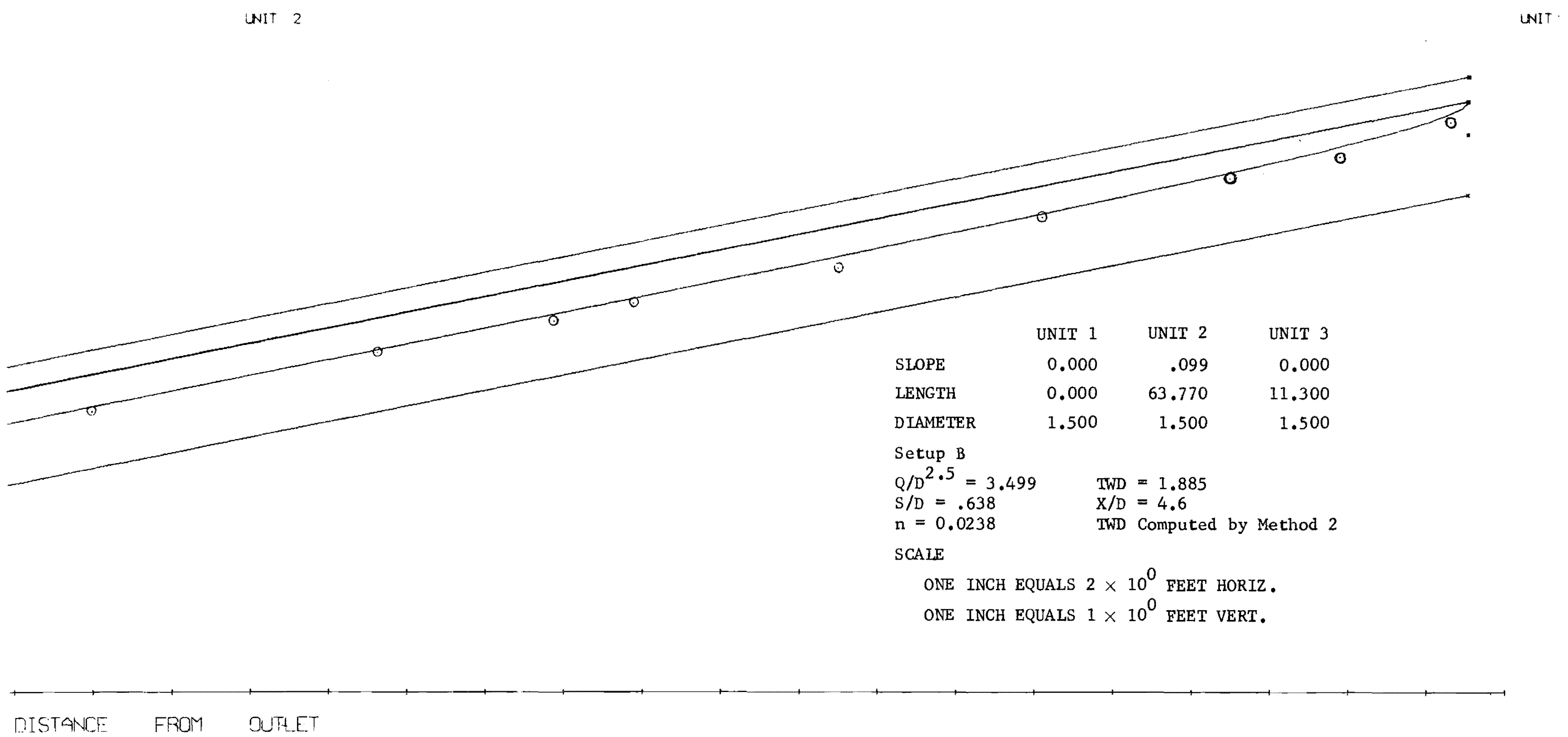

Figure 4-9. (Continued)

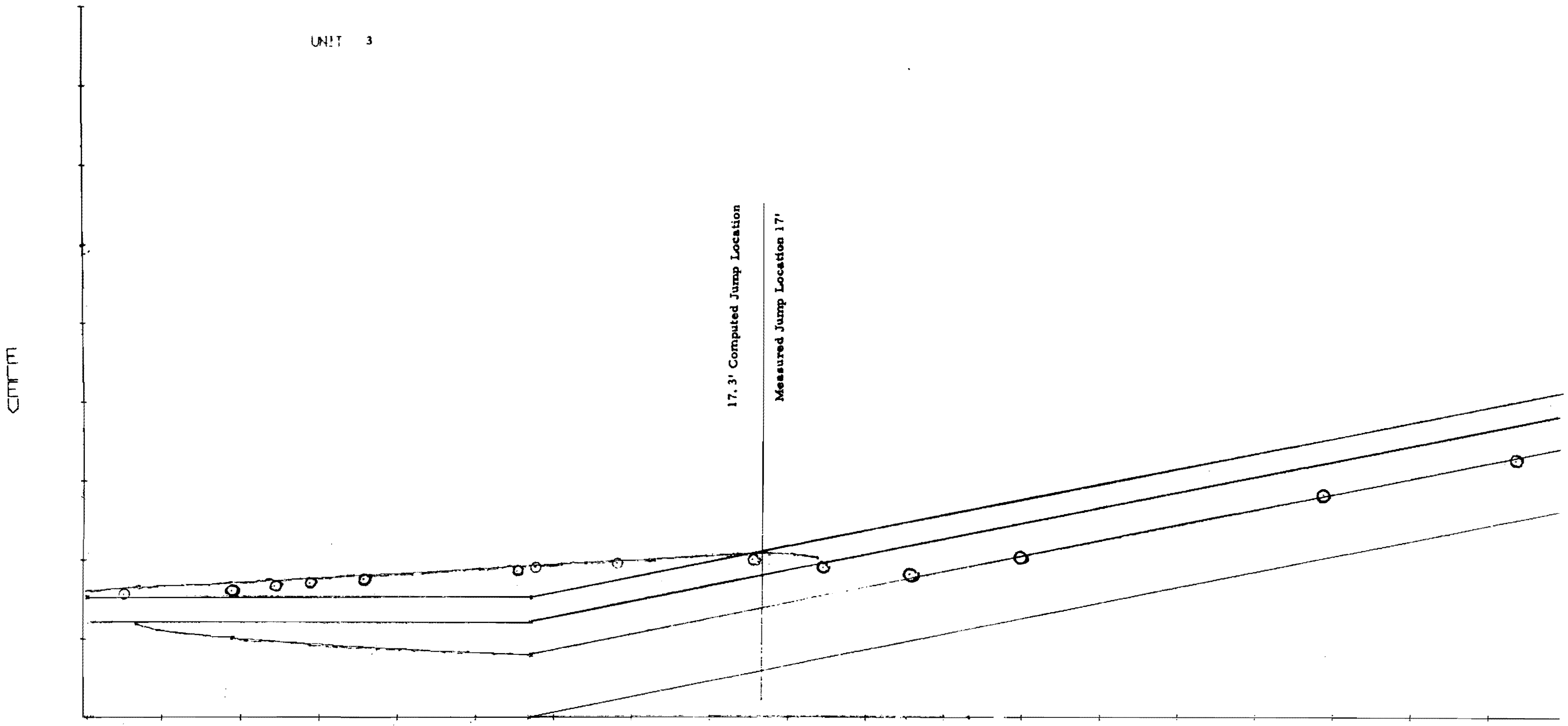

Figure 4-10. Measured and Computed Surface Profiles - Setup B (Continued)

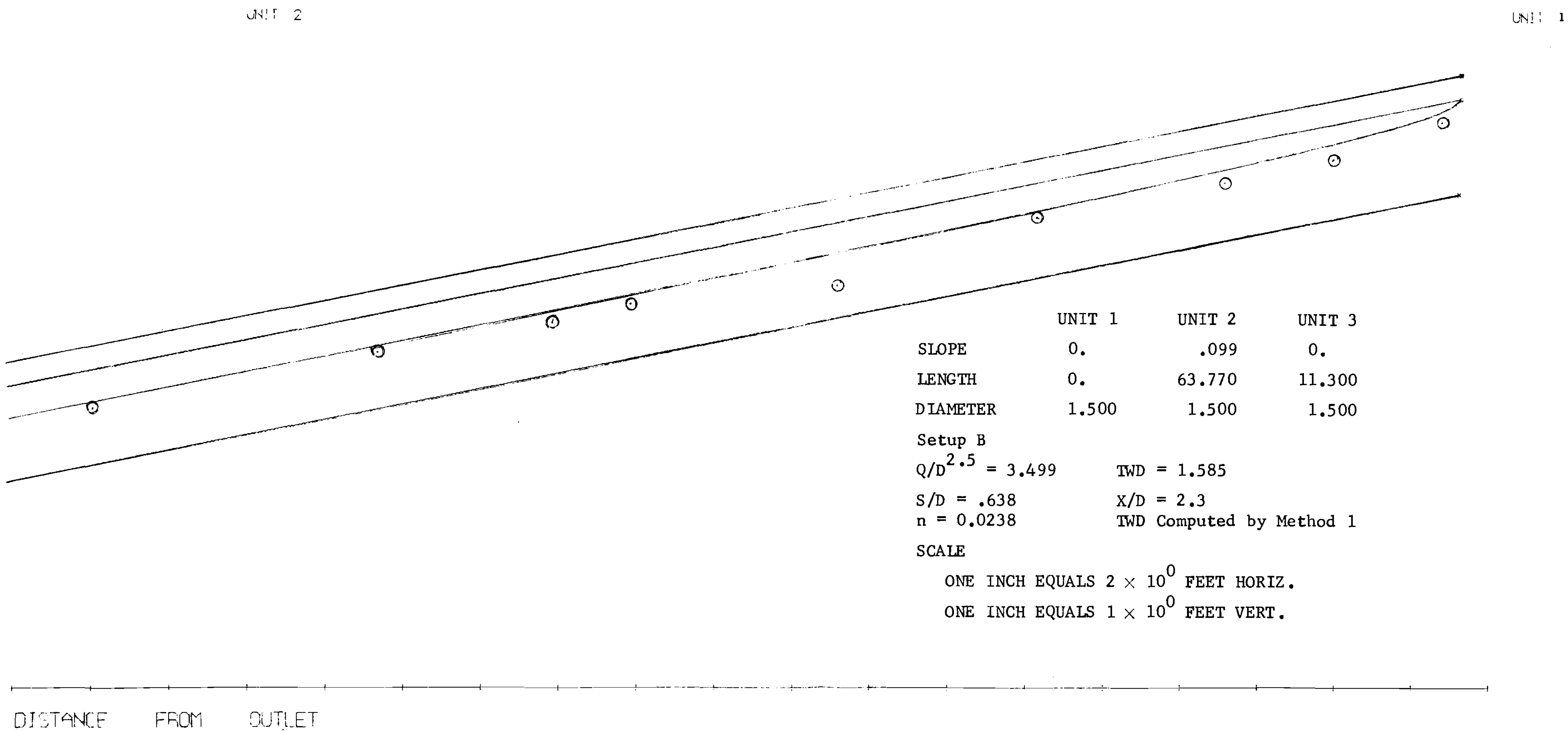

	UNIT 1	UNIT 2	UNIT 3
SLOPE	0.	.099	0.
LENGTH	0.	63.770	11.300
DIAMETER	1.500	1.500	1.500

Setup B

$Q/D^{2.5}$ = 3.499 TWD = 1.585

S/D = .638 X/D = 2.3

n = 0.0238 TWD Computed by Method 1

SCALE

ONE INCH EQUALS 2×10^0 FEET HORIZ.

ONE INCH EQUALS 1×10^0 FEET VERT.

Figure 4-10. (Continued)

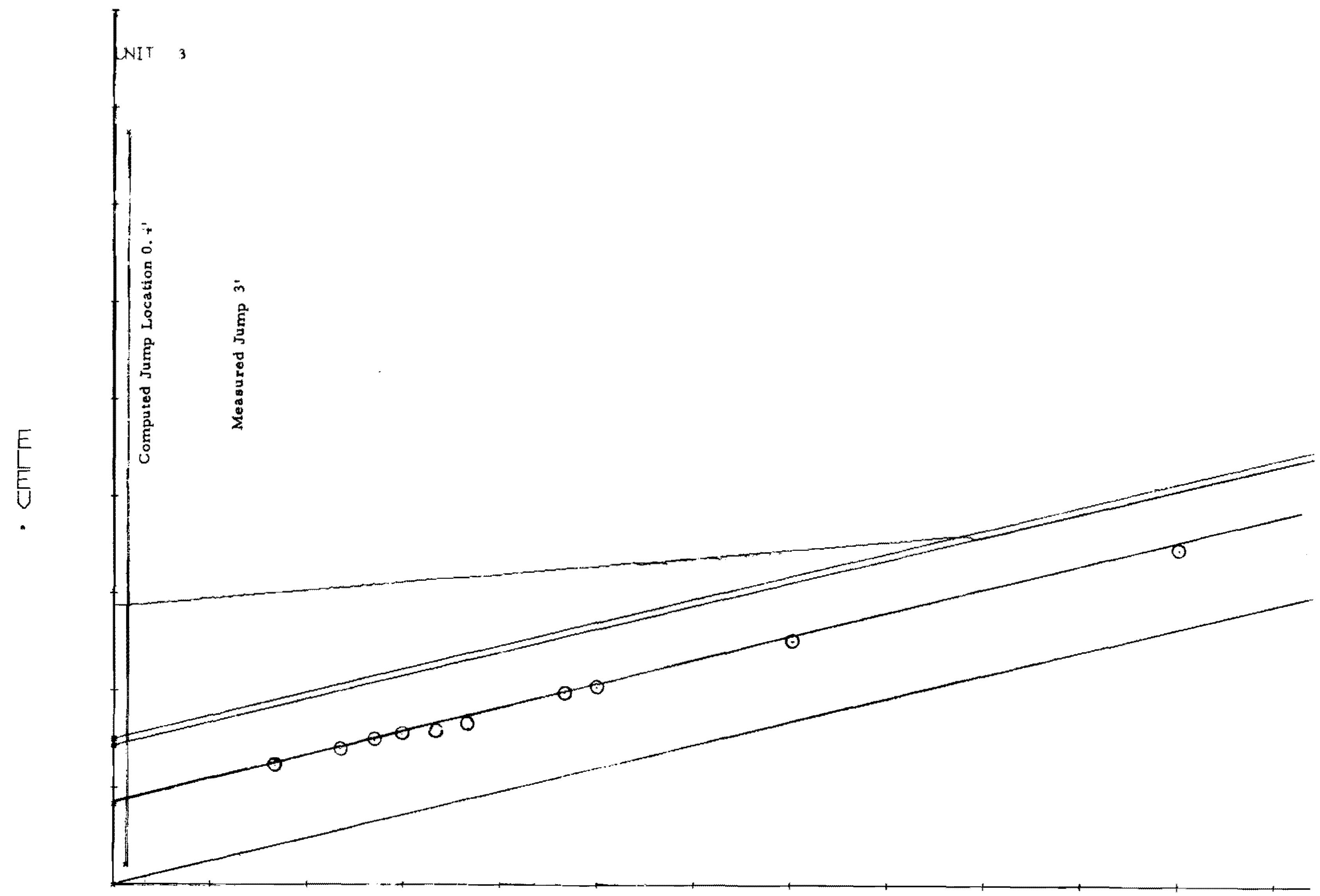

Figure 4-11. Measured and Computed Surface Profiles - Setup D

(Continued)

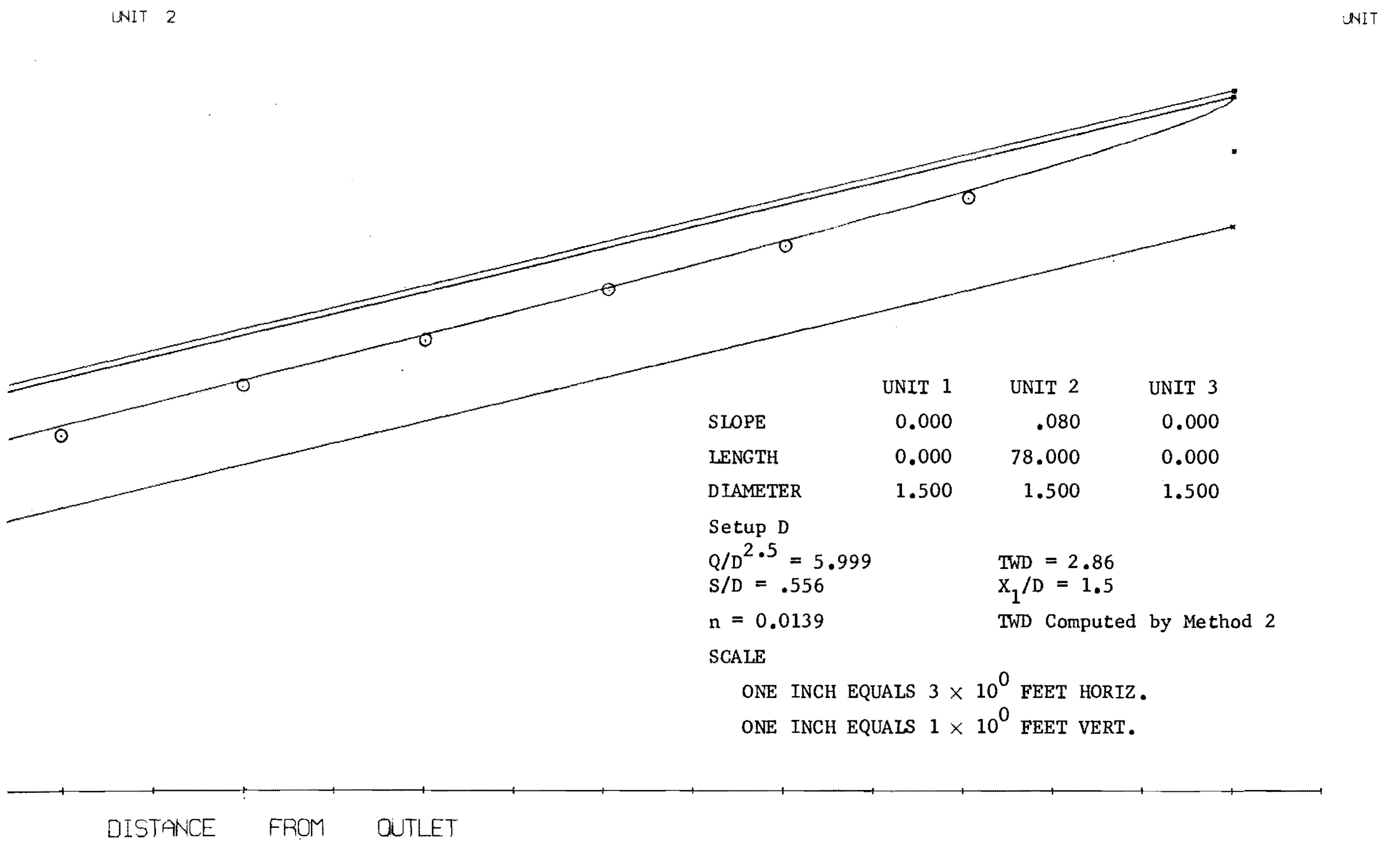

	UNIT 1	UNIT 2	UNIT 3
SLOPE	0.000	.080	0.000
LENGTH	0.000	78.000	0.000
DIAMETER	1.500	1.500	1.500

Setup D

$Q/D^{2.5} = 5.999$ TWD = 2.86

$S/D = .556$ $X_1/D = 1.5$

n = 0.0139 TWD Computed by Method 2

SCALE

ONE INCH EQUALS 3×10^0 FEET HORIZ.

ONE INCH EQUALS 1×10^0 FEET VERT.

Figure 4-11. (Continued)

flow profiles minor variations in the location of the critical depth section at the culvert inlet have been disregarded in the prediction of jump location.

Double Sill Tests on Corrugated Metal Pipe Model

In the tests described above studies of water surface profiles and jump locations were carried out with a single sill placed either at the mid-point or the end of the standard flared wing walls for Setups A, B and C. At the termination of these tests the study was reoriented to investigate the performance of two sills. These tests were begun with Setup C. The data from double sill tests with Setup C are summarized in Appendix A, Tables A-8 through A-11.

The following general procedure was followed in the selection of double sill arrangement. The height of the mid-sill, i.e., the sill nearest the culvert outlet was selected to force the jump inside the culvert. The second sill or end sill was then placed downstream of the mid-sill to form a pool to dissipate the energy of the nappe from the mid-sill and to distribute the flow uniformly to the downstream channel. The height of the second sill was selected by trial and was always lower than the mid-sill.

Data were collected to determine the effectiveness of two sills for producing uniform flow in the downstream channel by comparing their performance with the cases of (a) no sill, and (b) a single sill. Many double sill configurations were investigated over the full range of discharge to obtain the nine best combinations described in Figure 2-4. Depth profiles at Sections 8D and 11D downstream from the culvert outlet were measured for cases with (a) no sill, (b) a single sill, and (c) double sills. For each flow rate these profiles were compared to determine which produced the higher downstream channel depths and least severe velocity concentrations. These conditions were used as a measure of the performance of the various sill arrangements. A summary of these transverse depth profiles for the nine double sill configurations identified in Figure 2-4 are shown in Figures 4-12 through 4-15.

An evaluation of the variables affecting the double sill arrangements again is helpful at this point. In a manner similar to that used in Chapter III, the functional relationship between the variables is:

$$\bar{Y} = \phi[Q, \rho, g, D, X_1, \Delta X, s_1, s_2, n, B, L, \theta] \qquad (4\text{-}1)$$

where B is the channel width; $\bar{Y}$ is the average depth in the channel at a distance L from the culvert outlet; s_1 and s_2 are the heights of the mid and end sills respectively and ΔX is the distance between the sills. The rest of these variables are as defined in Figure 2-4. From dimensional analysis it is possible to group these variables in the following forms after setting the Manning's n, width, length and flare angle as constants for the tests.

$$\bar{Y}/D = \phi[Q/g^{0.5}D^{2.5}, X_1/D, \Delta X/D, s_1/D, s_2/D] \qquad (4\text{-}2)$$

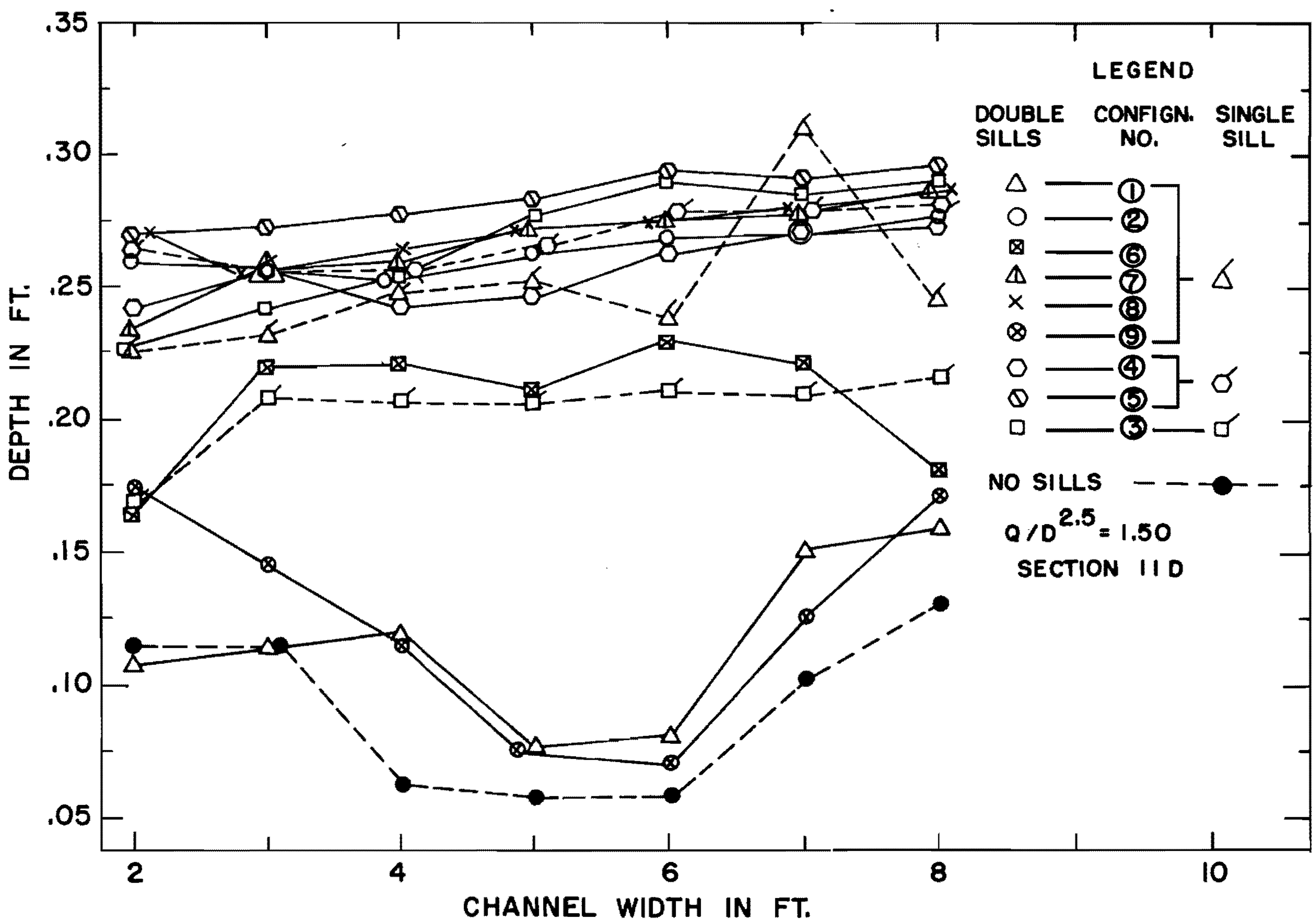

Figure 4-12. Depth Distributions for Different Sill Configurations

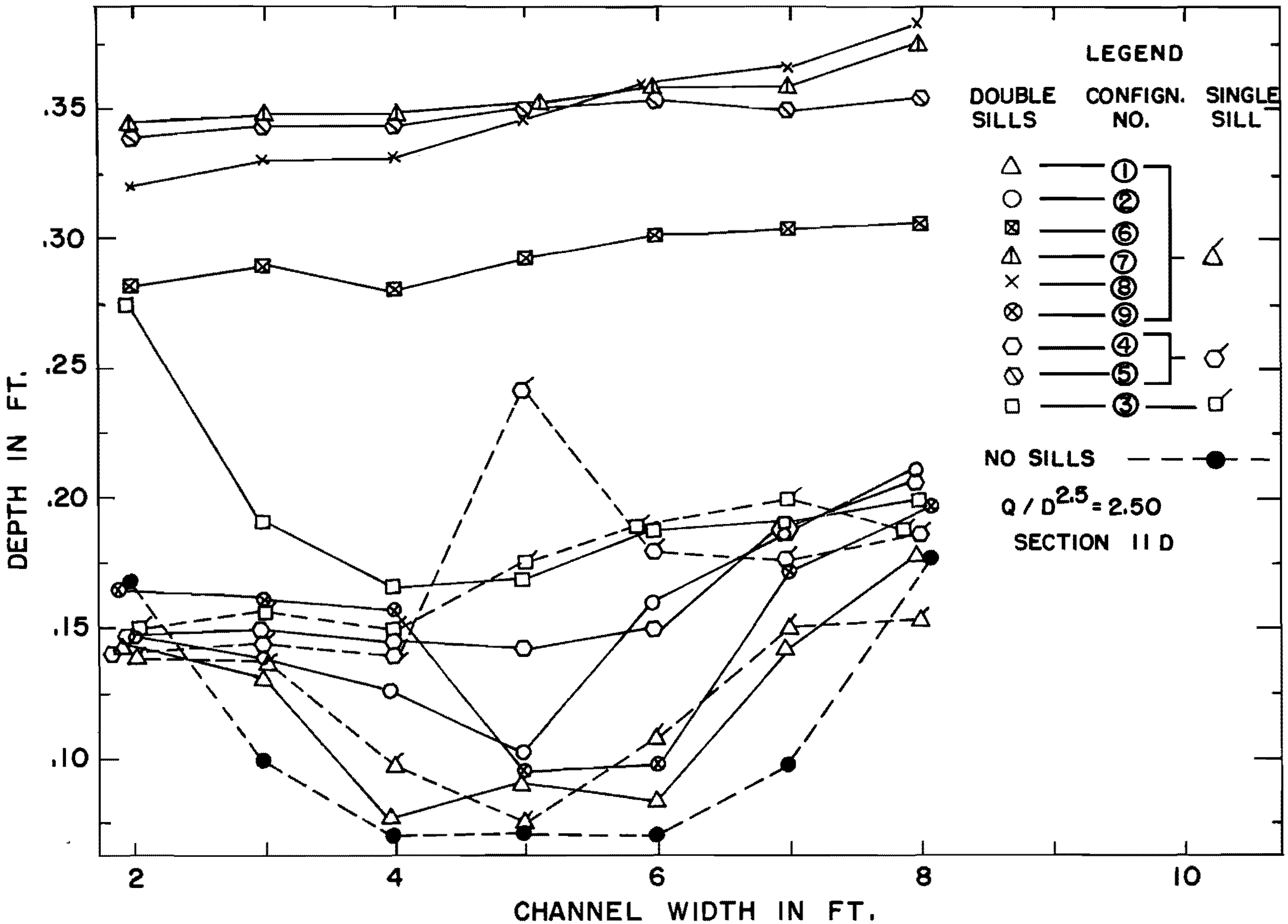

Figure 4-13. Depth Distributions for Different Sill Configurations

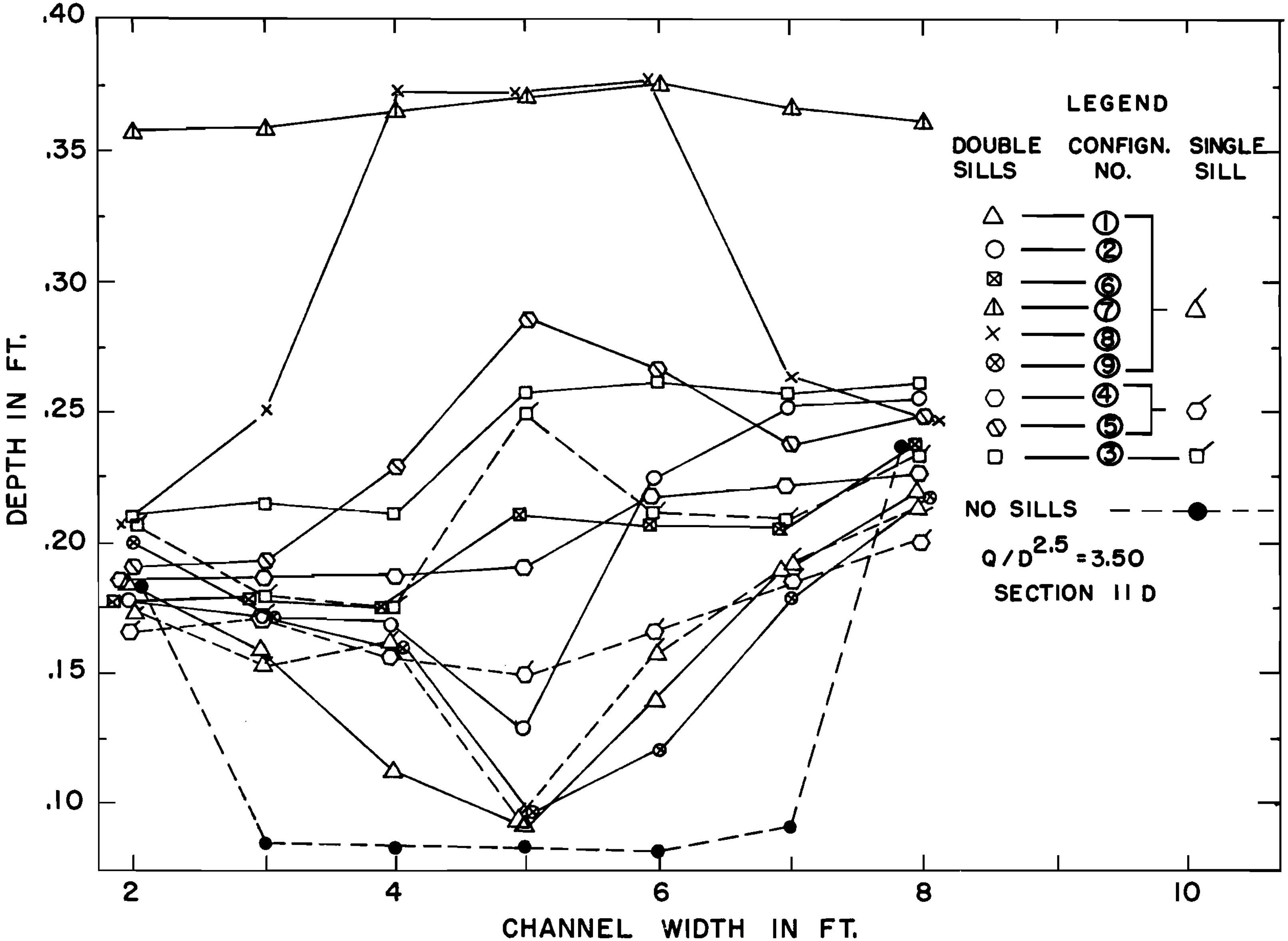

Figure 4-14. Depth Distributions for Different Sill Configurations

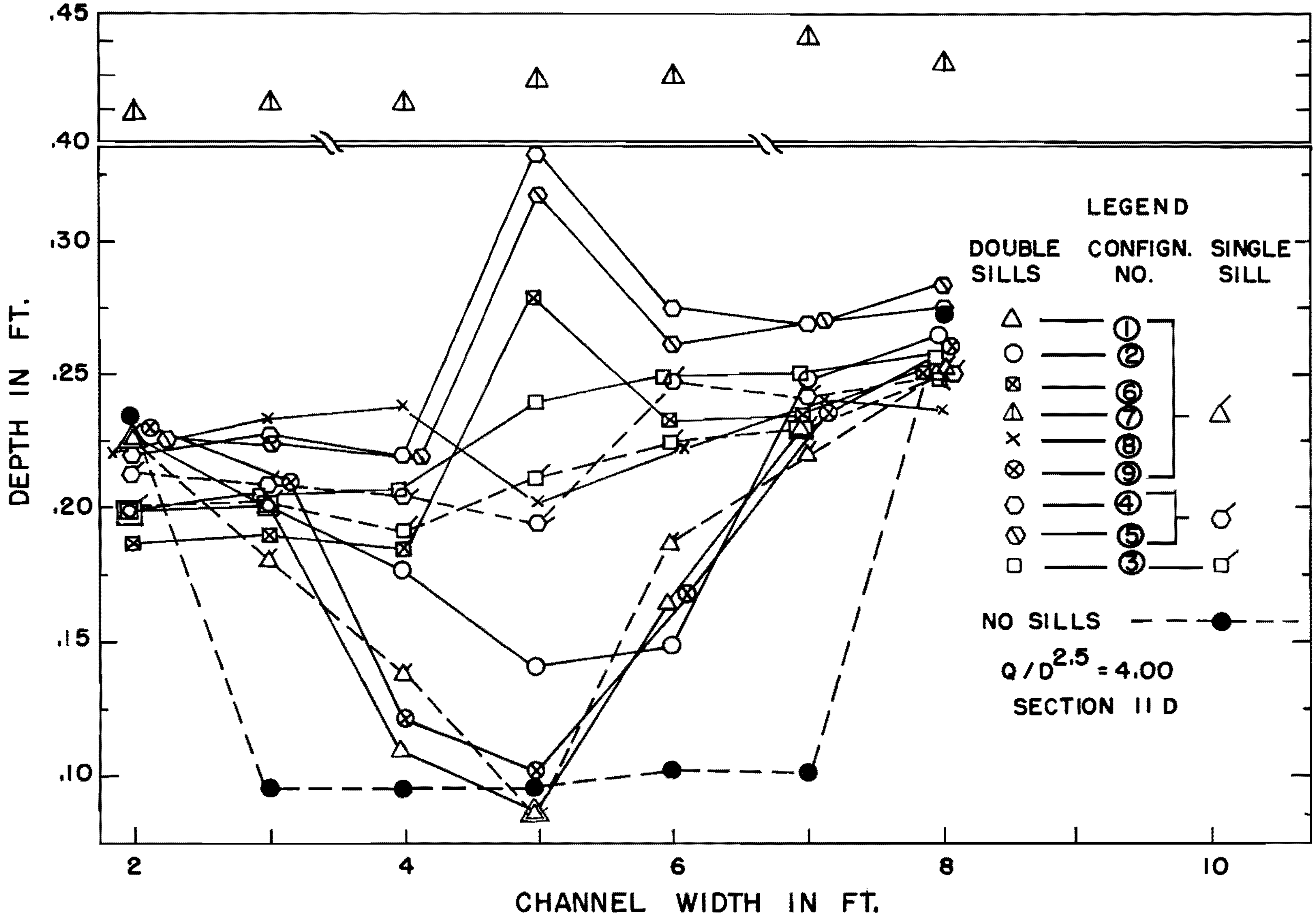

Figure 4-15. Depth Distribution for Different Sill Configurations

$$\bar{Y}/X_1 = \phi\,[Q/g^{0.5}D^{2.5},\ s_1/D,\ s_2/D,\ \Delta X/X_1] \tag{4-3}$$

All the significant geometrical features of the nine different double sill configurations used in Setup C are summarized in Table 4-3. The effect of the distance between sills, ΔX, on the downstream depth ($\bar{Y}$) is illustrated in Figure 4-16. Here the average relative depth is plotted against the relative sill spacing for specified values of the discharge ratio and mid and end sill heights. While the shape of the curve is affected by cross-waves and other disturbances in the downstream channel, the plot clearly shows that the average depth increases with increased spacing between sills. Also it is noted that for a given discharge factor large average depths can be produced closer to the culvert outlet by decreasing the height of the end sill, s_2.

Another set of plots, (Figures 4-17 and 4-18) relate the downstream depth in terms of culvert diameter and distance to the mid-sill to X_1/X_2. The curves show that as X_1/X_2 becomes smaller higher depths again are produced in the downstream channel. Figure 4-19 shows the relationship between the downstream depth and the ratio of sill heights s_1/s_2. Here it is seen that when the end sill is high the relative downstream depth is low indicating high velocities for a given discharge factor. As the height of the end sill is reduced, the downstream depth increases slightly and then becomes relatively insensitive to the relative sill height until a value of about 3.0 is reached beyond which the depths increase significantly. This

TABLE 4-3. GEOMETRY OF THE DOUBLE SILL CONFIGURATIONS

Double Sill No.	X_1 in Ft.	X_2 in Ft.	s_1 in Ft.	s_2 in Ft.	X_1/D	X_2/D	s_1/D	s_2/D	ΔX	$\Delta X/D$	s_1/s_2	$\Delta X/X_1$	s_1/X_1	X_1/X_2
1	1.00	2.00	0.75	0.50	0.667	1.333	0.500	0.333	1.00	0.667	1.50	1.00	0.750	0.500
2	1.00	3.45	0.75	0.50	0.667	2.300	0.500	0.333	2.45	1.633	1.50	2.45	0.750	0.289
3	3.45	6.90	0.96	0.50	2.300	4.600	0.638	0.333	3.45	2.300	1.92	1.00	0.378	0.500
4	2.25	4.50	0.83	0.50	1.500	3.000	0.556	0.333	2.25	1.500	1.67	1.00	0.370	0.500
5	2.25	4.50	0.83	0.25	1.500	3.000	0.556	0.167	2.25	1.500	3.33	1.00	0.370	0.500
6	1.00	6.90	0.75	0.50	0.667	4.600	0.500	0.333	5.90	3.933	1.50	5.90	0.750	0.145
7	1.00	6.90	0.75	0.25	0.667	4.600	0.500	0.167	5.90	3.933	3.00	5.90	0.750	0.145
8	1.00	4.50	0.75	0.25	0.667	3.000	0.500	0.167	3.50	2.333	3.00	3.50	0.750	0.222
9	1.00	2.00	0.75	0.25	0.667	1.333	0.500	0.167	1.00	0.667	3.00	1.00	0.750	0.500

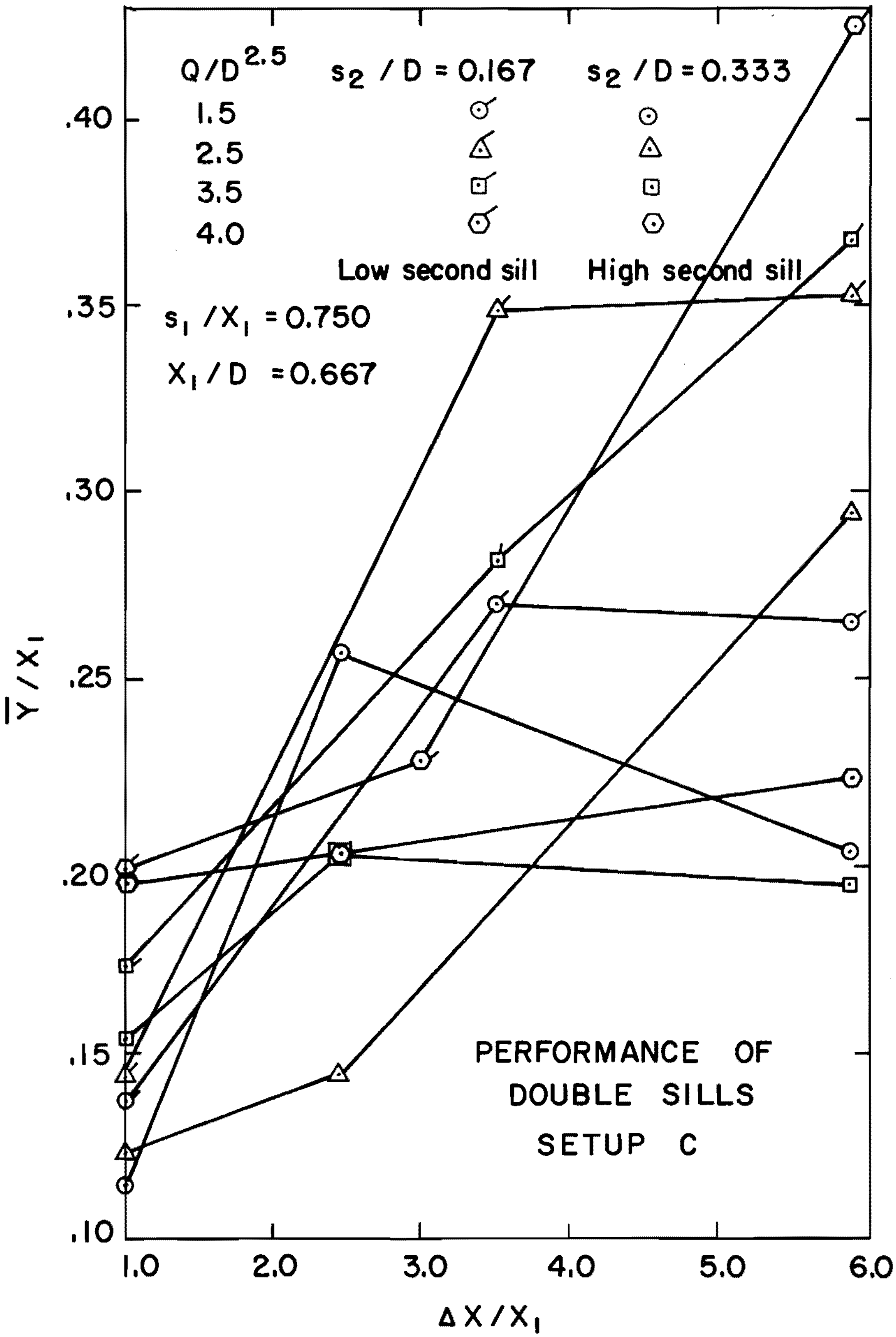

Figure 4-16. Downstream Channel Depth Variation with Relative Sill Spacing

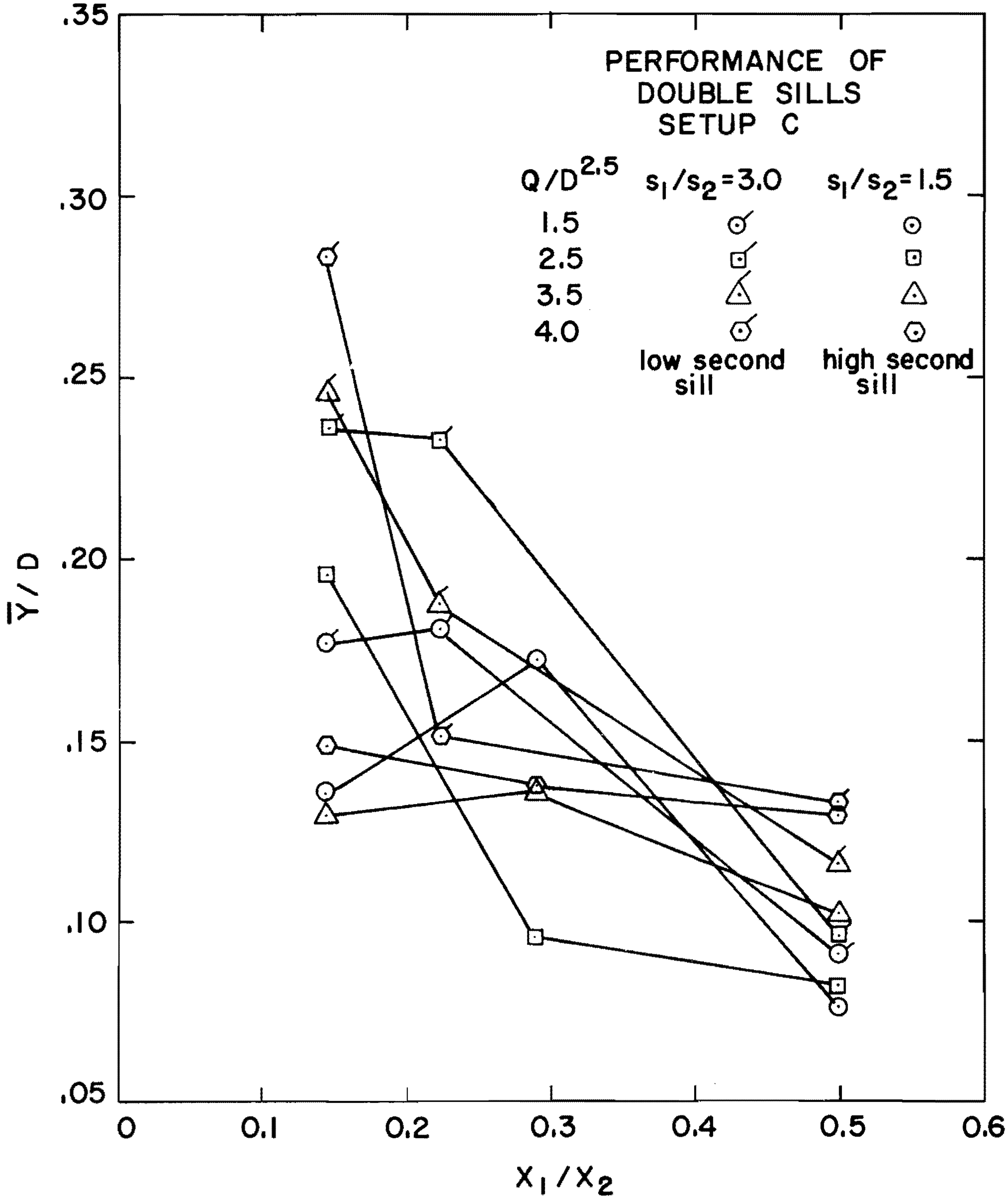

Figure 4-17. Downstream Channel Depth Variation with the Ratio of Sill Locations

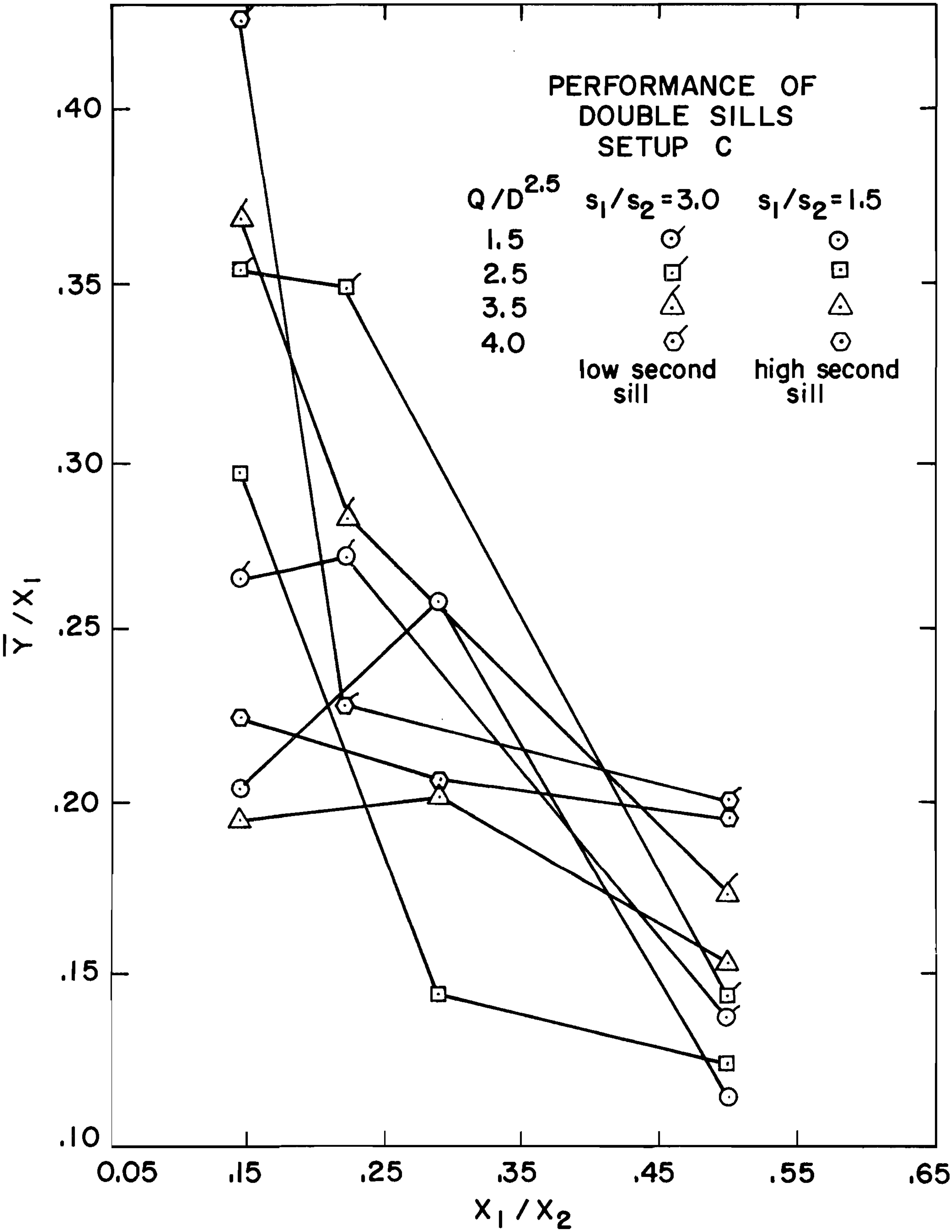

Figure 4-18. Downstream Channel Depth Variation with the Ratio of Sill Locations

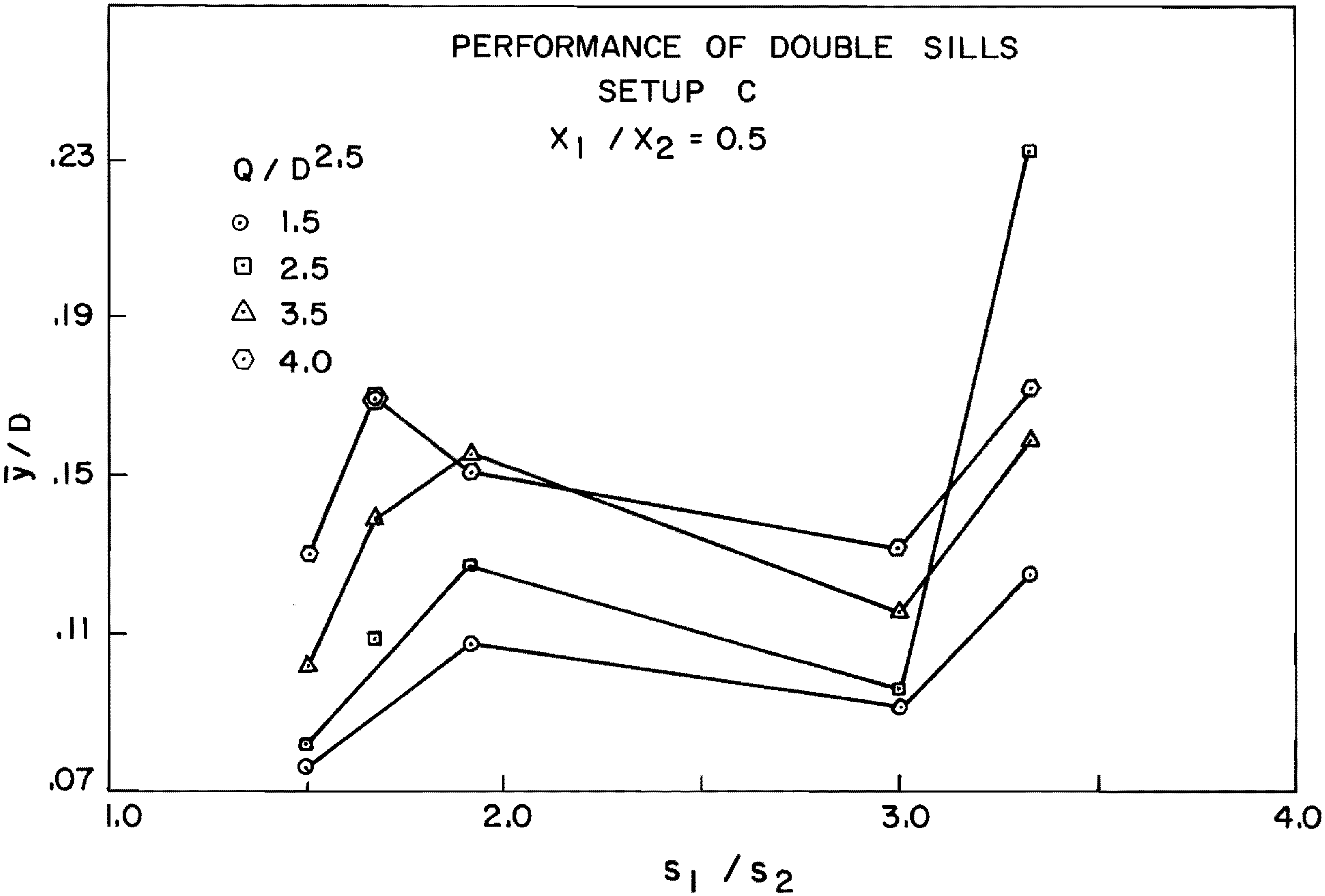

Figure 4-19. Downstream Channel Depth Variation with Ratio of Sill Heights

trend, however, would not be expected to continue because as the end sill is reduced further the pool available for dissipating energy of the falling nappe becomes very shallow and hence the effectiveness of the end sill is minimized.

The above curves are not intended to be design graphs but rather are attempts to present the extensive depth profile data collection in this study in condensed graphical form. An examination of the transverse depth profiles produced by the nine best double sill configurations under different flow ratios is perhaps the most meaningful method for selecting a desirable double sill configuration. These data show that the most desirable positioning of the two sills corresponds to a low end sill and a large spacing between the sills. The increase in spacing, ΔX, results in a larger pool for energy dissipation while a low end sill reduces the head produced upstream of the second sill. It is primarily this head and its even distribution across the end sill that determines the uniformity of the downstream flow conditions. Another useful plot of the experimental data of the double sill configurations is Figure 4-20 which shows the relationship between the downstream Froude number and the discharge factor for the nine different double sill configurations together with the corresponding single sill and no sill configurations. The downstream Froude number is computed from the average depth obtained from measurements across the width of the downstream channel at a Section 11D from the culvert outlet. Obviously,

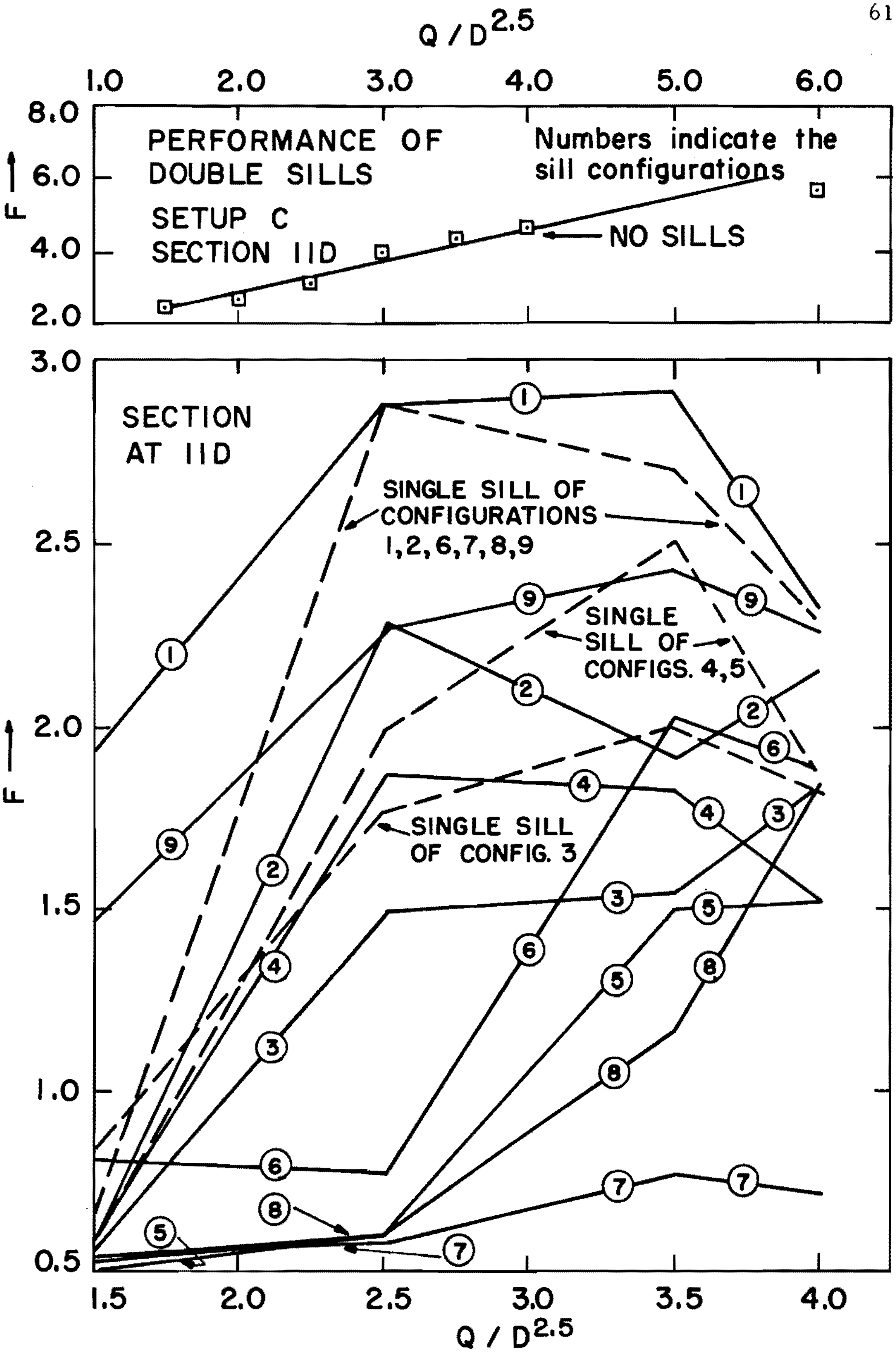

Figure 4-20. Relationship between Channel and Pipe Froudian Numbers for Different Sill Configurations

a desirable sill configuration should produce low Froude numbers in the downstream channel near the wing walls. Figure 4-20 shows this condition is best achieved by sill configurations Nos. 7, 8 and 5 in that order. Although sill arrangement No. 7 is clearly better than either 8, or 5, it requires that the standard wing walls be lengthened to accomodate the location of the end sill. If it is not possible to lengthen the wing walls, then either configurations Nos. 8 or 5 must be used. In the case of configuration No. 8, the mid-sill is quite close to the culvert outlet and produces a large amount of spray and occasional over topping of the wing walls. Consequently, if this configuration is selected, the height of the wing walls must be increased. Although configuration No. 5 would not require changes to the standard wing walls, it does compromise the sill performance in the downstream channel.

Tables 4-4 and 4-5 summarize the results obtained from the double sill tests on Setup C. Average flow depths at distances 8D and 11D downstream of the culvert outlet are tabulated for each discharge factor and double sill configuration together with the corresponding cases with single sill and no sill. Table 4-6 summarizes the percent reduction in total energy provided by the various sill configurations relative to the total energy for the case of no sill. It can be noted in Table 4-6, that the percent energy reduction again is constantly higher for configurations Nos. 7, 8 and 5. It may also be noted that the percent reduction is higher at Section 8D than 11D. This, however, is expected since the relative differences in the

TABLE 4-4. SUMMARY OF RESULTS ON DOUBLE SILL PERFORMANCE

TESTS (Test Section at 11D)

$Q/D^{2.5} = 1.5$			$Q/D^{2.5} = 2.5$			$Q/D^{2.5} = 3.5$			$Q/D^{2.5} = 4.0$			Sill Con-fign. No.
$\bar{Y}$ In Ft.	H In Ft.	F In Ft.	$\bar{Y}$ In Ft	H In Ft	F In Ft	$\bar{Y}$ In Ft	H In Ft	F In Ft	$\bar{Y}$ In Ft	H In Ft	F In Ft	
.233	.285	0.67	.123	.637	2.89	.161	.748	2.70	.198	.703	2.26	1S.S.*
.144	.329	1.94	.123	.637	2.89	.153	.801	2.92	.195	.717	2.32	1
.258	.300	0.57	.144	.517	2.28	.203	.574	1.91	.205	.677	2.15	2
.204	.271	0.81	.295	.385	0.78	.195	.597	2.03	.224	.621	1.88	6
.265	.305	0.55	.354	.416	0.59	.368	.480	0.78	.426	.536	0.72	7
.271	.309	0.53	.349	.413	0.61	.282	.475	1.17	.228	.610	1.83	8
.137	.286	1.48	.144	.517	2.28	.173	.682	2.43	.199	.700	2.25	9
.264	.304	0.55	.157	.471	2.00	.170	.699	2.50	.225	.619	1.87	4S.S.*
.254	.297	0.59	.164	.453	1.88	.209	.560	1.83	.256	.559	1.54	4
.282	.317	0.50	.349	.413	0.61	.238	.507	1.50	.258	.556	1.52	5
.200	.270	0.83	.169	.439	1.70	.197	.591	2.00	.230	.604	1.81	3S.S.*
.260	.301	0.56	.190	.405	1.50	.234	.513	1.54	.227	.613	1.85	3
.095	.404	2.55	.115	.703	3.20	.117	1.227	4.35	.121	1.470	4.74	No Sills

*S.S. - Single Sill; Note that sill configurations 1, 2, 6, 7, 8 and 9 have common single sill and configurations 4 and 5 have again a common single sill.

H = Total energy at Section 11D.

F = Froude's Number of the channel at Section 11D.

TABLE 4-5. SUMMARY OF RESULTS ON DOUBLE SILL PERFORMANCE TESTS

$Q/D^{2.5} = 1.5$			$Q/D^{2.5} = 2.5$			$Q/D^{2.5} = 3.5$			$Q/D^{2.5} = 4.0$			Designation of the Double Sill Configuration
Y	F	H	Y	F	H	Y	F	H	Y	F	H	
.092	2.68	.423	.094	4.32	.969	.112	4.67	1.332	.126	4.46	1.376	1 S.S.*
.082	3.24	.506	.091	4.54	1.024	.120	4.19	1.170	.158	3.17	.951	1
.248	0.60	.293	.117	3.10	.680	.181	2.27	0.646	.176	2.70	.819	2
.189	0.91	.267	.292	0.79	.383	.148	3.12	0.865	.179	2.64	.799	6
.257	0.57	.299	.355	0.59	.417	.324	0.94	.469	.251	1.58	.565	7
.235	0.66	.285	.156	2.02	.472	.209	1.83	.559	.174	2.74	.829	8
.100	2.36	.379	.097	4.10	.921	.127	3.86	1.072	.170	2.84	.836	9
.107	2.13	.350	.131	2.63	.583	.135	3.52	.970	.215	2.00	.643	4 S.S.
.111	2.02	.337	.137	2.45	.549	.202	1.92	.576	.213	2.03	.649	4
.275	0.52	.312	.186	1.55	.409	.232	1.56	.514	.235	1.75	.593	5
.103	2.26	.367	.134	2.54	.568	.156	2.84	.782	.217	1.97	.637	3 S.S.
.206	0.80	.272	.143	2.30	.521	.196	2.01	.592	.145	3.62	1.090	3
.068	4.46	.674	.078	5.70	1.348	.099	5.60	1.649	.110	5.44	1.740	No Sills

*S.S. - Single Sills. Note that sill configurations 1, 2, 6, 7, 8, and 9 have common single sill and configurations 4 and 5 have again a common single sill.

H = Total energy at Section 8D.

F = Froude's number of the channel at Section 8D.

TABLE 4-6. PERCENTAGE REDUCTION IN THE TOTAL ENERGY BY THE USE OF DOUBLE SILLS

Sill Confign. No.	Percentage Difference in Total Energy Levels Between the 'No Sill' and 'With Sill' Cases ($\Delta H/H_o$)*							
	SECTION AT 11D				SECTION AT 8D			
	$Q/D^{2.5}$ VALUES				$Q/D^{2.5}$ VALUES			
	1.5	2.5	3.5	4.0	1.5	2.5	3.5	4.0
1	18.6	9.4	34.7	51.2	24.8	24.1	29.2	45.3
2	25.8	26.5	53.2	54.0	56.2	49.6	60.6	52.9
6	33.0	45.3	51.3	57.8	60.2	71.6	47.6	54.1
7	24.6	40.8	60.8	63.6	55.4	69.2	71.6	67.5
8	23.6	41.3	61.3	58.6	57.4	65.1	66.2	52.3
9	29.3	26.5	44.4	52.4	43.5	31.7	35.1	51.9
4	26.5	35.6	54.4	62.0	49.2	59.4	65.0	62.7
5	21.6	41.3	58.6	62.2	53.6	69.8	68.8	66.0
3	25.6	42.4	58.2	58.3	59.6	61.4	64.2	37.4
1 S.S.	29.5	9.4	39.0	52.2	37.3	28.2	19.3	20.9
4 S.S.	24.8	33.0	43.0	57.8	48.0	56.7	41.2	63.1
3 S.S.	33.2	37.6	51.8	58.3	45.5	57.9	52.7	63.4

* ΔH = Difference is total energy at a given Section (8D or 11D) between the cases of 'No Sills' and 'With Sills'.

H_o = Total energy at a given section for the case of 'No Sill' situation.

performance of the various double sill patterns are more pronounced near the culvert outlet. On the other hand, it is recognized that measurements made near the culvert outlet, i.e., at 8D, are more susceptible to error than corresponding measurements made further downstream.

Double Sill Tests on Concrete Pipe Models

All results on the performance of double sills presented above were obtained with a corrugated metal pipe culvert (Setup C). Based on these results it was found that extensive testing with the concrete pipe models was not required. A few trial runs indicated, however, that the selected double sill configurations for corrugated metal pipe models were not necessarily suitable for the concrete pipe models.

Rather it was found that the relative spacing of sills (ΔX) needed to be increased in order to dissipate the energy of higher velocity flows obtained with two concrete pipe models. Accordingly the best double sill configuration for the concrete pipe corresponds to the following dimensions: $X_1 = 1.5D$, $X_2 = 4.6D$, $s_2 = 0.167D$ with the mid-sill height varying between 0.5D and 0.556D depending upon the setup. The data from the concrete pipe Setups D to G are summarized in Appendix A, Tables A-12 through A-26.

To illustrate the performance of double sills with the concrete pipe, transverse depth and velocity profiles were again measured for representative discharge factors and different culvert geometries. These data shown in Figures 4-21 through 4-31 indicate that sills produce a consistent and marked increase in depths (corresponding to reduction in velocities) at Sections 8D and 11D downstream of the culvert outlet. The relative performances of double sills together with the 'no sill' case are summarized in Table 4-7 which also includes corresponding energy levels in the downstream channel. Table 4-7 shows an average energy reduction of 73% at Section 11D if sills are used. This percentage reduction is indicative of the effectiveness of the sills. Furthermore, the percent energy change between the upstream section of the hydraulic jump and the 11D section was found to be about 86% on average although this energy change varied with the culvert configuration and the discharge factor.

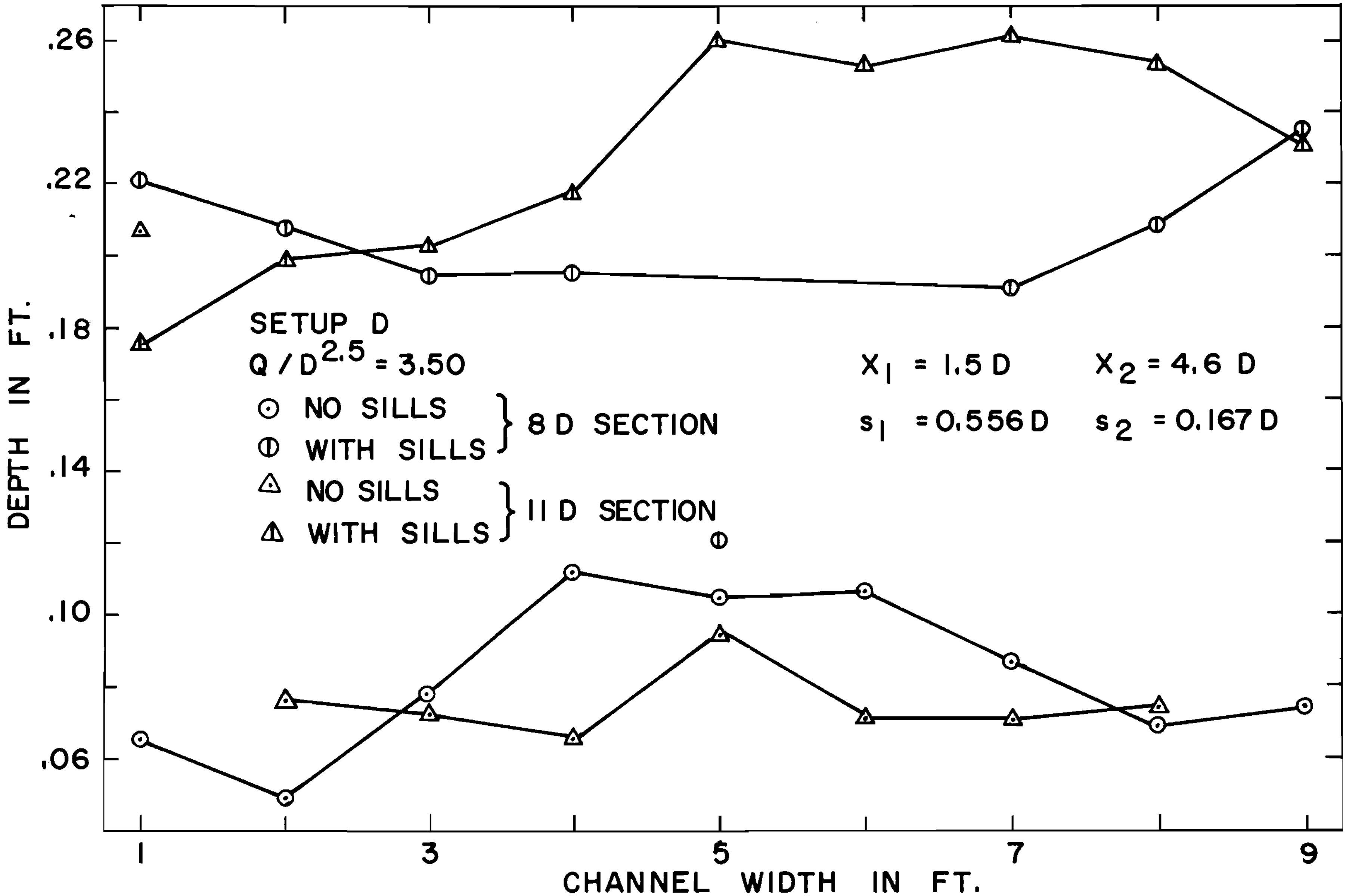

Figure 4-21. Downstream Channel Transverse Depth Profiles

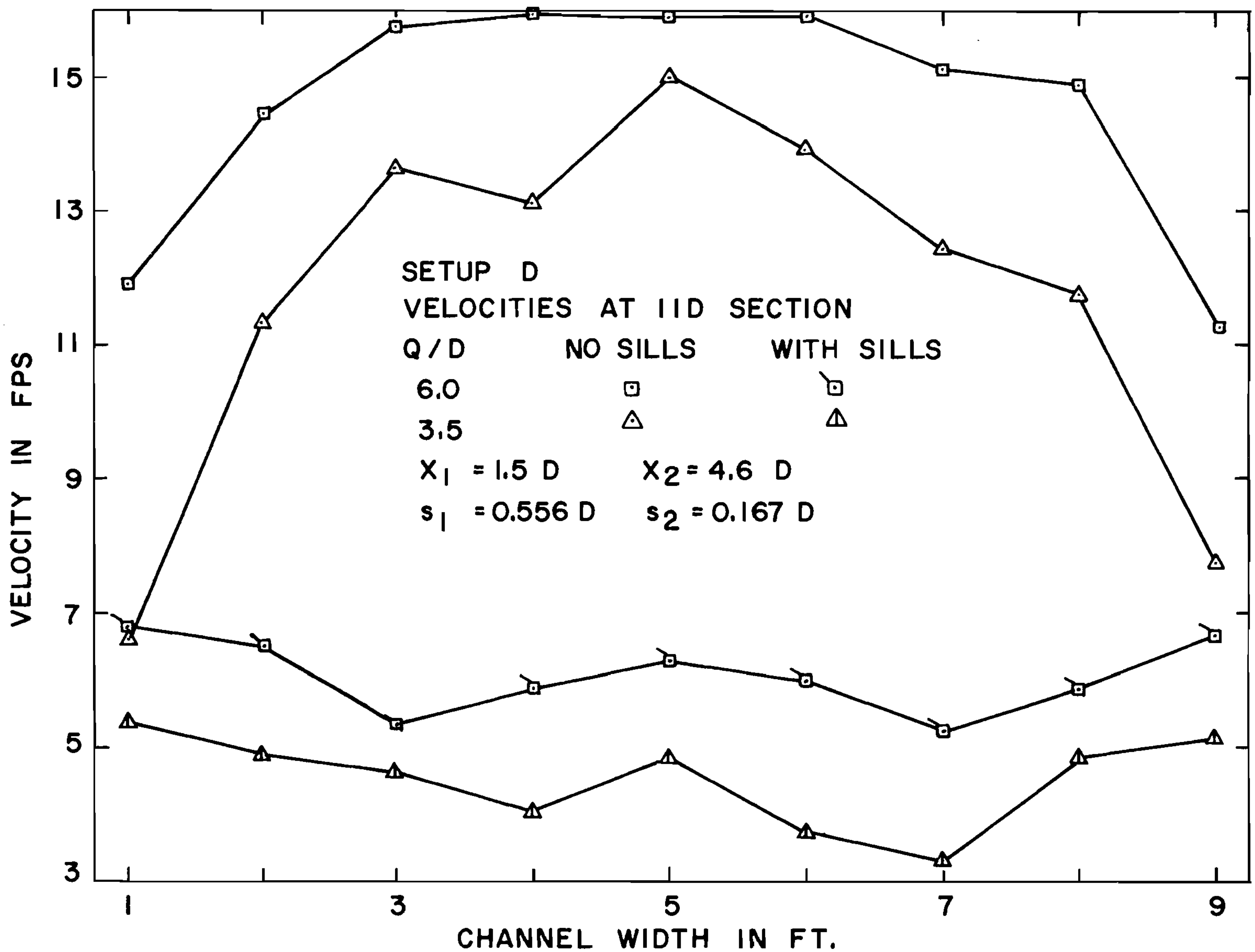

Figure 4-22. Downstream Channel Transverse Velocity Profiles

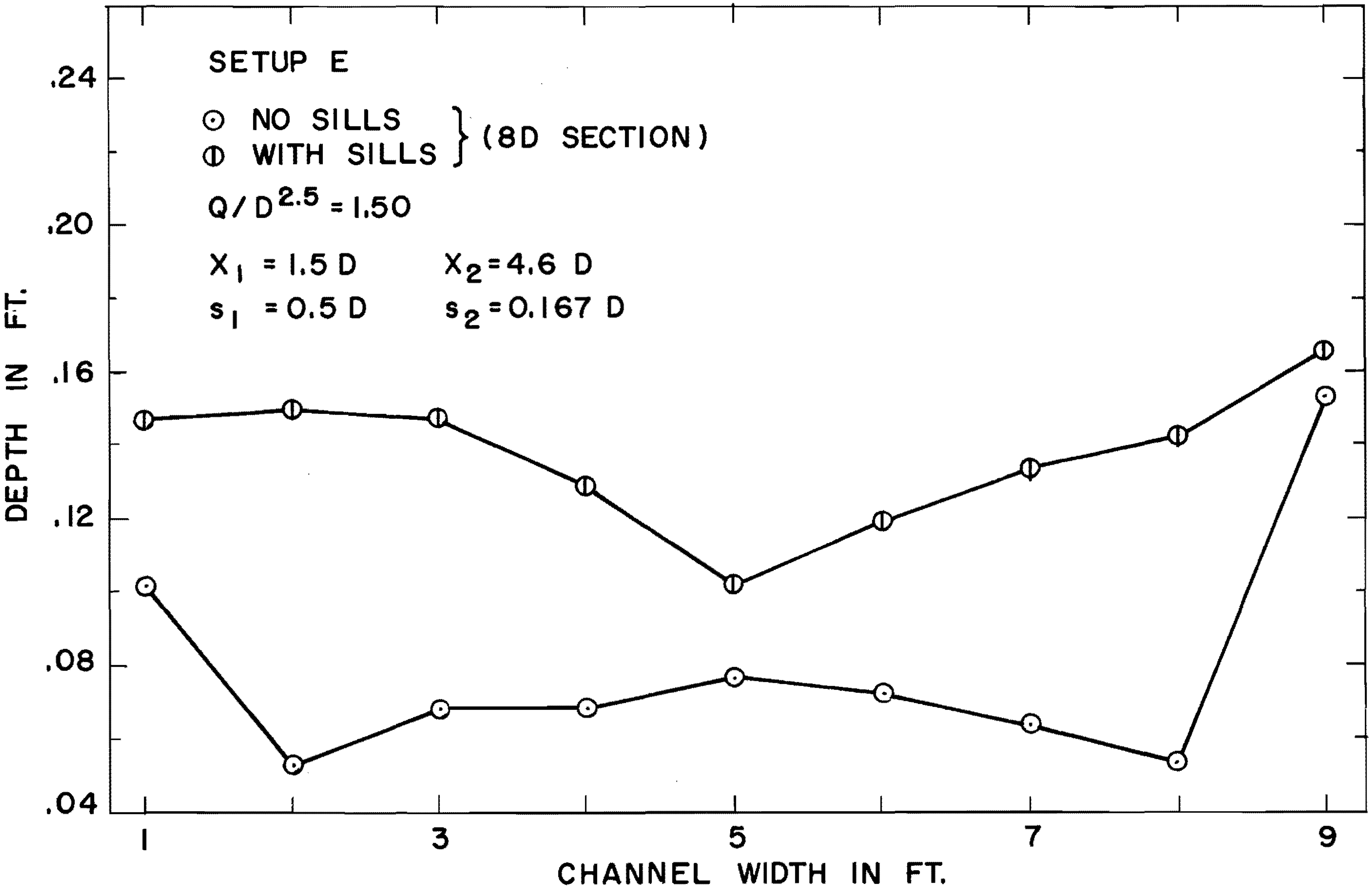

Figure 4-23. Downstream Channel Transverse Depth Profiles

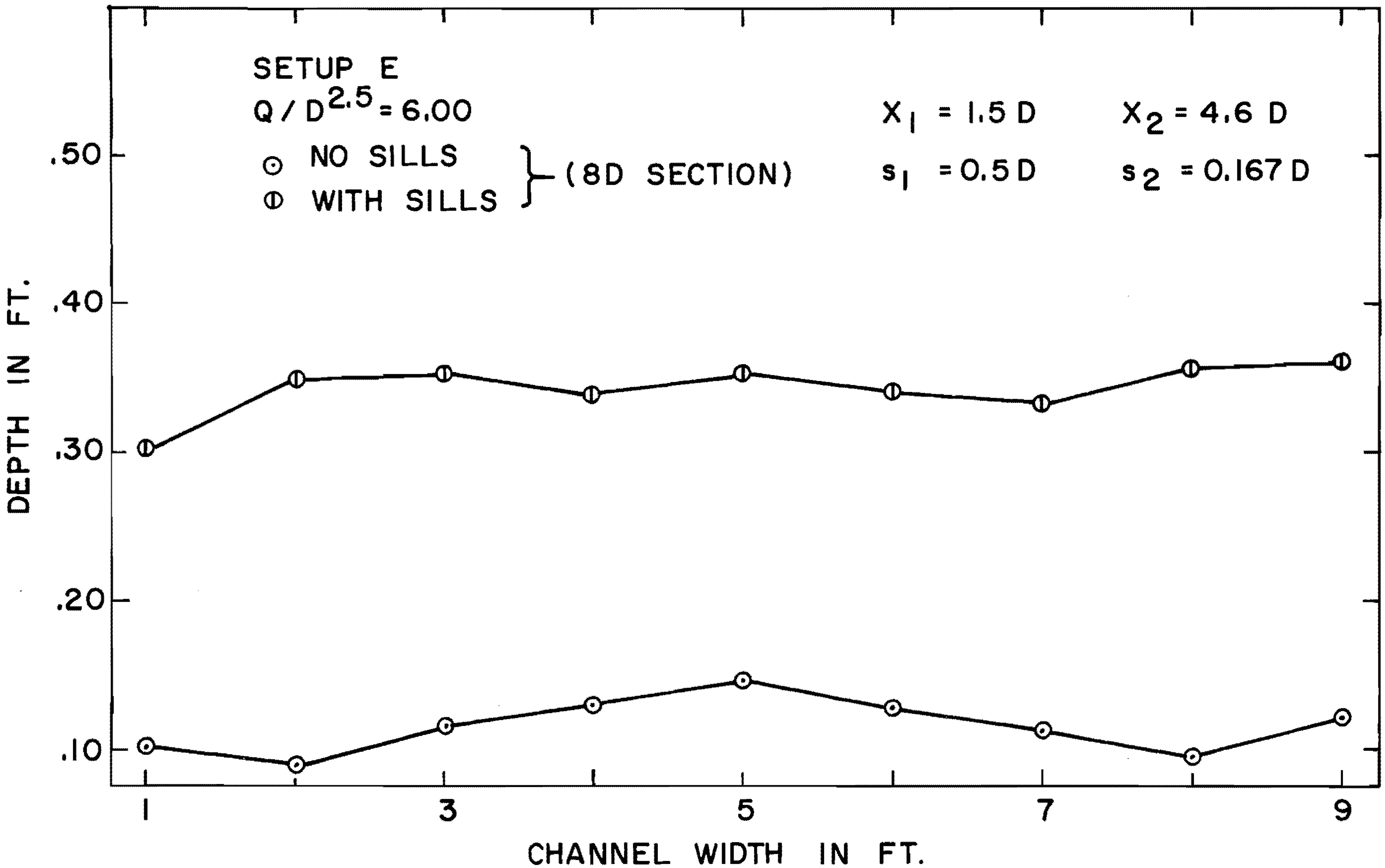

Figure 4-24. Downstream Channel Transverse Depth Profiles

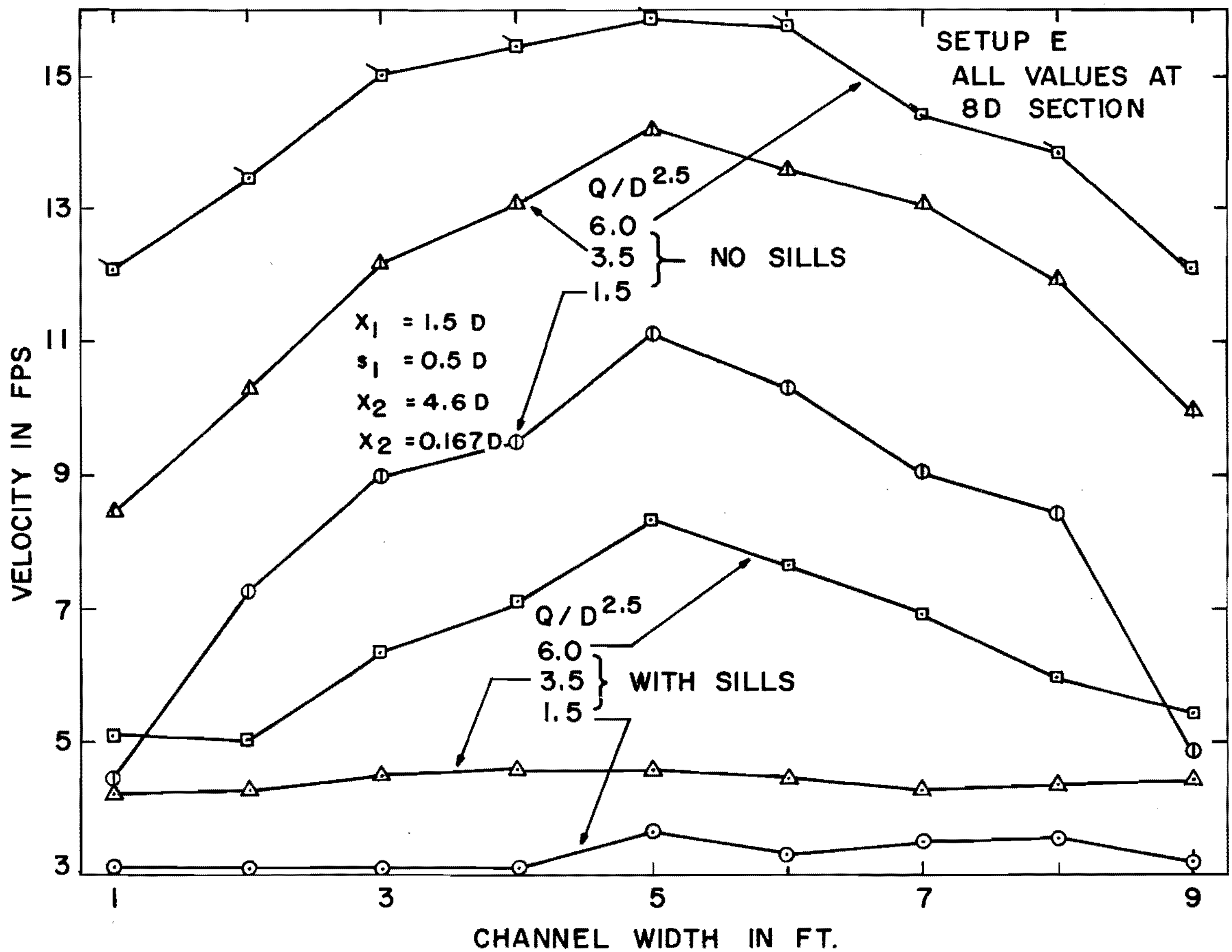

Figure 4-25. Downstream Channel Transverse Velocity Profiles

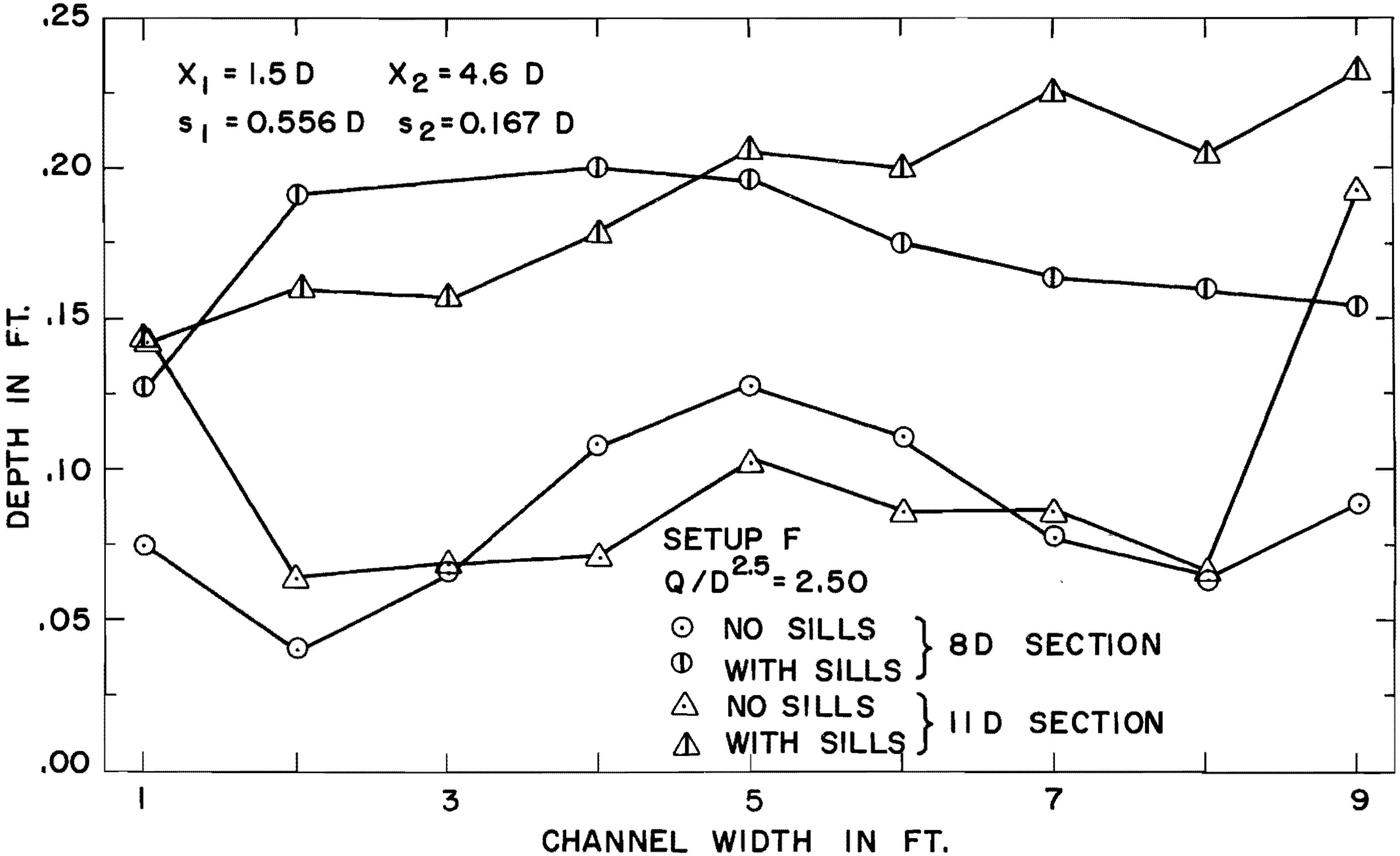

Figure 4-26. Downstream Channel Transverse Depth Profiles

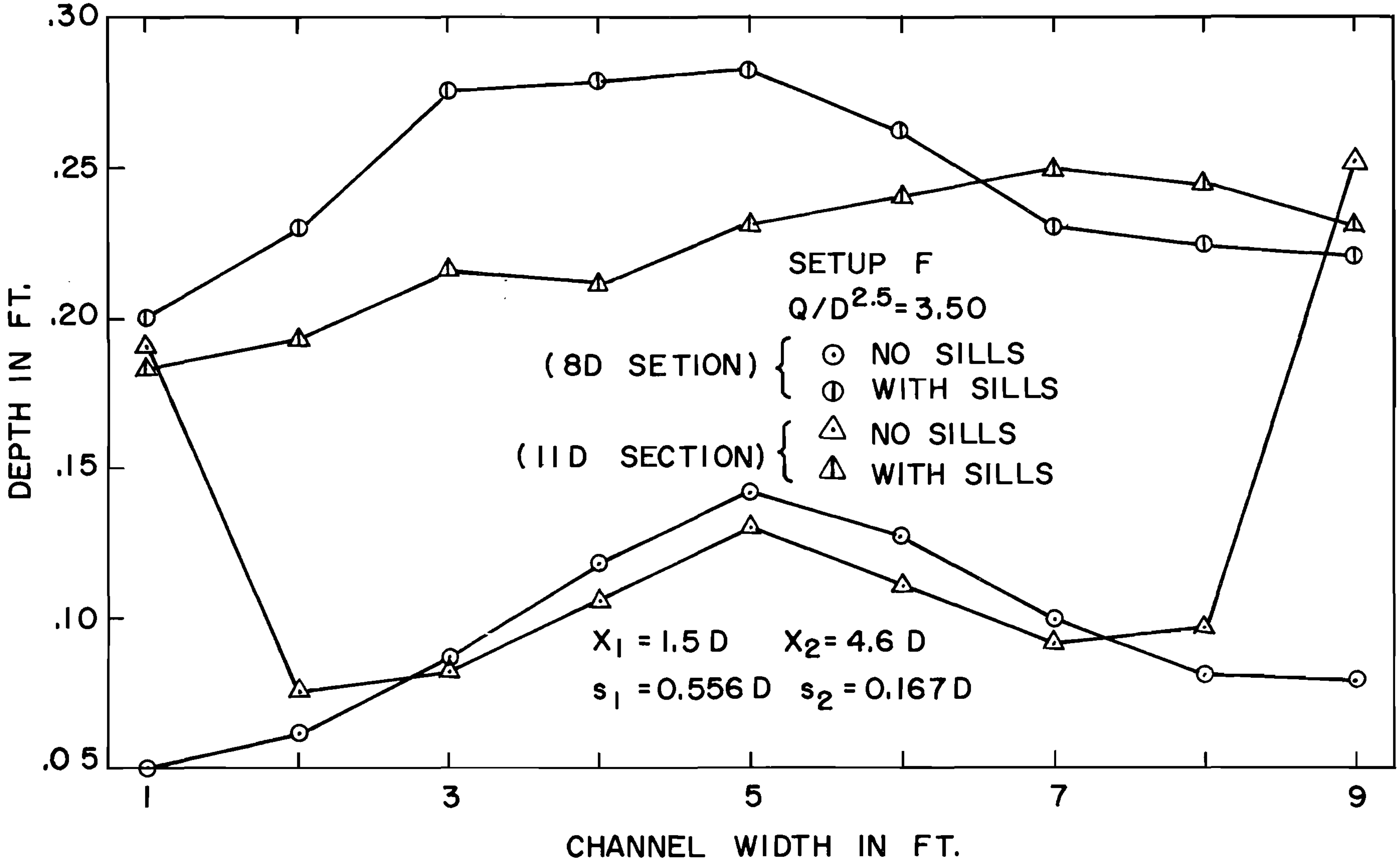

Figure 4-27. Downstream Channel Transverse Depth Profiles

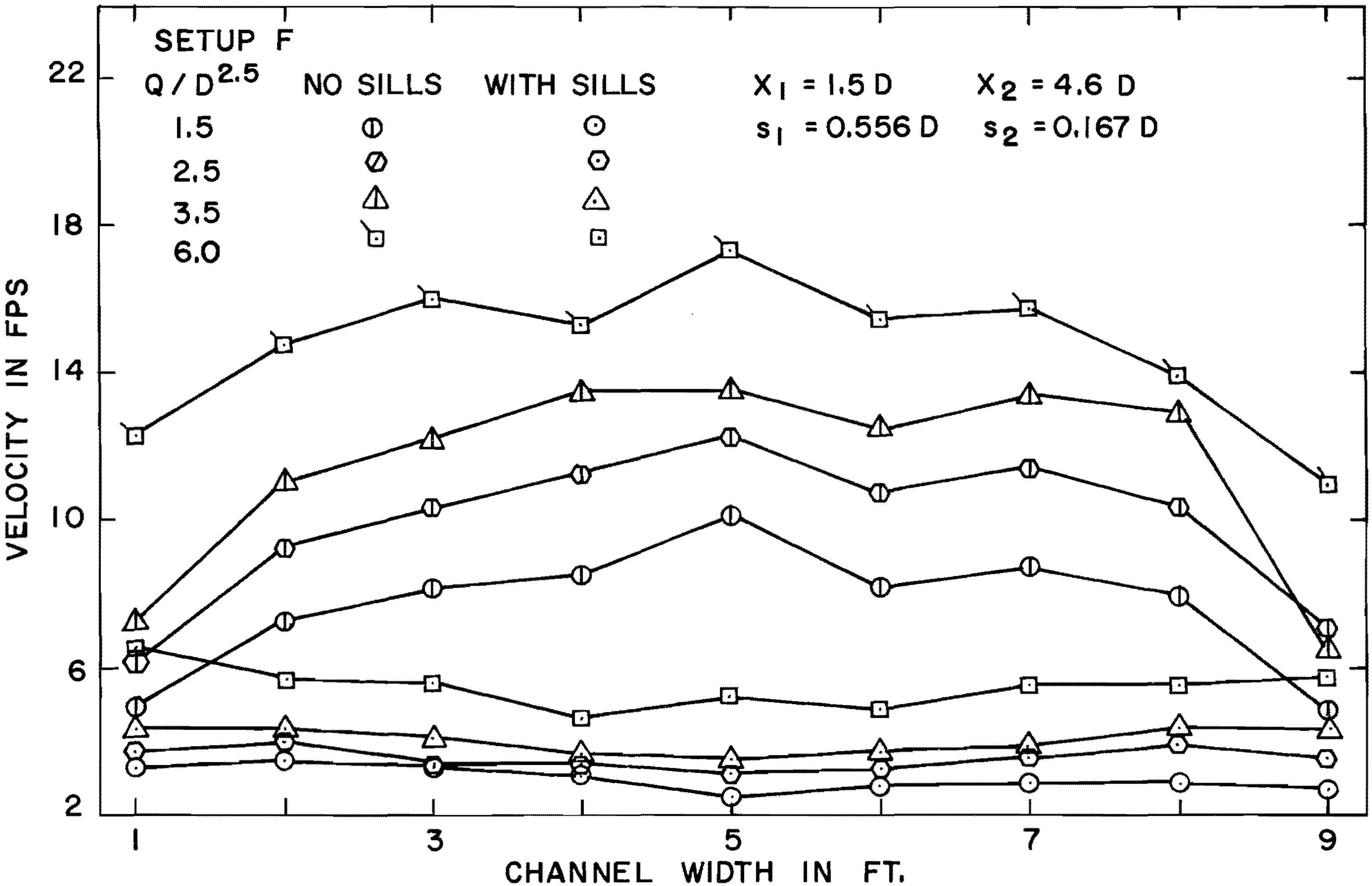

Figure 4-28. Downstream Channel Transverse Velocity Profiles

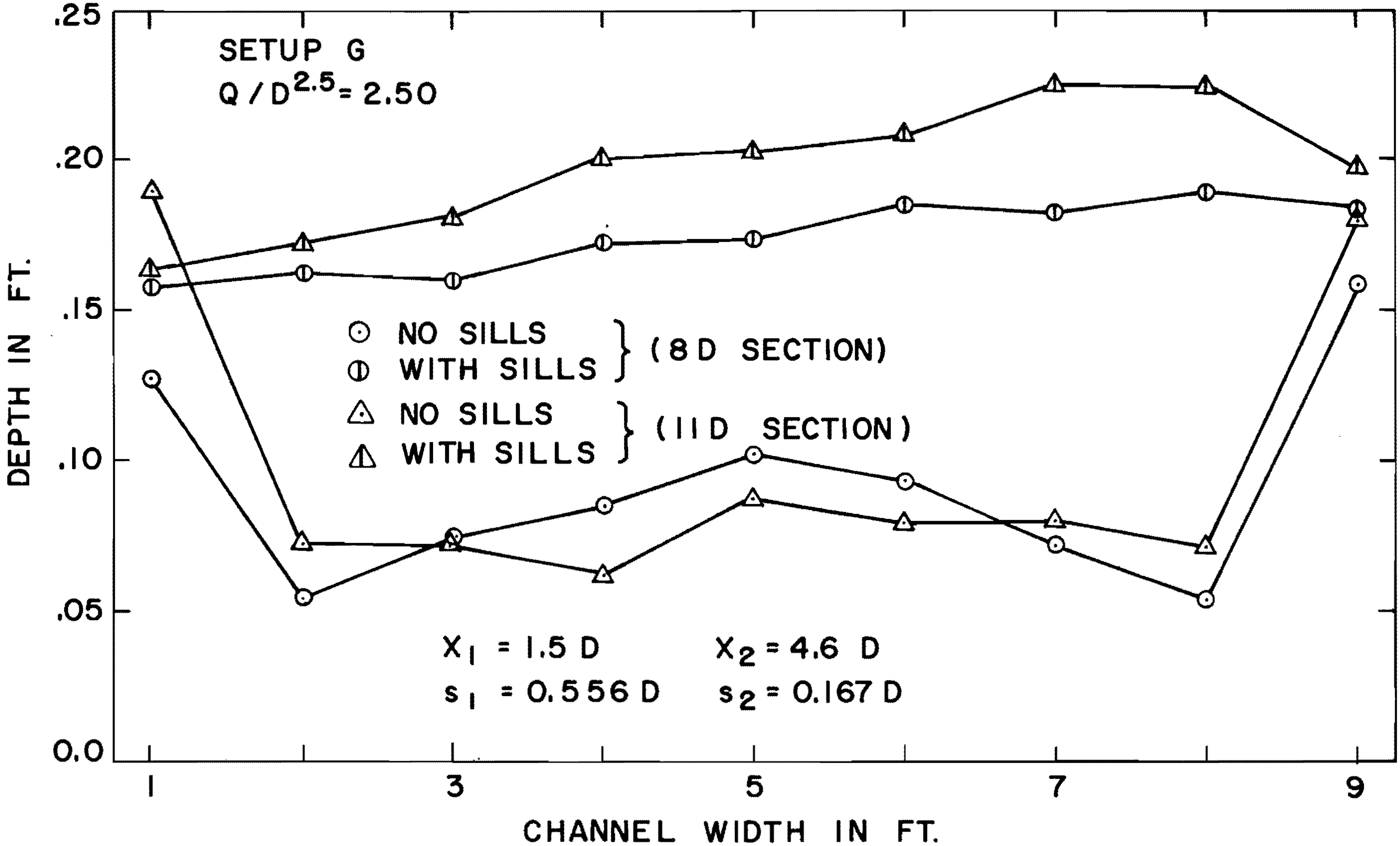

Figure 4-29. Downstream Channel Transverse Depth Profiles

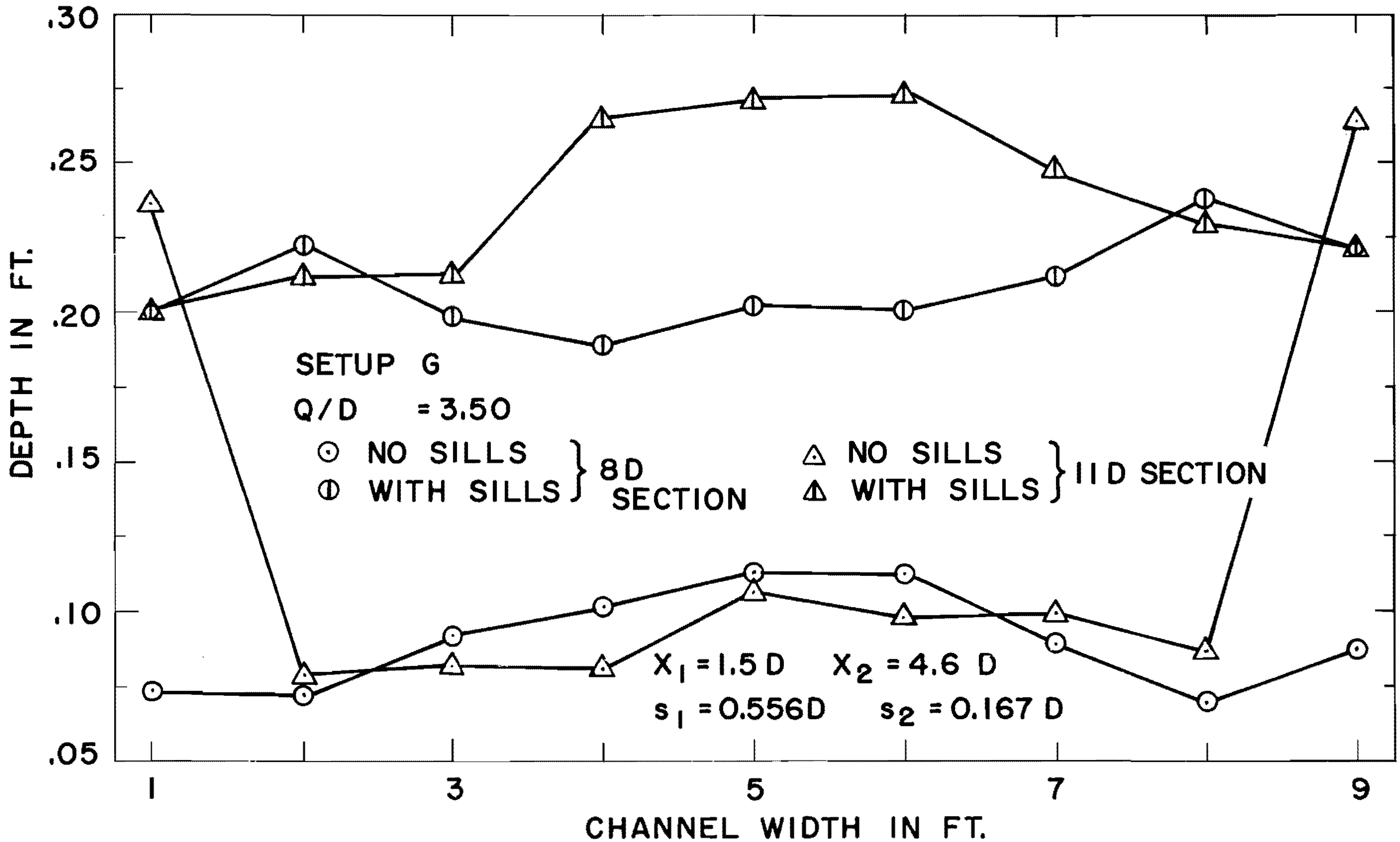

Figure 4-30. Downstream Channel Transverse Depth Profiles

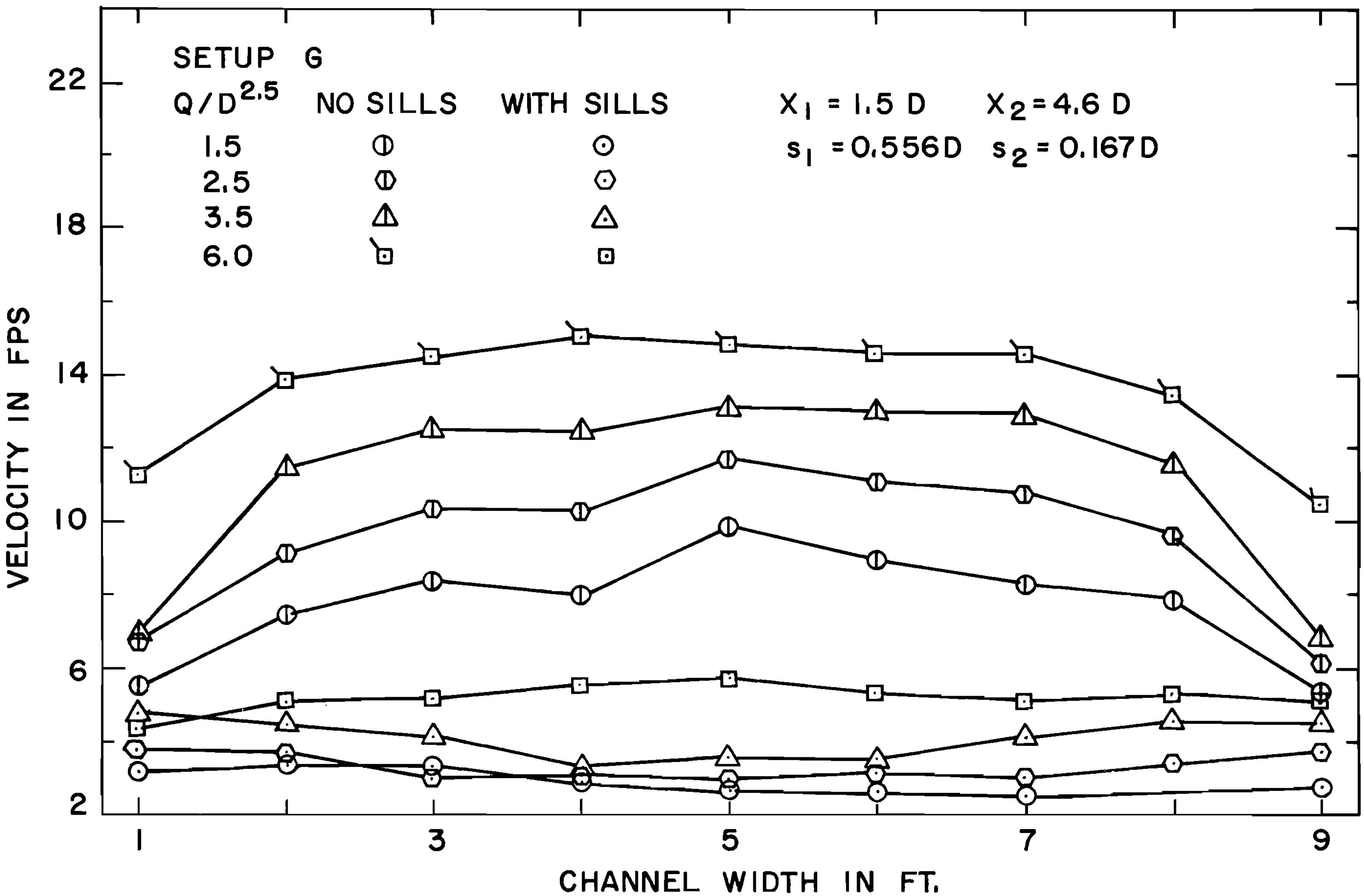

Figure 4-31. Downstream Channel Transverse Velocity Profiles

TABLE 4-7. SUMMARY OF RESULTS ON ENERGY DISSIPATION

(TEST SECTION 11D)

$Q/D^{2.5}$	Y_1	H_1	Y_o	H_o	Y_s	H_s	$\frac{H_1 - H_s}{H_1}$	$\frac{H_o - H_s}{H_s}$	Setup
6.0	.834	4.994	.100	4.550	.341	.725	.855	.840	
3.5	.610	3.770	.076	2.706	.235	.512	.864	.810	
2.5	.521	3.011	.073	1.533	.223	.379	.873	.755	D
1.5	.380	2.530	.052	1.085	.163	.268	.894	.754	
6.0	.900	4.360	.113	3.603	.374	.694	.840	.806	
3.5	.675	3.105	.090	1.960	.240	.500	.838	.744	
2.5	.550	2.680	.092	1.012	.195	.395	.853	.708	E
1.5	.425	1.995	.064	0.744	.139	.279	.860	.625	
6.0	.835	4.985	.122	3.122	.288	.825	.834	.735	
3.5	.605	3.855	.099	1.639	.228	.518	.865	.685	
2.5	.486	3.486	.077	1.387	.184	.414	.880	.701	F
1.5	.355	2.935	.064	0.744	.141	.281	.903	.623	

Y_1 = upstream depth of the jump.

H_1 = energy before the jump.

Y_o = downstream channel depth at Section 11D for 'No Sill' case.

Y_s = downstream channel depth at Section 11D for 'With Sill' case.

H_o, H_s = energy levels corresponding to the case of 'No Sills' and 'With Sills'.

CHAPTER V

SUMMARY AND CONCLUSIONS

Based on tests conducted on the hydraulic performance of 18-inch corrugated metal pipe and concrete pipe culvert models the following conclusions are justified:

1. The head water depth-discharge factor relationships for corrugated metal and concrete pipe culverts operating with sharp edged entrances are identical up to a discharge factor, $Q/D^{2.5} = 2.5$.

2. Under ventilated conditions the corrugated metal pipe displayed a slug and mixture control in the range of $2.5 < Q/D^{2.5} < 4.5$ whereas the concrete pipe displayed an orifice control in the range of $2.5 < Q/D^{2.5} < 6.5$. Beyond $Q/D^{2.5} = 4.5$ the corrugated metal pipe operated under pipe control.

3. The hydraulic jump in the steep sloped corrugated metal pipe culvert models were influenced significantly by the presence of horizontal unit (Unit 3) and the sharp change in grade between Unit 2 and Unit 3 whereas the jump position was little affected in the case of concrete pipe culvert models operated with similar geometrical configurations and discharge factors.

4. A jump can be produced without a sill for cases in which Unit 3 was sufficiently long or rough to cause critical depth to be obtained in the horizontal section of the culvert.

5. A sill was necessary to force a hydraulic jump to form inside the culvert for those cases where there was either an absence or insufficient length of horizontal unit at the end of steep unit of the culvert. For the culvert configurations and discharge factors

tested it was found that the jump position was relatively insensitive to sill height except for the case of highest sill of the order of 0.8D.

6. A one-dimensional method of analysis to predict water surface profiles and approximate jump locations was found to yield satisfactory results as long as the following were well-defined (a) upstream control, (b) downstream control, and (c) Manning's n or the friction factor. Based on the agreement between the measured and computed surface profiles and jump locations it may be stated that the supercritical normal depth is produced within a short distance from the beginning of Unit 2 and hence minor variations in the location of upstream control are relatively unimportant for rough pipe culverts. The factors which can be expected to cause large errors in the prediction of surface profiles and jump locations are due to inadequate representation of downstream control, Manning's n of the pipe and the effect of sudden change in grade between Unit 2 and Unit 3.

7. Methods suggested in this study to estimate the tail water depth produced by a specified sill configuration are approximate. In particular, it was recommended that the downstream control depth be taken as the sum of the height of jump producing mid-sill, the head over the sill as computed from standard weir formulae and the velocity head at the pipe outlet for purposes of jump location.

8. A sill was essential at the downstream of culvert outlet regardless of its requirement to force a hydraulic jump to the inside of culvert pipe. Without a sill the high velocity jet from the culvert outlet assumes a supercritical state in the downstream channel for extended lengths before a second jump occurs.

9. Based on the inter-comparisons of depth distributions in the downstream channel for a wide range of flow and for the cases of 'no sills', 'single sill', and 'double sills' it is concluded that the use of two sills was more effective and desirable from the following view points (a) to be able to force a jump to the inside of the pipe and retard the high velocity flow from the culvert outlet, (b) to dissipate the energy of the nappe following the jump producing mid-sill by creating a pool in the space between the two sills, and (c) to aid the flow in distributing itself more uniformly across the width of the downstream channel.

10. Higher downstream channel depths are produced by decreasing the ratio of sill spacing (X_1/X_2) and by increasing the ratio of sill heights (s_1/s_2).

11. The most desirable double sill configuration was associated with greater relative sill spacing (ΔX) and a smaller end sill height (s_2). This condition obviously required greater length of wing walls although this disadvantage was compensated for by the reduction in downstream velocity concentrations and accomplishment of relative uniformity of flows across the channel width.

12. Based on the double sill performance tests with the corrugated metal pipe culvert model it was recommended that two sills be placed at distances 1.5 and 3.0 pipe diameters from the culvert outlet. The height of the mid-sill was fixed on the criteria for jump formation within the culvert whereas the height of the end sill could be of the order of 0.167D. For the case of concrete pipe culverts the above double sill configuration was found to be unsuitable due to the fact that the high velocity jet following the mid-sill springs clear off the end sill. This necessiated an increase of the location of the end sill (X_2) up to a distance of 4.6D.

It is expected that the results obtained from the large sized culvert models are relatively free of scale effects. Furthermore, the upper limit of the experimental range corresponds to the extremes in regard to both the discharge factor as well as the steepness of Unit 2. Hence the experimentally observed values in this study are believed to adequately represent the hydraulic state of affairs associated with prototype culvert installations.

REFERENCES

1. Price, B. E., and Masch, F. D., 1967. "Performance of Circular Culverts on Steep Grades", Research Report Number 92-2, Center for Highway Research, The University of Texas at Austin.

2. Brandes, R. J., Masch, F. D., and Rao, Manam V. P., 1969. "End Sills and the Forced Hydraulic Jump in Circular Culverts Operating at Low Discharge Factors", Research Report Number 92-4, Center for Highway Research, The University of Texas at Austin.

3. MacDonald, T. C., 1969. "Energy Dissipators for Large Culverts", Journal of the Hydraulic Division, ASCE, Vol. 95, No. HY 6, November 1969, pp. 1941-1958.

4. Blaisdell, F. W., 1966. "Culvert Flow and Related Design Philosophies", Journal of the Hydraulic Division, ASCE, Vol. 92, No. HY 2, March 1966, pp. 19-31.

5. French, J. L., 1961. "Fourth Progress Report on Hydraulics of Culverts - Hydraulics of Improved Inlet Structures for Pipe Culverts", National Bureau of Standards Report No. 7178, 132 pp.

APPENDIX

(Data Tables)

Table A-1. Headwater Depth and Discharge Data for Different Culvert Set Ups

$Q/D^{2.5}$	HW/D	Set Up
1.500	0.800	
2.000	0.950	
2.500	1.100	A
3.000	1.125	
3.500	1.175	
1.500	0.779	
1.780	0.849	
2.062	0.943	
2.480	1.053	
2.500	1.050	
2.740	1.096	
2.875	1.102	
3.000	1.055	B
3.000	1.135	
3.000	1.133	
3.320	1.133	
3.500	1.133	
3.635	1.153	
4.000	1.145	
5.075	1.207	
5.690	2.200	
6.010	1.950	
6.100	2.813	
6.280	2.598	
6.420	2.690	

$Q/D^{2.5}$	HW/D	Set Up
2.500	1.052	
3.000	1.240	
3.500	1.340	C
3.500	1.403	
3.500	1.103	
1.300	0.680	
1.500	- - -	
1.575	0.687	
1.890	0.853	
2.130	0.926	
2.500	1.023	
2.500	1.053	
2.780	1.210	
2.940	1.190	D
3.480	1.400	
3.500	- - -	
3.970	1.640	
4.660	2.003	
5.225	2.220	
5.980	2.953	
6.275	3.186	
6.530	3.280	

$Q/D^{2.5}$	HW/D	Set Up
1.500	- - -	
2.500	1.030	E
3.500	1.400	
6.000	1.968	
1.018	0.600	
1.270	0.673	
1.450	0.730	
1.765	0.813	
1.890	0.883	
2.240	0.947	
2.510	1.037	
2.850	1.156	
3.090	1.260	F
3.284	1.320	
3.500	1.400	
3.554	1.427	
3.880	1.613	
4.220	1.792	
4.570	1.967	
5.040	2.317	
5.580	2.687	
5.990	1.967	

TABLE A-2

SURFACE PROFILE DATA - SET UP A ($Q/D^{2.5} = 2.0$)

Piezometer No.	X/D = 4.6 with different s/D values					X/D = 2.3 with different s/D values				
	.806	.750	.638	.500	.333	0.00	.806	.638	.500	.333
1	1.53	1.44	1.29	1.12	1.10	1.01	1.66	1.37	1.17	1.04
2	1.56	1.46	1.34	1.20	1.16	1.16	1.69	1.41	1.24	1.17
3	1.57	1.48	1.35	1.22	1.19	1.18	1.70	1.42	1.26	1.19
4	1.58	1.50	1.38	1.27	1.23	1.23	1.71	1.43	1.29	1.25
5	1.59	1.51	1.40	1.29	1.25	1.25	1.72	1.45	1.31	1.27
6	1.60	1.53	1.43	1.32	1.29	1.28	1.74	1.47	1.33	1.29
7	1.64	1.57	1.45	1.33	1.29	1.30	1.79	1.52	1.38	1.32
8	- - -	1.58	1.47	1.33	1.28	1.29	1.80	1.53	1.36	1.30
9	1.67	1.56	1.35	1.13	1.08	1.08	1.81	1.45	1.20	1.10
10	1.40	1.42	1.40	1.38	1.36	1.38	1.68	1.38	1.37	1.38
11	2.02	2.05	2.05	2.01	2.02	2.01	2.02	2.02	2.01	2.02
12	2.58	2.63	2.60	2.58	2.57	2.56	2.57	2.58	2.57	2.58
13	3.25	3.25	3.22	3.22	3.22	3.20	3.21	3.22	3.21	3.21
14	3.85	3.89	3.90	3.88	3.85	3.85	3.86	3.85	3.25	3.86
15	4.48	4.49	4.48	4.48	4.45	4.46	4.46	4.47	4.47	4.50
16	5.10	5.12	5.10	5.10	5.10	5.09	5.11	5.11	5.09	5.12
17	5.67	5.67	5.68	5.67	5.68	5.67	5.66	5.67	5.66	5.66
18	6.20	6.22	6.22	6.21	6.19	6.20	6.20	6.21	6.19	6.21
19	6.89	6.91	6.93	6.90	6.88	6.89	6.89	6.91	6.89	6.91
20	7.08	7.10	7.10	7.08	7.08	7.08	7.09	7.07	7.07	7.08
21	7.15	7.16	7.16	7.14	7.15	7.16	7.15	7.15	7.14	7.15
22	7.18	7.23	7.21	7.20	7.17	7.20	7.19	7.19	7.18	7.19
23	7.31	7.36	7.36	7.31	7.31	7.31	7.32	7.32	7.32	7.31

TABLE A-3

SURFACE PROFILE DATA - SET UP A ($Q/D^{2.5}$ = 2.5)

No.	X/D = 4.6 with different s/D Values							X/D = 2.3 with different s/D				
	.806	.750	.694	.638	.557	.503	.333	0.00	.806	.638	.500	.333
1	1.54	1.48	1.42	1.34	1.24	1.19	1.10	1.11	1.71	1.45	1.23	1.13
2	1.57	1.53	1.48	1.40	1.34	1.32	1.28	1.28	1.75	1.50	1.32	1.27
3	1.58	1.54	1.49	1.42	1.36	1.35	1.31	1.32	1.76	1.52	1.34	1.31
4	1.61	1.57	1.53	1.46	1.41	1.39	1.36	1.36	1.78	1.54	1.39	1.36
5	1.63	1.58	1.54	1.49	1.43	1.42	1.39	1.40	1.79	1.55	1.42	1.38
6	1.65	1.61	1.57	1.52	1.47	1.45	1.42	1.42	1.82	1.57	1.44	1.41
7	1.73	1.68	1.62	1.58	1.54	1.52	1.48	1.49	1.89	1.64	1.52	1.49
8	1.75	1.71	1.65	1.61	1.55	1.53	1.49	1.49	1.91	1.65	1.52	1.49
9	1.76	1.70	1.62	1.54	1.44	1.42	1.32	1.30	1.93	1.63	1.38	1.32
10	1.48	1.48	1.47	1.47	1.46	1.44	1.45	1.44	1.87	1.45	1.45	1.45
11	2.09	2.09	2.09	2.09	2.07	2.06	2.08	2.07	2.10	2.08	2.08	2.08
12	2.65	2.65	2.64	2.63	2.63	2.63	2.62	2.62	2.66	2.64	2.62	2.62
13	3.30	3.31	3.29	3.26	3.27	3.27	3.26	3.27	3.30	3.28	3.28	3.28
14	3.93	3.93	3.94	3.93	3.92	3.93	3.91	3.93	3.93	3.95	3.92	3.93
15	4.55	4.55	4.54	4.53	4.52	4.54	4.53	4.52	4.54	4.53	4.54	4.53
16	5.17	5.18	5.15	5.16	5.17	5.16	5.16	5.17	5.19	5.19	5.17	5.17
17	5.70	5.72	5.71	5.70	5.72	5.71	5.70	5.70	5.73	5.70	5.70	5.70
18	6.26	6.27	6.26	6.25	6.27	6.24	6.24	6.25	6.28	6.27	6.25	6.27
19	6.98	6.99	7.00	7.00	7.01	6.98	6.98	6.99	6.98	6.98	6.98	6.97
20	7.15	7.15	7.15	7.15	7.13	7.14	7.13	7.15	7.15	7.15	7.15	7.14
21	7.20	7.20	7.20	7.21	7.19	7.20	7.19	7.21	7.23	7.23	7.23	7.23
22	7.25	7.26	7.24	7.25	7.23	7.24	7.23	7.24	7.26	7.28	7.27	7.27
23	7.40	7.38	7.37	7.36	7.39	7.39	7.40	7.41	7.45	7.44	7.44	7.44

TABLE A-4

SURFACE PROFILE DATA - SET UP A ($Q/D^{2.5} = 3.0$)

Piezo-meter No.	X/D = 4.6 with different s/D Values						X/D = 2.3 with different s/D values				
	.806	.750	.694	.638	.500	.333	0.00	.806	.638	.500	.333
1	1.59	1.53	1.46	1.39	1.25	1.17	1.17	1.77	1.46	1.31	1.22
2	1.65	1.59	1.53	1.48	1.39	1.36	1.36	1.82	1.54	1.43	1.40
3	1.67	1.61	1.56	1.51	1.44	1.40	1.40	1.84	1.56	1.47	1.44
4	1.69	1.65	1.60	1.56	1.48	1.45	1.46	1.87	1.59	1.52	1.51
5	1.72	1.67	1.62	1.58	1.51	1.48	1.48	1.89	1.61	1.55	1.52
6	1.75	1.69	1.64	1.61	1.55	1.52	1.52	1.92	1.65	1.58	1.56
7	1.87	1.80	1.75	1.72	1.65	1.63	1.62	2.03	1.75	1.67	1.65
8	1.88	1.84	1.79	1.74	1.67	1.65	1.65	2.04	1.76	1.69	1.67
9	1.91	1.88	1.83	1.79	1.68	1.65	1.65	2.07	1.77	1.67	1.63
10	2.03	1.96	1.89	1.83	1.45	1.43	1.42	2.17	1.54	1.55	1.55
11	1.95	1.95	1.93	1.94	2.07	2.02	2.02	2.14	2.16	2.15	2.15
12	2.58	2.57	2.58	2.56	2.59	2.59	2.60	2.70	2.71	2.70	2.69
13	3.23	3.23	3.23	3.23	3.24	3.20	3.25	3.35	3.35	3.35	3.35
14	3.86	3.87	3.83	3.84	3.90	3.87	3.88	4.01	4.02	4.01	4.01
15	4.48	4.47	4.46	4.45	4.49	4.49	4.49	4.63	4.62	4.61	4.61
16	5.19	5.18	5.21	5.00	5.13	5.11	5.16	5.25	5.25	5.25	5.25
17	5.70	5.72	5.73	5.71	5.74	5.69	5.69	5.80	5.77	5.77	5.80
18	6.27	6.34	6.30	6.27	6.23	6.21	6.22	6.34	6.35	6.34	6.32
19	7.01	7.05	7.01	7.02	6.98	6.95	6.93	7.08	7.08	7.08	7.10
20	7.12	7.12	7.15	7.09	7.10	7.10	7.10	7.26	7.25	7.25	7.26
21	7.19	7.19	7.17	7.18	7.17	7.16	7.18	7.34	7.33	7.33	7.33
22	7.26	7.25	7.26	7.24	7.22	7.22	7.22	7.43	7.43	7.43	7.44
23	7.43	7.42	7.41	7.37	7.38	7.38	7.38	7.54	7.54	7.54	7.54

TABLE A-5

SURFACE PROFILE DATA - SET UP A ($Q/D^{2.5} = 3.5$)

Piezo-meter No.	X/D = 4.6 with different s/D Values							X/D = 2.3 with different s/D Values			
	.806	.750	.694	.638	.557	.500	.333	0.00	.806	.638	.500
1	1.61	1.56	1.51	1.43	1.36	1.32	1.26	1.28	1.88	1.58	1.40
2	1.68	1.61	1.59	1.56	1.50	1.49	1.48	1.47	1.96	1.65	1.54
3	1.68	1.64	1.62	1.58	1.54	1.53	1.51	1.52	1.97	1.67	1.56
4	1.74	1.70	1.65	1.62	1.58	1.58	1.57	1.57	1.98	1.71	1.61
5	1.76	1.71	1.68	1.64	1.62	1.62	1.61	1.60	2.01	1.73	1.64
6	1.79	1.75	1.72	1.68	1.65	1.63	1.64	1.64	2.05	1.74	1.67
7	1.91	1.87	1.84	1.80	1.78	1.77	1.76	1.77	2.16	1.87	1.81
8	1.94	1.92	1.88	1.84	1.81	1.81	1.78	1.80	- -	- -	- -
9	2.01	1.95	1.91	1.87	1.85	1.86	1.84	1.85	2.23	1.97	1.85
10	2.14	2.11	2.07	2.03	2.02	1.99	1.97	1.96	2.37	2.09	1.99
11	2.05	1.96	1.91	1.86	1.85	1.86	1.92	1.93	2.56	1.95	1.93
12	2.51	2.48	2.49	2.49	2.49	2.48	2.47	2.45	2.50	2.50	2.52
13	3.15	3.10	3.11	3.13	3.12	3.10	3.11	3.11	3.14	3.14	3.14
14	3.74	3.76	3.76	3.75	3.74	3.76	3.76	3.77	3.78	3.78	3.80
15	4.37	4.36	4.40	4.38	4.39	4.38	4.41	4.38	4.42	4.44	4.42
16	5.05	5.06	5.08	4.98	4.98	5.01	4.99	5.02	5.04	5.09	5.04
17	5.64	5.63	5.60	5.60	5.61	5.60	5.59	5.55	5.61	5.63	5.60
18	6.15	6.15	6.16	6.14	6.13	6.12	6.14	6.12	6.16	6.13	6.12
19	6.88	6.88	6.86	6.87	6.84	6.84	6.83	6.82	6.87	6.85	6.84
20	6.93	6.93	6.93	6.93	6.93	6.93	6.95	6.92	6.97	6.98	6.99
21	7.03	7.04	7.03	7.03	7.02	7.02	7.04	7.05	7.09	7.07	7.09
22	7.17	7.18	7.16	7.17	7.16	7.15	7.11	7.11	7.20	7.18	7.15
23	7.28	7.29	7.33	7.30	7.32	7.30	7.29	7.30	7.35	7.32	7.34

TABLE A-6

SURFACE PROFILE DATA - SET UP B

Piezo-meter No.	$Q/D^{2.5} = 1.5$		$Q/D^{2.5} = 2.0$		$Q/D^{2.5} = 2.5$		
	X/D = 2.3	X/D = 4.6	X/D = 2.3	X/D = 4.6	X/D = 2.3	No Sill	X/D = 4.6
1	1.44	1.23	1.425	1.28	1.42	1.11	1.320
2	1.46	1.26	1.450	1.33	1.54	1.31	1.410
3	1.47	1.28	1.480	1.35	1.56	1.33	1.430
4	1.48	1.29	1.490	1.35	1.58	1.35	1.465
5	1.49	1.30	1.490	1.38	1.60	1.34	1.470
6	1.52	1.32	1.530	1.36	1.63	1.05	1.430
7	1.51	1.28	1.520	1.32	1.61	1.09	1.350
8	1.50	1.18	1.410	1.15	1.45	1.21	1.220
9	1.32	1.31	1.400	1.41	1.50	1.51	1.520
10	1.46	1.44	1.540	1.55	1.64	1.65	1.640
11	1.77	1.75	1.840	1.86	1.95	1.93	1.950
12	2.04	2.03	2.120	2.13	2.20	2.20	2.210
13	2.80	2.79	2.870	2.92	2.97	2.97	2.965
14	3.23	3.20	3.320	3.35	3.39	3.39	3.380
15	3.52	3.52	3.610	3.62	3.71	3.70	3.670
16	4.21	4.21	4.330	4.33	4.42	4.43	4.410
17	4.59	4.57	4.710	4.65	4.80	4.80	4.770
18	4.82	4.78	4.950	4.92	5.03	5.02	5.020
19	5.17	5.19	5.240	5.26	5.32	5.32	5.310
20	5.89	5.86	6.050	6.00	6.12	6.10	6.060
21	6.34	6.33	6.500	6.43	6.54	6.55	6.530
22	6.62	6.64	6.700	6.75	6.82	6.82	6.820
23	7.04	7.04	7.180	7.21	7.35	7.35	7.340

All water surface elevations pertain to s/D = 0.638 except the column of 'No Sill'.

TABLE A-7

SURFACE PROFILE DATA - SET UP B

Piezo-meter No.	$Q/D^{2.5} = 3.00$			$Q/D^{2.5} = 3.50$			$Q/D^{2.5} = 4.0$
	X/D = 2.3	X/D = 4.6	No Sills	X/D = 2.3	X/D = 4.6	No Sills	X/D = 4.6
1	1.53	1.36	1.21	1.57	1.43	1.28	1.530
2	1.59	1.48	1.42	1.65	1.57	1.53	1.650
3	1.64	1.52	1.46	1.67	1.59	1.58	1.670
4	1.66	1.55	1.52	1.71	1.64	1.50	1.720
5	1.68	1.58	1.54	1.76	1.67	1.63	1.760
6	1.79	1.65	1.59	1.87	1.83	1.77	1.950
7	1.79	1.64	1.60	1.91	1.84	1.82	1.960
8	1.75	1.48	1.35	1.96	1.89	1.83	2.030
9	1.52	1.53	1.47	1.97	1.80	1.77	2.175
10	1.62	1.63	1.63	1.93	1.68	1.56	2.220
11	1.95	1.97	1.95	1.85	1.80	1.80	2.350
12	2.16	2.17	2.14	2.05	2.00	2.05	2.320
13	2.97	2.97	2.94	2.85	2.82	2.84	2.610
14	3.39	3.37	3.36	3.29	3.23	3.26	3.030
15	3.71	3.71	3.71	3.58	3.49	3.56	3.310
16	4.40	4.42	4.40	4.29	4.21	4.27	4.050
17	4.79	4.76	4.77	4.66	4.58	4.65	4.420
18	5.02	4.99	4.99	4.86	4.78	4.88	4.570
19	5.28	5.30	5.30	5.14	5.12	5.13	4.920
20	6.14	6.12	6.15	6.00	5.95	6.00	5.750
21	6.57	6.56	6.58	6.45	6.42	6.44	6.220
22	6.87	6.87	6.79	6.78	6.72	6.73	6.530
23	7.35	7.34	7.34	7.24	7.25	7.24	7.050

All water surface elevations pertain to s/D = 0.638 except the column of 'No Sills.'

TABLE A-8

Depth Distribution Data at Section 8D for the Different Sill Configurations (Set Up C)

SILL CONFIGURATION NUMBER												No Sills	$Q/D^{2.5}$
1	2	6	7	8	9	4	5	3	1*	4*	3*		
0.107	0.203	0.159	0.239	0.223	0.120	0.110	0.247	0.126	0.138	0.130	0.167	0.146	
0.109	0.248	0.168	0.246	0.243	0.076	0.103	0.250	0.137	0.115	0.095	0.168	0.088	
0.091	0.249	0.183	0.252	0.264	0.080	0.102	0.270	0.271	0.082	0.081	0.082	0.064	
0.097	0.257	0.188	0.246	0.263	0.094	0.103	0.268	0.249	0.079	0.082	0.089	0.064	
0.053	0.251	0.199	0.248	0.276	0.095	0.100	0.271	0.207	0.077	0.081	0.099	0.068	1.5
0.059	0.251	0.202	0.271	0.277	0.094	0.104	0.273	0.219	0.081	0.081	0.093	0.064	
0.051	0.253	0.197	0.264	0.283	0.086	0.104	0.291	0.213	0.078	0.086	0.073	0.062	
0.132	0.259	0.198	0.268	0.283	0.088	0.131	0.305	0.203	0.131	0.141	0.129	0.068	
0.139	0.263	0.209	0.278	0.285	0.170	0.139	0.299	0.227	0.156	0.186	0.126	0.167	
0.146	0.180	0.247	0.324	0.185	0.165	0.176	0.207	0.129	0.145	0.194	0.201	0.192	
0.076	0.111	0.287	0.340	0.172	0.097	0.136	0.205	0.118	0.076	0.193	0.197	0.082	
0.103	0.118	0.289	0.345	0.127	0.091	0.111	0.149	0.119	0.087	0.121	0.123	0.080	
0.092	0.135	0.293	0.350	0.125	0.101	0.129	0.149	0.125	0.084	0.113	0.115	0.074	
0.089	0.126	0.293	0.351	0.137	0.103	0.133	0.158	0.148	0.086	0.095	0.099	0.074	2.5
0.096	0.128	0.309	0.363	0.136	0.107	0.136	0.163	0.170	0.087	0.096	0.097	0.076	
0.095	0.123	0.309	0.369	0.137	0.110	0.131	0.147	0.156	0.097	0.114	0.108	0.076	
0.090	0.138	0.307	0.374	0.231	0.113	0.140	0.245	0.159	0.102	0.230	0.239	0.085	
0.198	0.234	0.317	0.380	0.248	0.231	0.213	0.252	0.163	0.180	0.239	0.249	0.247	

* Single Sills - all the rest of the data are depths (in feet) for double sill configurations

TABLE A-9

Depth Distribution Data at Section 8D for the Different Sill Configurations (Set Up C)

SILL CONFIGURATION NUMBER												No Sills	$Q/D^{2.5}$
1	2	6	7	8	9	4	5	3	1*	4*	3*		
0.156	0.189	0.157	0.305	0.228	0.212	0.253	0.252	0.119	0.261	0.235	0.269	0.276	
0.147	0.166	0.153	0.259	0.226	0.120	0.251	0.258	0.149	0.114	0.172	0.229	0.097	
0.119	0.179	0.157	0.298	0.174	0.112	0.136	0.272	0.249	0.123	0.133	0.177	0.099	
0.082	0.158	0.166	0.299	0.148	0.107	0.145	0.171	0.251	0.106	0.117	0.146	0.096	
0.083	0.149	0.173	0.305	0.146	0.109	0.150	0.173	0.188	0.097	0.092	0.089	0.094	3.5
0.095	0.161	0.189	0.307	0.147	0.111	0.154	0.175	0.209	0.110	0.096	0.127	0.097	
0.150	0.192	0.208	0.302	0.219	0.114	0.147	0.173	0.198	0.115	0.130	0.167	0.105	
0.178	0.193	0.205	0.313	0.296	0.132	0.288	0.303	0.200	0.121	0.206	0.209	0.104	
0.180	0.198	0.202	0.363	0.298	0.274	0.297	0.315	0.202	- - -	0.252	0.249	0.352	
0.198	0.175	0.157	0.286	0.142	0.199	0.276	0.264	0.102	0.245	0.275	0.280	0.309	
0.191	0.160	0.158	0.292	0.170	0.198	0.279	0.275	0.119	0.132	0.277	0.296	0.098	
0.199	0.162	0.187	0.229	0.168	0.189	0.172	0.182	0.129	0.122	0.174	0.185	0.112	
0.095	0.177	0.157	0.206	0.176	0.111	0.169	0.179	0.127	0.106	0.163	0.173	0.113	
0.059	0.105	0.242	0.208	0.149	0.091	0.169	0.173	0.159	0.112	0.131	0.142	0.109	4.0
0.138	0.107	0.207	0.207	0.166	0.125	0.173	0.176	0.162	0.113	0.136	0.136	0.110	
0.185	0.189	0.207	0.252	0.191	0.201	0.172	0.187	0.168	0.113	0.162	0.167	0.113	
0.200	0.227	0.223	0.324	0.191	0.201	0.296	0.343	0.165	0.183	0.298	0.283	0.115	
0.232	0.231	0.237	0.344	0.211	0.213	0.323	0.332	0.177	0.293	0.317	0.292	0.372	

* Single Sills - all the rest of the data are depths (in feet) for double sill configurations.

TABLE A-10

Depth Distribution Data at Section 11D for the Different Sill Configurations (Set Up C)

SILL CONFIGURATION NUMBER												No Sill	
1	2	6	7	8	9	4	5	3	1*	4*	3*		$Q/D^{2.5}$
0.103	0.209	0.188	0.239	0.257	0.175	0.232	0.267	0.205	0.209	0.315	0.170	0.119	
0.110	0.261	0.167	0.235	0.265	0.176	0.242	0.267	0.225	0.227	0.262	0.167	0.115	
0.110	0.254	0.228	0.257	0.261	0.147	0.244	0.273	0.241	0.237	0.256	0.210	0.115	
0.123	0.255	0.221	0.258	0.263	0.117	0.244	0.277	0.246	0.256	0.256	0.207	0.062	
0.074	0.262	0.212	0.273	0.271	0.073	0.247	0.282	0.274	0.277	0.264	0.207	0.056	1.5
0.079	0.267	0.230	0.276	0.273	0.072	0.263	0.291	0.288	0.225	0.275	0.211	0.058	
0.150	0.267	0.223	0.278	0.279	0.125	0.272	0.287	0.283	0.290	0.277	0.208	0.102	
0.165	0.275	0.184	0.282	0.280	0.179	0.267	0.299	0.287	0.180	0.242	0.207	0.150	
0.140	0.142	0.291	0.350	0.320	0.159	0.137	0.337	0.247	0.125	0.140	0.139	0.165	
0.145	0.147	0.282	0.344	0.320	0.165	0.142	0.339	0.275	0.138	0.140	0.149	0.167	
0.130	0.141	0.290	0.346	0.335	0.161	0.150	0.344	0.191	0.137	0.144	0.157	0.099	
0.077	0.128	0.280	0.346	0.335	0.107	0.145	0.344	0.166	0.096	0.139	0.149	0.070	
0.090	0.103	0.293	0.351	0.346	0.094	0.143	0.349	0.169	0.076	0.241	0.178	0.072	2.5
0.083	0.160	0.301	0.357	0.359	0.097	0.151	0.354	0.188	0.108	0.108	0.179	0.189	
0.143	0.186	0.303	0.357	0.366	0.171	0.192	0.350	0.189	0.150	0.175	0.199	0.097	
0.177	0.210	0.305	0.371	0.385	0.196	0.208	0.356	0.199	0.152	0.184	0.188	0.176	
0.197	0.217	0.310	0.364	0.371	0.205	0.211	0.364	0.229	0.160	0.194	0.205	0.202	

* Single Sills - all the rest of the data is depths (in feet) for double sill configurations.

TABLE A-11

Depth Distribution Data at Section 11D for the Different Sill Configurations (Set Up C)

SILL CONFIGURATION NUMBER												No Sills	$Q/D^{2.5}$
1	2	6	7	8	9	4	5	3	1*	4*	3*		
0.195	0.184	0.189	0.373	0.207	0.187	0.197	0.177	0.177	0.189	0.178	0.180	0.205	
0.186	0.178	0.187	0.360	0.207	0.200	0.186	0.190	0.210	0.177	0.169	0.178	0.183	
0.158	0.172	0.183	0.362	0.251	0.172	0.191	0.193	0.215	0.156	0.175	0.179	0.086	
0.113	0.169	0.177	0.368	0.371	0.160	0.189	0.227	0.211	0.163	0.161	0.176	0.084	
0.092	0.129	0.213	0.374	0.371	0.097	0.193	0.286	0.258	0.095	0.153	0.251	0.086	3.5
0.140	0.225	0.210	0.379	0.378	0.121	0.222	0.265	0.262	0.160	0.166	0.211	0.084	
0.190	0.252	0.209	0.366	0.263	0.180	0.225	0.239	0.258	0.190	0.191	0.207	0.092	
0.220	0.256	0.240	0.363	0.249	0.218	0.231	0.251	0.261	0.215	0.203	0.234	0.238	
0.228	0.258	0.251	0.433	0.242	0.224	0.245	0.256	0.255	0.230	0.204	0.235	0.256	
0.229	0.192	0.189	0.427	0.201	0.227	0.221	0.226	0.181	0.229	0.213	0.194	0.247	
0.227	0.200	0.189	0.412	0.220	0.229	0.221	0.226	0.199	0.226	0.212	0.207	0.235	
0.202	0.201	0.192	0.416	0.229	0.210	0.228	0.225	0.209	0.182	0.210	0.204	0.095	
0.109	0.177	0.187	0.416	0.237	0.121	0.219	0.220	0.206	0.138	0.205	0.191	0.095	
0.087	0.141	0.279	0.423	0.201	0.101	0.332	0.318	0.239	0.085	0.195	0.307	0.096	4.0
0.165	0.149	0.234	0.425	0.223	0.167	0.273	0.262	0.243	0.186	0.247	0.226	0.102	
0.230	0.249	0.232	0.439	0.241	0.236	0.270	0.271	0.249	0.220	0.243	0.247	0.102	
0.250	0.264	0.253	0.431	0.237	0.259	0.275	0.286	0.262	0.250	0.249	0.252	0.272	
0.260	0.271	0.261	0.444	0.275	0.239	0.268	0.291	0.259	0.263	0.252	0.245	0.280	

* Single Sills - are all the rest of the data depths (in feet) for double sill configurations

Table A-12. Surface Profile Data from Set Up D

Station Number	$Q/D^{2.5}$ = 1.5		2.5		3.5		6.0	
	DEPTHS IN FEET							
	*	**	*	**	*	**	*	**
1	0.403	0.384	0.495	----	0.573	----	0.804	----
2	.390	.376	.456	----	.546	----	.790	----
3	.394	.382	.453	0.463	.565	0.595	.798	0.800
4	.388	.405	.446	.450	.551	.575	.812	.801
5	.372	.406	.440	.458	.536	.572	.840	.835
6	.401	.394	.479	.462	.572	.607	.888	.862
7	.417	.388	.483	----	.566	.627	.867	.867
8	.400	.389	.498	----	.570	.620	.827	.838
9	.405	.363	.475	----	.596	.616	.794	.809
10	.393	.373	.482	----	.592	.620	.808	.818
11	.371	.375	.458	----	.583	.598	.839	.847
12	.393	----	.450	----	.575	.604	.865	.875
13	.390	----	.439	----	.580	----	.848	.846
14	.385	----	.416	----	.564	----	.793	----
15	.367	----	.484	----	.596	----	.793	----
16	.400	----	.488	----	.558	----	.837	----
17	.386	----	.479	----	.596	----	.811	----
18	.426	----	.468	----	.613	----	.849	----
19	.414	----	.412	----	.610	----	.859	----
20	.437	----	.572	----	.626	----	.859	----
21	.442	----	.577	----	.652	----	.969	----
22	.511	----	.672	----	.704	----	----	----
23	.658	----	.696	----	----	----	----	----

* No Sills

** No Sills (Repeated Data)

Table A-13. TRANSVERSE DEPTH PROFILE DATA FROM SET UP D

(Double Sill Confign. $X_1 = 1.5D$, $X_2 = 4.6D$, $S_1 = 0.556D$ and $S_2 = 0.167D$)

Station Number	$Q/D^{2.5} = 1.50$				$Q/D^{2.5} = 2.50$			
	Section at 11D		Section at 8D		Section at 11D		Section at 8D	
	no sills	with sills	no sills	with sills	no sills	with sills	no sills	with sills
1	0.106	0.152	0.078	0.089	0.055	0.178	0.094	0.162
2	.058	.131	.028	.115	.067	.200	.044	.207
3	.047	.136	.048	.129	.076	.193	.071	.225
4	.044	.135	.065	.157	.075	.187	.099	.254
5	.075	.178	.060	.152	.093	.222	.099	.238
6	.047	.198	.071	.168	.076	.212	.116	.244
7	.040	.211	.048	.152	.069	.222	.071	.232
8	.056	.265	.042	.161	.074	.248	.054	.234
9	.148	.249	.119	.167	.094	.264	.072	.232

Table A-14. TRANSVERSE DEPTH PROFILE DATA FROM SET UP D

(Double Sill Confign. $X_1 = 1.5D$, $X_2 = 4.6D$, $S_1 = 0.556D$ and $S_2 = 0.167D$)

Station Number	$Q/D^{2.5} = 3.50$				$Q/D^{2.5} = 6.00$			
	Section at 11D		Section at 8D		Section at 11D		Section at 8D	
	no sills	with sills	no sills	with sills	no sills	with sills	no sills	with sills
1	0.207	0.176	0.066	0.204	- - - -	0.351	0.064	- - - -
2	.076	.200	.048	.209	0.098	.342	.060	- - - -
3	.073	.203	.078	.218	.099	.328	.111	- - - -
4	.066	.218	.113	.245	.096	.318	.142	- - - -
5	.095	.261	.105	.236	.122	.346	.145	- - - -
6	.072	.253	.108	.232	.102	.332	.138	- - - -
7	.071	.263	.088	.219	.101	.343	.113	- - - -
8	.076	.255	.070	.234	.106	.352	.095	- - - -
9	.287	.230	.076	.238	- - - -	.354	.101	- - - -

Table A-15. Velocity Profile Data from Set Up D

	VELOCITY IN FPS								
STA.	$Q/D^{2.5} = 1.5$		3.5				6.0		
	11D sec	8D sec	11D sec	11D sec	8D sec	8D sec	11D sec	11D sec	8D sec
	*	*	*	**	*	**	*	**	*
1	5.50	4.95	6.62	5.38	9.42	4.74	11.88	6.76	11.71
2	8.22	8.24	11.33	4.88	11.94	5.84	14.40	6.47	14.04
3	9.46	9.31	13.64	4.65	13.24	5.52	15.70	5.30	16.35
4	8.86	11.15	13.10	4.09	14.87	5.14	15.90	5.87	17.40
5	9.96	12.80	15.14	4.88	15.83	5.17	16.18	6.23	17.95
6	9.48	12.34	13.91	3.76	15.50	5.14	16.43	5.96	17.67
7	8.56	10.40	12.45	4.17	14.35	5.38	15.10	5.27	16.54
8	7.45	9.05	11.78	4.84	13.12	5.52	14.83	5.82	15.42
9	5.14	15.02	7.74	5.10	10.52	5.36	11.25	6.63	13.10

* No Sills

** With Sills ($X_1 = 1.5D$, $X_2 = 4.6D$, $S_1 = 0.556D$ and $S_2 = 0.167D$)

Table A-16. Surface Profile Data from Set Up E

Station Number	$Q/D^{2.5} = 1.5$		2.5		3.5		6.0	
	DEPTHS IN FEET							
	*	**	*	**	*	**	*	**
1	0.412	1.007	0.532	- - - -	0.624	- - - -	0.850	- - - -
2	.423	.989	.552	- - - -	.649	1.025	.851	- - - -
3	.431	.756	.564	0.491	.661	.731	.852	0.906
4	.426	.431	.561	.511	.630	.641	.835	.848
5	.397	.396	.545	.509	.624	.628	.840	.980
6	.399	.382	.591	.507	.601	.614	.838	.819
7	.426	.414	.538	.514	.631	.627	.845	.855
8	.413	.413	.518	.490	.622	.611	.834	.868
9	.396	.415	.515	.473	.607	.617	.862	.925
10	.375	.394	.512	.473	.605	.625	.930	1.088
11	.391	.413	.503	.481	.639	.709	1.019	.802
12	.394	.384	.518	.484	.607	.592	.817	.772
13	.389	.385	.515	.489	.609	.620	.792	- - - -
14	.389	.374	.512	- - - -	.605	- - - -	.789	- - - -
15	.367	.374	.484	- - - -	.584	- - - -	.793	- - - -
16	.364	.374	.470	.453	.578	.581	.804	.814
17	.377	.368	.500	- - - -	.593	- - - -	.857	- - - -
18	.395	.392	.539	- - - -	.621	- - - -	.860	- - - -
19	.391	.378	.541	- - - -	.626	- - - -	.834	- - - -
20	.385	.387	.527	.498	.618	- - - -	.808	- - - -
21	.388	.388	.533	- - - -	.602	- - - -	.806	- - - -
22	.362	.377	.483	- - - -	.581	- - - -	.791	- - - -
23	.375	.361	.509	- - - -	.587	- - - -	.839	- - - -
24	.374	.370	.513	- - - -	.579	- - - -	.826	- - - -
25	.374	.386	.519	.472	.623	- - - -	.790	- - - -
26	.387	.381	.507	- - - -	.641	- - - -	.842	- - - -
27	.402	.415	.546	.504	.599	.597	.833	.879
28	.433	.426	.508	- - - -	.631	- - - -	.844	- - - -
29	.425	.416	.521	- - - -	.664	- - - -	.888	- - - -
30	.390	.375	.528	.530	.654	- - - -	.833	- - - -
31	.419	.410	.607	- - - -	.669	- - - -	.857	- - - -
32	.454	.434	.644	.635	.681	- - - -	.949	- - - -
33	.543	.515	.699	- - - -	.752	- - - -	1.108	- - - -
34	.623	.590	.713	- - - -	.844	- - - -	- - - -	- - - -

* No Sills

** With Sills ($X_1 = 1.5D$, $X_2 = 4.6D$, $S_1 = 0.5D$, $S_2 = 0.167D$)

Table A-17. TRANSVERSE DEPTH PROFILE DATA FROM SET UP E

(Double Sill Confign. $X_1 = 1.5D$, $X_2 = 4.6D$, $S_1 = 0.5D$, and $S_2 = 0.167D$)

Station Number	$Q/D^{2.5} = 1.50$		$Q/D^{2.5} = 2.50$		$Q/D^{2.5} = 3.50$		$Q/D^{2.5} = 6.0$	
	Section at 8D		Section at 8D		Section at 8D		Section at 8D	
	no sills	with sills	no sills	with sills	no sills	with sills	no sills	with sills
1	0.101	0.148	0.159	0.196	0.120	0.233	0.105	0.303
2	.052	.150	.062	.200	.068	.231	.090	.350
3	.068	.148	.087	.199	.095	.233	.117	.353
4	.068	.129	.100	.185	.100	.220	.130	.340
5	.076	.102	.111	.187	.114	.240	.148	.354
6	.071	.119	.115	.188	.103	.251	.129	.343
7	.063	.134	.089	.191	.079	.248	.114	.335
8	.052	.143	.078	.206	.070	.261	.097	.355
9	.153	.166	.184	.203	.123	.247	.123	.360

Table A-18. Velocity Profile Data from Set Up E

STA.	VELOCITY IN FPS $Q/D^{2.5}$ = 1.5		3.5		6.0	
	8D Sec	8D Sec	8D Sec	8D Sec	8D Sec	8D Sec
	*	**	*	**	*	**
1	4.58	3.16	8.49	4.35	12.09	5.12
2	7.31	3.16	10.30	4.32	13.68	5.10
3	9.04	2.98	12.20	4.58	15.00	6.37
4	9.57	3.04	13.07	4.65	15.48	7.13
5	11.15	3.72	14.18	4.65	15.88	8.34
6	10.38	3.42	13.57	4.51	15.71	7.71
7	9.10	3.63	13.10	4.30	14.41	6.89
8	8.45	3.68	11.88	4.43	13.87	6.00
9	4.96	3.31	9.93	4.47	12.12	5.46

* No Sills

** With Sills (X_1 = 1.5D, X_2 = 4.6D, S_1 = 0.5D, and S_2 = 0.167D)

Table A-19. Surface Profile Data from Set Up F

Station Number	$Q/D^{2.5} = 1.5$		2.5		3.5		6.0	
	DEPTHS IN FEET							
	*	**	*	**	*	**	*	**
1	0.385	1.011	0.481	- - - -	0.569	- - - -	0.767	- - - -
2	.416	.903	.523	0.972	.585	0.992	.775	- - - -
3	.410	.659	.532	.577	.580	.902	.816	0.906
4	.417	.356	.544	.490	.662	.613	.896	.884
5	.418	.351	.551	.522	.726	.603	.934	.870
6	.416	.397	.485	.485	.606	.599	.787	.769
7	.391	.339	.483	.466	.612	.593	.840	.773
8	.356	.339	.523	.496	.564	.555	.799	.796
9	.384	.361	.512	.491	.619	.598	.843	.799
10	.414	.404	.482	.486	.653	.627	.854	.847
11	.440	.434	.530	.533	.661	.667	.855	.870
12	.463	.470	.588	.582	.650	.668	- - - -	- - - -
13	.526	.529	.656	.652	.725	.703	- - - -	1.071
14	.589	.584	.703	.713	.852	.787	- - - -	- - - -

* No Sills

** With Sills ($X_1 = 1.5D$, $X_2 = 4.6D$, $S_1 = 0.556D$ and $S_2 = 0.167D$)

Table A-20. TRANSVERSE DEPTH PROFILE DATA FROM SET UP F

(Double Sill Confign. $X_1 = 1.5D$, $X_2 = 4.6D$, $S_1 = 0.556D$ and $S_2 = 0.167D$)

Station Number	$Q/D^{2.5} = 1.50$				$Q/D^{2.5} = 2.50$			
	Section at 11D		Section at 8D		Section at 11D		Section at 8D	
	no sills	with sills	no sills	with sills	no sills	with sills	no sills	with sills
1	0.105	0.094	0.063	0.095	0.143	0.141	0.074	0.127
2	.057	.146	.037	.101	.063	.159	.040	.191
3	.060	.119	.050	.122	.167	.157	.066	.226
4	.051	.118	.077	.126	.070	.179	.108	.201
5	.094	.149	.087	.131	.104	.206	.127	.197
6	.066	.150	.086	.135	.086	.201	.111	.175
7	.063	.159	.065	.128	.086	.224	.077	.163
8	.060	.155	.050	.130	.065	.206	.063	.159
9	.146	.186	.099	.108	.192	.232	.087	.153

Table A-21. TRANSVERSE DEPTH PROFILE DATA FROM SET UP F

(Double Sill Confign. $X_1 = 1.5D$, $X_2 = 4.6D$, $S_1 = 0.556D$ and $S_2 = 0.167D$)

Station Number	$Q/D^{2.5} = 3.50$				$Q/D^{2.5} = 6.00$			
	Section at 11D		Section at 8D		Section at 11D		Section at 8D	
	no sills	with sills	no sills	with sills	no sills	with sills	no sills	with sills
1	0.190	0.183	0.049	0.200	0.322	0.280	0.113	- - - -
2	.075	.193	.061	.230	.105	.261	.080	- - - -
3	.083	.217	.087	.275	.111	.273	.115	- - - -
4	.105	.212	.118	.278	.126	.281	.134	- - - -
5	.130	.237	.141	.282	.146	.296	.148	- - - -
6	.111	.240	.127	.261	.134	.297	.133	- - - -
7	.091	.249	.098	.229	.116	.306	.117	- - - -
8	.098	.244	.080	.224	.117	.307	.091	- - - -
9	.253	.230	.078	.220	.363	.295	.196	- - - -

Table A-22. Velocity Profile Data from Set Up F

STA	VELOCITY IN FPS							
	$Q/D^{2.5} = 1.5$		2.5		3.5		6.0	
	11D sec	11D sec	11D sec	11D sec	11D sec	11D sec	11D sec	11D sec
	*	**	*	**	*	**	*	**
1	4.87	3.25	6.20	3.72	7.22	4.36	12.30	6.56
2	7.23	3.52	9.25	4.02	11.15	4.30	14.80	5.44
3	8.17	3.25	10.35	3.48	12.20	4.06	16.00	5.60
4	8.47	3.07	11.25	3.46	13.45	3.73	15.25	4.68
5	10.15	2.55	12.35	3.17	13.58	3.50	17.35	5.23
6	8.20	2.78	10.78	3.25	12.55	3.77	15.50	4.94
7	8.80	2.86	11.46	3.72	13.40	3.94	15.80	5.54
8	7.92	2.86	10.40	3.96	12.90	4.39	13.90	5.54
9	4.86	2.72	7.08	3.62	6.50	4.35	10.95	5.74

* No Sills

** With Sills ($X_1 = 1.5D$, $X_2 = 4.6D$, $S_1 = 0.556D$, $S_2 = 0.167D$)

Table A-23. Surface Profile Data from Set Up G

Station Number	$Q/D^{2.5}$ = 1.5 *	**	2.5 *	**	3.5 *	**	6.0 *	**
	DEPTHS IN FEET							
1	0.387	----	0.537	----	0.645	----	0.783	----
2	.379	0.954	.552	1.028	.640	----	.812	----
3	.375	.890	.540	.887	.633	1.008	.827	1.002
4	.366	.375	.527	.530	.622	.785	.836	.937
5	.374	.398	.530	.532	.609	.642	.849	.901
6	.384	.415	.533	.534	.617	.621	.832	.877
7	.404	.426	.560	.547	.614	.611	.807	.867
8	.380	.390	.541	.526	.598	.601	.775	.841
9	.352	.355	.505	.478	.609	.603	.764	.818
10	.347	.338	.500	.480	.619	.651	.869	.850
11	.348	.352	.521	.472	.654	.752	.928	.955
12	.338	.353	.463	.464	.554	.563	.764	.838
13	.353	.365	.486	.491	.551	.571	.755	.834
14	.360	.376	.494	.494	.552	.566	.784	.810
15	.348	.358	.483	.477	.549	.544	.796	.871
16	.337	.331	.494	.480	----	.705	.845	.893
17	.378	.377	.468	.471	.581	.590	.763	.845
18	.311	.331	.452	.453	.569	.594	.763	.807
19	.334	.344	.487	.507	.553	.555	.763	.822
20	.363	.375	.478	.499	.608	.608	.818	----
21	.381	.404	.471	.476	.620	.652	.840	----
22	.412	.429	.526	.517	.642	.642	.842	----
23	.443	.453	.591	.571	.655	.646	----	----
24	.510	.520	.637	.653	.698	.719	1.020	----
25	.538	.531	.696	.703	.783	.807	----	----

* No Sills

** With Sills (X_1 = 1.5D, X_2 = 4.6D, S_1 = 0.556D and S_2 = 0.167D)

Table A-24. TRANSVERSE DEPTH PROFILE DATA FROM SET UP G

(Double Sill Confign. $X_1 = 1.5D$, $X_2 = 4.6D$, $S_1 = 0.556D$ and $S_2 = 0.167D$)

Station Number	$Q/D^{2.5} = 1.5$				$Q/D^{2.5} = 2.5$			
	Section at 11D		Section at 8D		Section at 11D		Section at 8D	
	no sills	with sills	no sills	with sills	no sills	with sills	no sills	with sills
1	0.144	0.155	0.115	0.118	0.190	0.164	0.127	0.158
2	.055	.152	.046	.127	.072	.171	.054	.163
3	.057	.165	.060	.123	.071	.180	.074	.159
4	.050	.186	.068	.124	.061	.200	.086	.173
5	.077	.221	.076	.115	.088	.203	.103	.174
6	.062	.231	.074	.124	.079	.208	.094	.186
7	.058	.219	.056	.133	.080	.224	.072	.182
8	.055	.227	.047	.137	.070	.225	.055	.189
9	.140	.220	.122	.144	.181	.197	.160	.184

Table A-25. TRANSVERSE DEPTH PROFILE DATA FROM SET UP G IN FEET

(Double Sill Configuration $X_1 = 1.5D$, $X_2 = 4.6D$, $S_1 = 0.556D$ and $S_2 = 0.167D$)

	$Q/D^{2.5} = 3.5$				$Q/D^{2.5} = 6.0$			
	Section at 11D		Section at 8D		Section at 11D		Section at 8D	
	no sills	with sills	no sills	with sills	no sills	with sills	no sills	with sills
1	0.238	0.201	0.073	0.201	0.215	0.275	0.102	- - - -
2	0.079	0.212	0.072	0.222	0.102	0.279	0.104	- - - -
3	0.083	0.213	0.092	0.199	0.117	0.271	0.133	- - - -
4	0.082	0.266	0.102	0.189	0.122	0.298	0.142	- - - -
5	0.108	0.271	0.113	0.203	0.137	0.281	0.160	- - - -
6	0.100	0.273	0.113	0.202	0.131	0.279	0.156	- - - -
7	0.100	0.249	0.089	0.213	0.133	0.288	0.128	- - - -
8	0.880	0.230	0.070	0.239	0.131	0.301	0.090	- - - -
9	0.266	0.223	0.088	0.220	0.331	0.283	0.175	- - - -

Table A-26. Velocity Profile Data From Set Up G

STA.	VELOCITY IN FPS							
	$Q/D^{2.5}$ = 1.5		2.5		3.5		6.0	
	*	**	*	**	*	**	*	**
1	5.51	3.17	6.73	3.80	6.97	4.73	11.30	4.35
2	7.63	3.38	9.15	3.68	11.50	4.29	13.87	5.10
3	8.39	3.25	10.26	3.06	12.55	4.18	14.50	5.20
4	8.05	2.88	10.30	3.11	12.53	3.31	15.10	5.57
5	9.85	2.70	11.76	3.00	13.15	3.59	14.84	5.80
6	8.90	2.63	11.07	3.19	13.01	3.55	14.64	5.36
7	8.21	2.52	10.79	3.05	12.94	4.10	14.60	5.14
8	7.84	1.56	9.64	3.41	11.59	4.57	13.51	5.36
9	5.38	2.71	6.13	3.74	6.83	4.55	10.47	5.12

* No Sills

** With Sills (X_1 = 1.5D, X_2 = 4.6D, S_1 = 0.556D and S_2 = 0.167D)

All Values at 11D Section